Optimal Renewable Energy Integration into the Process Industry and Energy Infrastructure Using the Multi-Energy Hub Approach with Economic and Environmental Considerations

by

Syed Taha Haider Taqvi

A thesis

presented to the University of Waterloo

in fulfillment of the

thesis requirement for the degree of

Doctor of Philosophy

in

Chemical Engineering

Waterloo, Ontario, Canada, 2018

Examining Committee Membership

The following served on the Examining Committee for this thesis. The decision of the Examining Committee is by majority vote.

External Examiner	SIMANT UPRETI Professor
Supervisor(s)	ALI ELKAMEL Professor
Internal Member	ERIC CROISET Professor
Internal Member	TIZAZU MEKONNEN Assistant Professor
Internal-external Member	FATMA GZARA Associate Professor

Author's Declaration

This thesis consists of material all of which I authored or co-authored: see Statement of Contributions included in the thesis. This is a true copy of the thesis, including any required final revisions, as accepted by my examiners.

I understand that my thesis may be made electronically available to the public.

Statement of Contributions

Chapter 2 of this dissertation includes excerpts from a book chapter and a review paper that was co-authored by me, Dr. Azadeh Maroufmashat, a post-doctoral fellow, Prof. Michael Fowler and my supervisor, Prof. Ali Elkamel. I conducted the literature review on energy hubs and classified all relevant studies in different sections based on different themes (i.e. Planning & Operation, Economic and Environmental Considerations, Applications). Moreover, I had presented the energy hub modelling technique with storage and network considerations. Excerpts from sections I had authored in these manuscripts have been presented in this dissertation.

Abstract

Fossil fuels are an integral part of the current energy infrastructure and the major contributor towards carbon emissions. Energy intensive industries and local energy framework, inclusive of the transport sector, can be integrated with distributed renewable energy technology (RET), to mitigate this problem. Cases exist in literature where the impact of a particular RET on system effectiveness is studied. In this work, however, a comprehensive model is developed, based on the multi-energy hub approach, to optimally integrate renewable energy into the process industry and the energy infrastructure in a systematic manner. MILP models are developed to evaluate optimal energy distribution within an upstream oil supply chain (USOSC) and a refinery, as well as the transport sector. Case studies are carried out on Abu Dhabi, where different scenarios, including varying EROI, implementation of EOR+ technology (i.e. carbon capture and re-injection) and employment of carbon cap-and-trade program (CC&T), are considered. On the other hand, the refinery is simulated using Aspen HYSYS. Various energy generation systems, with and without storage, are considered in order to meet effective demand. In the last phase, a study is conducted assessing rooftop area of structures within Abu Dhabi city, for the deployment of RET, designing an electric vehicle (EV) charging infrastructure. MATLAB image segmentation and region analyzing tools are employed. The optimal configuration of multi-energy systems is determined for both, minimum economic cost and CO_2 emissions, using CPLEX 11.1.1 solver.

Acknowledgements

I would like to acknowledge and thank Prof. Ali Elkamel for his supervision, guidance, and persistent support during my research years. Moreover, I am grateful to the examining committee members, Prof. Eric Croiset, Prof. Fatma Gzara, Prof. Tizazu Mekonnen and Prof. Simant Upreti for reviewing the presented work and providing insightful feedback.

I am truly indebt to dear Sh. ‘*Abul Hasan’* Muhammad Yasin who constantly guides me in every stage of life. I recognize the contributions of The Batool [as] Foundation, especially Sayyid Imran, Dr. Zoheir Ali Esmail, Sh. Riaz Esmail and the entire organization.

Lastly, I would like to thank my wife for always being by my side and my beautiful family, my brothers and sisters, who always remember me in their prayers.

Dedication

To Mamma and Abbu

Table of Contents

List of Figures

List of Tables

Nomenclature

Sets

Q Storage technology

S Energy hub

T Time period (30 yrs)

X Carbon capture technology

Y Carbon storage technology

Z Carbon transport technology

Parameters

A^{ch} Charging efficiencies of storage technologies in diagonal matrix form

A^{dis} Discharging efficiencies of storage technologies in diagonal matrix form

A_{swept} Area swept by a blade in wind turbine technology

$Aperture_{SCA}$ Aperture area of a solar collector assembly in CSP technology

$Area$ Area of a single unit of energy production technology (e.g. PV module)

$Area^{max}$ Maximum area allocated for the technology at a particular energy hub

$Areamax$ Total number of parking spaces available at a particular energy hub

b Unit conversion vector

C Coupling matrix

C^{cap} Capital cost per unit of power for a particular energy carrier

C^{DR} Disposal and recycling costs of a particular storage technology

C^{fixed} Fixed operating cost per unit energy produced for a particular energy

C^{fuel} Fuel cost per unit energy, mass or volume for a particular energy

C^{LCC} Life-cycle costs for a particular storage technology

C^{Rep} Replacement cost for a particular storage technology

C^{st-cap} Capital cost for a particular storage technology per unit energy

C^{st-var} Variable operating cost for particular storage technology per unit energy

$C^{st-fixed}$ Fixed operating cost for particular storage technology per unit energy

C^{var} Variable operating cost per unit energy produced for a particular input energy carrier

$C^{var\ O\&M}$ Operating and maintenance costs of an energy production technology

CCH Capital cost of an electric vehicle charger

CCI^{cap} Amortized capital cost of an electric vehicle charger

CF Capacity factor of a particular energy production technology

$CO2$ Carbon emissions produced per unit of energy demanded or produced

$CO2_{credit}$ Price at which carbon emissions are traded (i.e. carbon credit value)

CRF Capital Recovery Factor

D Discount rate aka interest rate (Chapter 2)

D_{PV} Depreciated present value

$Demand^{min}$ Minimum volume of crude oil demanded

$Demand^{max}$ Maximum volume of crude oil demanded

DNI Direct Normal Irradiation exposed to CSP technology

EOR Ratio of incremental oil as a result of the EOR process

FSP^{min} Minimum flow of crude oil from source to pool as dictated by pipeline capacity

FSP^{max} Maximum flow of crude oil from source to pool as dictated by pipeline capacity

GHI Global Horizontal Irradiance per surface area

g Acceleration due to gravity (i.e. 9.8 m/s^2) (Chapter 3)

g^{EV} Amount of carbon emissions produced by an average BEV

g^{ICE} Amount of carbon emissions produced by an average ICE vehicle

g^{PHEV} Amount of carbon emissions produced by an average PHEV

h Number of hours in a year (i.e. 8760)

$head$ Pressure head

$h_{j/q}$ Number of operating hours of a particular technology (*j* or *q*)

km^{EV} Average range of an average battery electric vehicle on a full charge

km^{ICE} Average range of an average internal combustion vehicle on a full tank

km^{PHEV} Average range of an average plug-in electric vehicle on a full charge

$LCOS$ Levelized cost of storage for a particular storage technology

LEC Levelized energy cost for a particular energy production technology

LHV Low heating value of a particular fuel

$length_{SCA}$ Length of a single solar collector assembly in CSP technology

Lim^{carbon} Allowed limit of carbon emissions set by governing authorities

M^{min} Minimum storage capacity of a particular storage technology

M^{max} Maximum storage capacity of a particular storage technology

$\dot{m}$ Mass of heat transfer fluid

m^{fuel} Mass of fuel used for a particular energy production technology

n Number of discharges cycles of a particular storage technology

N_{CH} Lifetime of electric vehicle charger in years

nch_{min} Minimum number of chargers for electric vehicles to be installed

nch_{max} Maximum number of chargers for electric vehicles allowed to be installed

Nev_{min} Minimum number of electric vehicles that need to be charged

Nev_{min} Maximum number of electric vehicles that can be charged

Np Number of amortized payments

$N_{storage}^{min}$ Minimum number of storage technologies allowed

$N_{storage}^{max}$ Maximum number of storage technologies allowed

N_{tech}^{min} Minimum number of energy production technologies allowed

N_{tech}^{max} Maximum number of energy production technologies allowed

P^{min} Minimum energy production capacity of for input energy carrier at energy hub s

P^{max} Maximum energy production capacity of for input energy carrier j at a particular energy hub

$Park^{min}$ Minimum parking ratio allowed designated for charging electric vehicles

$Park^{max}$ Maximum parking ratio allowed designated for charging electric vehicles

$Power$ Power rating of a single unit of a particular energy production technology

$Price$ Price of crude oil per unit of volume

$Price^{carbon}$ Price at which carbon emissions are traded (i.e. carbon credit value)

$Prod^{min}$ Minimum volume of production

$Prod^{max}$ Maximum volume of production

PR Performance ratio of a particular energy production technology

$Q^{ch,min}$ Minimum flow of energy into a particular storage technology

$Q^{ch,max}$ Maximum flow of energy into a particular storage technology

$Q^{dis,min}$ Minimum flow of energy out of a particular storage technology

$Q^{dis,max}$ Maximum flow of energy out of a particular storage technology

$rotor_{WT}$ Rotor diameter of the blades of WT technology

$Source^{min}$ Minimum flow of crude oil from the oil reservoirs

$Source^{max}$ Maximum flow of crude oil from the oil reservoirs

T Tax rate

T^{min} Minimum amount of energy transferred from an energy hub

T^{max} Maximum amount of energy transferred from an energy hub

t^{rep} Replacement period for a particular storage technology

v Flow of water stream

V^{fuel} Volume of fuel used for a particular energy production technology

VS Quality of crude oil at the source

VT Quality of crude desired at the terminal

ws Wind speed

α Matrix defining the connections between energy hubs

α^{ch} Charging efficiency of a particular storage technology

α^{dis} Discharging efficiency of a particular storage technology

β Matrix defining the connections between energy hubs

η Overall efficiency of a particular storage technology

ρ_{air} Density of air

ρ_{water} Density of water

ΔH Change in enthalpy

Continuous Variables

C_{trade} Revenue generated from carbon emissions trade

C_{CCS}^{T} Total carbon capture and storage costs for CCS technology

$C_{CC\&T}^{T}$ Total cost of carbon emissions traded

Car^{cap} Carbon emissions captured using CCS technology

Car^{stor} Carbon emissions stored using CCS technology

Car^{trans} Carbon emissions transported using CCS technology

CCH^{T} Total cost of electric vehicle chargers

CE^{T} Total cost of energy produced from energy production technology

CI^{T} Total cost of charging infrastructure

$Cost_{cap}^{T}$ Total capital cost of a particular energy production plant

$Cost^{CCS}$ Carbon capture and storage cost for a particular energy hub

$Cost_{CCS}^{T}$ Total carbon capture and storage costs for CCS technology

$Cost^{capture}$ Carbon emissions capture cost for a particular CCS technology

$Cost_{energy}^{T}$ Total cost of energy produced from energy production technology

$Cost_{fuel}^{T}$ Total fuel costs of a particular energy production plants

$Cost_{op}^{T}$ Total operating cost of a particular energy production plant

$Cost_{Rep}^{T}$ Total replacement cost of energy storage technologies

$Cost_{storage}^{T}$ Total cost of energy storage

$Cost^{storage}$ Carbon emissions storage cost for a particular CCS technology

$Cost_{st-cap}^{T}$ Total capital cost of energy storage technologies

$Cost_{st-op}^{T}$ Total operating cost of energy storage technologies

$Cost^{storage}$ Carbon emissions transport cost for a particular CCS technology

$CO2_{trade}$ Carbon emissions traded under cap-and-trade program

CS^{T} Total cost of energy storage

D Load energy demand by a particular energy hub (Chapters 3, 4, 5 and 6)

E Energy demand by a particular energy hub per unit product

FPT Flow of crude oil from pool to terminal

$Flow$ Flow of crude oil

FPT Flow of crude oil from pool to terminal

FSP Flow of crude oil from source to pool

g Amount of carbon emissions produced by a particular source

g^{Energy} Amount of carbon emission produced by energy production technologies

g^{T} Total amount of carbon emission produced

g^{Veh} Amount of carbon emissions produced from vehicles

L Load demand by a particular energy hub (Chapter 2)

$Land$ Land area occupied by a particular energy hub for certain technology

M Energy stored in technology in a particular time period

$\dot{M}$ Change in energy stored in technology with respect to a particular time period

M^{stdby} Energy losses in the storage technology

OE Energy demanded based on the production of crude oil

P Input energy carrier

$Prod$ Volume of production at a particular energy hub

Q^{ch} Energy flowing in to a particular storage technology (i.e. charging)

Q^{dis} Energy flow out of a particular storage technology (i.e. discharging)

$Revenue$ Revenue generated by the selling of crude oil

T Energy flowing out of a particular energy hub to all energy hubs

Tr Energy flowing from a particular energy hub to another

z_1 Total economic cost

z_2 Total amount of carbon dioxide emissions

Integer Variables

n^{EV} Number of battery electric vehicles

n^{ICE} Number of internal combustion engine vehicles

n^{PHEV} Number of plug-in hybrid electric vehicles

N Number of units of a particular energy production technology

nCH Number of electric chargers

Nev Number of electric vehicles charged

Binary Variables

δ^{ch} Indicates whether a particular storage technology is being charged (1), otherwise (0)

δ^{dis} Indicates whether a particular storage technology is being discharged (1), otherwise (0)

ε Indicates whether a particular storage technology is being used (1), otherwise (0)

γ Indicates whether a particular energy production technology is being used (1), otherwise (0)

List of Abbreviations/Acronyms

AD	Atmospheric Distillation Unit
AL	Alkylation Unit
AM	Amine Sweetening Unit
BESS	Battery Energy Storage System
BEV	Battery Electric Vehicle
BOP	Balance of Plant
CC	Catalytic Crack Unit
CCS	Carbon Capture and Storage
CHP	Combined Heat and Power
CSP	Concentrated Solar Power
DC	Delayed Coker
DH	Diesel Hydrotreating Unit
DNI	Direct Normal Irradition
EROEI	Energy Return on Energy Invested (aka EROI)
ESP	Electric Submersible Pumps
EV	Electric Vehicle
FCEV	Fuel Cell Electric Vehicle
GAMS	General Algebraic Modeling System
GHG	Greenhouse Gas
HC	Hydrocracker
HEV	Hybrid Electric Vehicle

HP	Hydrogen Production Plant
ICE	Internal Combustion Engine
IEA	International Energy Agency
IS	Isomerization Unit
KH	Kerosene Hydrotreating Unit
LCOS	Levelized Cost of Storage
LEC	Levelized Energy Cost (LCOE)
MILP	Mixed Integer Linear Program
MINLP	Mixed Integer Non-Linear Program
NH	Naphtha Hydrotreater
PCS	Power Conversion Systems
PHEV	Plug-in Hybrid Electric Vehicle
PV	Photovoltaic
RE	Reformer
RET	Renewable Energy Technology
SCA	Solar Collector Assemblies
SG	Saturated as Plant
SR	Sulfur Recovery Unit
TES	Thermal Energy Storage
UG	Unsaturated Gas Plant
USOSC	Upstream Oil Supply Chain
VD	Vacuum Distillation Unit
WT	Wind Turbines

Chapter 1 Introduction

1.1 Motivation

Fossil-based fuels are and have been the major source of energy, globally, ever since their discovery in the 1950s. Their reliability as an energy source as well as the simplicity with which energy can be derived, have made them technically feasible. With advancement of technology, the relatively low cost associated with their exploration and production, also, made it economical to use these fuels as the primary source of energy. Furthermore, most energy systems around the world have been designed to work on these non-renewable energy sources. However, due to their scarcity and adverse effects on nature, they have been regarded as environmentally hostile. This has raised interest amongst scientists, since the past few decades, to research on alternate sources of 'cleaner' energy.

On the other hand, renewable energy sources such as biomass (i.e. wood to fuel fires) date thousands of years before fossil-fuel discovery. People have been using wind energy to maneuver ships on seas for transport, for centuries. Yet, they are not perceived as economical or technically feasible choices, as compared to fossil-based energy sources. Renewables such as solar or wind are intermittent sources of energy and substantial research is being carried out, till this day, to address concerns regarding their reliability. Nevertheless, they are cleaner energy sources and unanimously agreed as favorable sources of future energy. Fossil-based fuels, in contrast to 'cleaner' options, may not necessarily be completely replaceable in the near future due to the relatively low cost and ease-of-use. However, energy intensive industries, relying on such resources and emitting enormous volume of carbon emissions, may be integrated with renewable energy, in this transition period. Thus, current energy systems can be integrated with renewable energy in order to reduce dependence on fossil-based fuels and promote sustainability. Moreover, several storage technologies may be employed to address reliability concerns. In future, with promising research, systems can be enhanced and harmful environmental effects, by conventional energy sources, can be further mitigated.

1.2 Background

There is no doubt that renewable energy makes significant contribution to global energy production. In 2015, about 5454 TWh (24%) of electricity produced was generated from renewable energy sources[1]. In addition, these cleaner alternatives have been to be more beneficial than conventional sources of energy in terms of their social, economic and environmental impacts[2], [3]. However, 66% of the electricity produced globally was fueled by fossil-based fuel as seen in Figure 1.1[1]. Moreover, these sources are known to be depleting over time and leading to the worsening of the global warming scenario.

Renewable energy, as defined by the EIA, is energy derived from regenerate sources that commonly include biomass, hydropower, geothermal, wind and solar[2], [4], [5]. A number of countries, in North America, South America and Europe depend on these means as their primary sources of energy. In 2015, Norway reported its share of renewables in electricity production to be as high as 98%[6]. On the other hand, most oil and gas producing countries show a high dependence on the conventional non-renewable sources of energy and with less or almost negligible contribution by the renewables. United Arab Emirates (UAE) was the 10th largest producer of global energy, producing about 2.5 GWh in 2015[6]. However, it had about 0.25% share of renewables in electricity production[7]. Nevertheless, Abu Dhabi, the capital of the United Arab Emirates, launched a policy, in 2009, to increase the city's power generation capacity from renewable sources by 2020[8]. Since then, considerable research has been carried out on this topic, in the region.

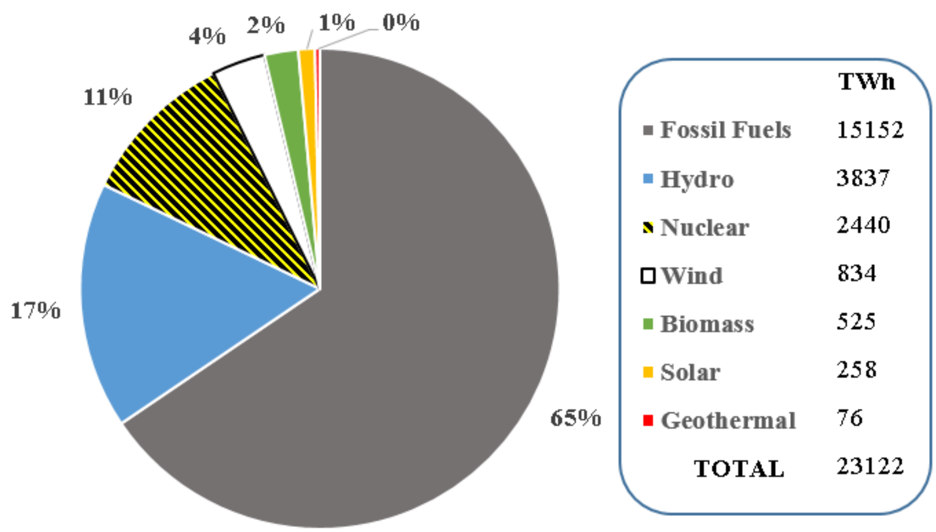

Figure 1.1 World electricity production from all energy sources in 2015 [1]

Traditionally, one of the factors affecting decision-making in using renewable energy was the cost associated with it. According to OpenEI, the levelized cost of energy (LCOE) of using Photovoltaic (PV) systems to generate electricity was averaged to \$0.62/kWh in 2004[9]. Whereas, the LCOE associated with electricity being produced using natural gas was averaged to \$0.07/kWh[10]. However, in 2014, LCOE of PV systems was reported as low as \$0.056/kWh while generation systems using natural gas was reported to be as low as $0.049/kWh[11]. Hence, making renewable energy competitive to use as compared to other types of energy in this aspect.

Over the past few years, in addition to competitive cost, renewable energy systems have been found to be technically feasible for small domestic applications such as solar charging stations and thermal desalination processes[12], [13]. Additionally, much research is being carried out on integrating renewable energy sources (RES) with existing power grid and electricity markets[14], [15]. Another major advantage of using renewables over non-renewables is the immense reduction of greenhouse gas emissions (GHG) and water pollution observed[2]. Though, it has been argued in a study that renewable energy sources, specifically hydropower, are not entirely ‘clean’ and emit significant pollutants[16]. Yet, according to statistics reported by International Energy Agency (IEA) in 1998, fossil-based power generation systems emitted roughly 60-100 times more GHG emissions per kWh than renewables[17]. Due to these growing environmental concerns, countries have taken interest in promoting use of renewable energy to meet targets set for reduced emission collectively (i.e. Paris Agreement) or by extending subsidies. This had a positive economic impact as ‘clean’ energy investments have increased, creating more jobs. In 2009, a study, outlining the economic benefits of investing in clean energy, depicted that an investment of a dollar in clean energy could produce more jobs as it would in the oil and gas industry[18]. All these benefits, collectively, lead to the social well-being of an individual in terms of health, work opportunities and technological advances[2]. Despite all these favorable arguments, conventional sources of energy receive 75 times more subsidies than renewables, till this day[3]. In fact, a tremendous amount of energy is consumed in the production of fossil fuels resulting in a vast amount of GHG emissions and hazardous wastewater[19].

A study on Abu Dhabi showed that 63% of its energy was consumed by the industry sector in 2010, as seen in Figure 1.2[20]. More than 30% of that grid-connected energy was expended by Abu Dhabi National Oil Company (ADNOC). Furthermore, it has been forecasted to exceed 2000 GWh/year by 2020[20]. Yet, this does not include energy consumption through off-grid energy sources. With declining Energy Return on Energy Investment (EROEI) of oil and gas, this demand is difficult to meet without utilization of alternate sources of energy[21]. In order to promote sustainability, two major challenges need to be overcome: (i) integrating high share of intermittent resources to current energy system and (ii) the transportation sector dependence on fossil fuels[22]. Since the most abundant and cleanest renewables are intermittent sources of energy (i.e. solar, wind), a major challenge that exists in integrating these renewables into the electricity grid is maintaining grid reliability[23]. Yet, there exist possibilities of integrating renewable energy sources to existing energy-related industries that require enormous amounts of energy to generate them (i.e. oil and gas)[19]. On the other hand, even though electric vehicles (EV) have overcome several technical and economic barriers (i.e. battery size, capacity, cost) in order to be more competitive with combustion engines, the lack of charging infrastructure is one of major challenges preventing its mass adoption[24].

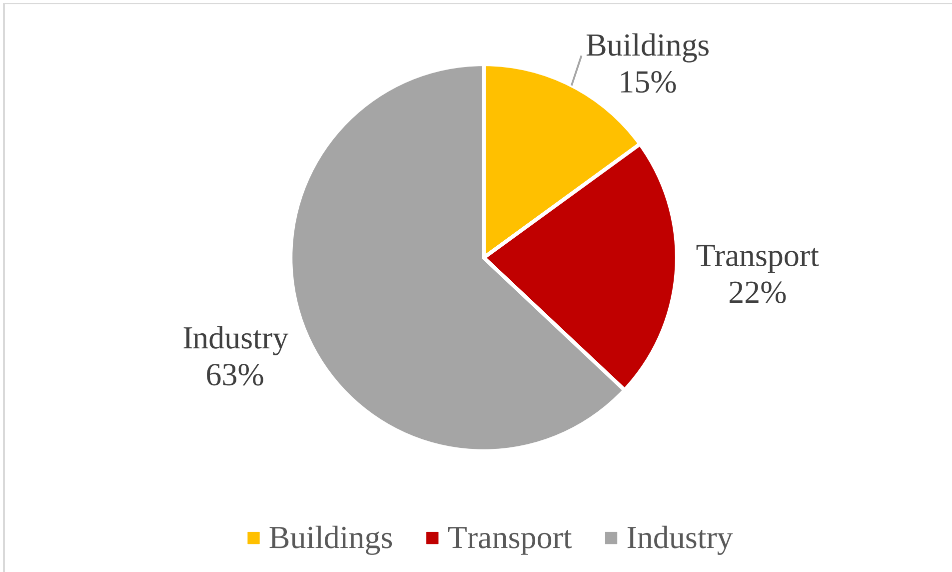

Figure 1.2 Energy consumption of Abu Dhabi by sector in 2010[20]

1.3 Research Objectives and Contributions

Considering the scenarios mentioned above, the main aim of this research is to develop a generic framework to optimally integrate renewable energy within the process industry and the current energy infrastructure, using the multi-energy hub approach. In line with this research work, the following are the objectives of this study:

- conduct a comprehensive literature review on the proposed energy hub approach to identify potential for process industry and energy infrastructure applications,

- develop a general framework for optimal renewable energy integration within a network of energy hubs with storage whilst making economic and environmental considerations,

- develop a multi-period model, based on the generic framework, for the process industry, specifically areas with high energy consumption

- develop a multi-period model, based on the generic framework, for an energy infrastructure application.

For the process industry application, the study focuses on studying all essential processes that take place within the industry and the associated CO_2 emissions. For the energy infrastructure application, the study focuses on identifying all potential energy consumers within the geographical location and the associated carbon emissions. For both applications, the general mathematical model is modified for the respective problems to meet effective demand while reducing GHG emissions at the operational level.

The main outcome of this study will be a general framework that can be generally used for the optimal integration of renewable energy within an energy intensive sector. The models developed can be applied to the process industry and to a current energy infrastructure, respectively, to optimally integrate renewable energy to them. Through the implementation of these models, areas of renewable energy integration can be identified, the total profit/cost and total CO_2 emissions can be calculated, based on various economic and environmental criteria. Within them, different possible constraints may be defined on product supply and demand, energy supply and demand, and CO_2 management constraints, due to possible limitations (e.g., upper and lower bounds) on the production limit, energy availability and/or technological restrictions. In all, decisions/policy makers will be able to assess the impact of integrating renewable energy to their current system and make informed decisions accordingly.

1.4 Dissertation Outline

Chapter 2 of this dissertation comprises of a comprehensive literature review on energy hubs. It classifies the studies based on different themes and identifies the different energy vectors and technologies utilized in each study. The energy hub approach is explicitly defined within this section. Moreover, the modeling of energy hubs and general optimization strategies are also discussed in this chapter. Through this work, potential of using this approach will be realized for the optimal integration of renewable energy within the desired sectors.

Chapter 3 shows the development of the general mathematical model for optimally integrating renewable energy within the process industry/energy infrastructure. It states the different objective criteria that can be considered and the various sets of constraints, incorporated within the model.

Chapter 4 shows the integration of renewable energy within the Upstream Oil Supply Chain (USOSC) of Abu Dhabi. Different nodes along different echelons within the USOSC are regarded as energy hubs. The problem is posed as a pooling problem. Renewable energy is optimally integrated based on economic and environmental objectives whilst maintaining oil production targets.

Chapter 5 discusses the development of a MILP model where renewable energy is integrated within a refinery. Processes within the refinery are simulated using Aspen HYSYS to yield energy consumption by each unit. General Algebraic

Modeling System (GAMS) software was used to solve the model and yield optimal energy allocation schemes whilst integrating renewable energy.

Chapter 6 discusses the study of integrating renewable energy within the current energy infrastructure of Abu Dhabi City. Energy hubs are considered in different areas within the city with available renewable energy sources. Primarily, these energy hubs are aimed to provide charging to electric vehicles throughout the city. Surplus energy, if any, may also be used towards meeting the domestic demand by buildings.

Chapter 7 draws conclusions from this research work; stating the significant findings from different studies presented in this work. Additionally, a set of recommendations are made for researchers with interest to conduct further work in this area.

Chapter 2 Literature Review[1,2]

In this chapter, literature review has been conducted on energy hubs to understand the energy hub approach. Moreover, to identify the potential this approach has to model the scenario for optimal integration of clean energy into existing energy systems. The proposed energy hub modeling technique is discussed, in detail.

2.1 Energy Hub

Synergy in energy systems has been a topic of interest for many decades. Several studies have been carried out in the area tackling optimal multi-energy carrier problems. The energy hub approach has played a vital role in addressing many such problems. Several researchers have utilized this methodology and extended this concept in modelling, optimization, and applications. In this chapter, we have reviewed and organized different literature on energy hub modelling. Furthermore, the need for energy hubs for future energy systems has been outlined whilst depicting the advancement to the energy hub approach since its inception.

In 2002, a research project titled, "Vision of Future Energy Networks (VoFEN)", was initiated with the aim of creating an optimal energy infrastructure for the

---

[1] A variant of the literature classification section in this chapter is submitted for publication: A. Maroufmashat, S. Taqvi, M. Fowler and A. Elkamel, "Energy Hubs – Modeling and Optimization: A Comprehensive Review"

2 A variant of the modeling section in this chapter is published: S. Taqvi, A. Maroufmashat, M. Fowler, A. Elkamel and S. Khavas, "Optimal Design, Operation, and Planning of Distributed Energy Systems Through the Multi-Energy Hub Network Approach," in *Operation, Planning, and Analysis of Energy Storage Systems in Smart Energy Hubs*, 1st Edition, B. Mohammadi-Ivatloo and F. Jabari (Eds.), Springer, 2018, pp. 365-389.

target year of 2050[25]. Based on a Greenfield approach, the project focused on developing a generic model and an analysis framework. In 2005, the research team introduced the concepts of Energy Hubs (EH) and Energy Interconnectors (EI)[26], [27]. The latter, though not in the scope of this study, was proposed as an application in multiple energy carrier transmission[28]. The research work was carried out envisioning the difficulty of traditional systems to be economically and environmentally sustainable[26]. By considering these bridging elements (i.e. energy hubs and interconnectors), Geidl et al.[28] believed that current sub-optimal systems can be transitioned to an optimal level.

2.1.1 Significance

Energy systems, for many centuries, have been successful in extracting energy from primary energy sources, transforming chemical and/or mechanical energy into electrical energy. However, they have been processing these forms of energy in a decentralized manner, Implying, energy generation and conversion taking place in different facilities, not administered by the end user. Moreover, emitting large volumes of carbon emissions. Also, as recent research interest increases in zero-emissions vehicles such as battery electric vehicles (BEV), plug-in hybrid electric vehicles (PHEV), and fuel cell vehicle (FCV), there is a drastic increase expected in distributed demand for electricity. Whilst, the current energy system lacks the ability to accommodate this growing energy demand without countering the problem of depleting resources. It does not allow for the integration of ‘cleaner’ energy sources whilst meeting the increasingly stringent environmental regulations[25]. Thus, the need arises for investment in poly-generation energy systems and decentralized technologies, allowing for a more flexible energy infrastructure in terms of operation and distribution[29]. Moreover, strategies need to be developed considering ecology, economy and functionality.

The Greenfield approach, as used in other fields of study, advocates a strategy to design future power systems that eliminate constraints set by previous energy systems, in order to achieve true optima by bridging different forms of energy to establish synergism, as a fundamental step towards an optimum state. Hence, the linking of multiple energy carriers in centralized units was proposed (i.e. energy hubs)[25], [28]. Moreover, these forms of energy may be transported in proposed single transmission devices as energy interconnectors[25]. By devising and utilizing such bridging systems, an optimal level of operation for energy systems may be attained.

2.1.2 Definition

The literature has referred to energy hubs as multi-energy systems, multiple energy carrier systems, multi-source multi-product systems, combined/hybrid energy systems, hybrid poly-generation energy systems and as distributed multi-generation systems. These hybrid energy systems can be defined as interconnected energy units which include energy generation, conversion, and storage systems [30]. In the optimal energy infrastructure of the future, the "Vision of Future Energy Networks" defines the energy hub as an interface between energy producers and consumers, which incorporates direct connections, energy conversion and storage technologies to couple multiple energy carriers to meet load demands [25]. An energy hub has inputs of various energy vectors such as electricity, natural gas (NG), heat, hydrogen, biogas, and liquid petroleum and alcohol fuels. Within an energy hub, energy may be generated or transformed with technologies such as wind turbines, solar photovoltaics, solar thermal, combined heat and power plants (CHP) heat exchangers, furnaces and boilers, and electrochemical devices such as fuel cells. Energy can be stored in technologies such as: batteries, as hydrogen, flow batteries, flywheels, compressed air energy storage (CAES), or thermal devices and arrays[31].

2.2 Literature classification of Energy hub

This section of the chapter aims at organizing and classifying literature regarding energy hubs, whilst identifying research gaps in this field of study. The areas focused in this chapter are (a) planning and operation, (b) economic and environmental impacts, and (c) various applications of energy hubs. Each area is explored in detail in its respective section.

Since the discovery of these optimal multiple energy carrier units, numerous studies have been carried out. Over the years, the proposed energy hub model has been modified and further developed for the purpose of enhancing reliability and control [32]–[35]. The principle of the energy hub concept has been applied across different regions and fields of study [36]–[38]. Planning of energy hub networks and their operation has been the focus of several research projects [39]–[42];specially, different aspects pertaining to the economics and environment have been considered [43]–[45]. In addition, recent studies have looked at the concepts of energy internet, smart energy hubs, virtual power plants, and smart grids based on the energy hub approach [46]–[52].

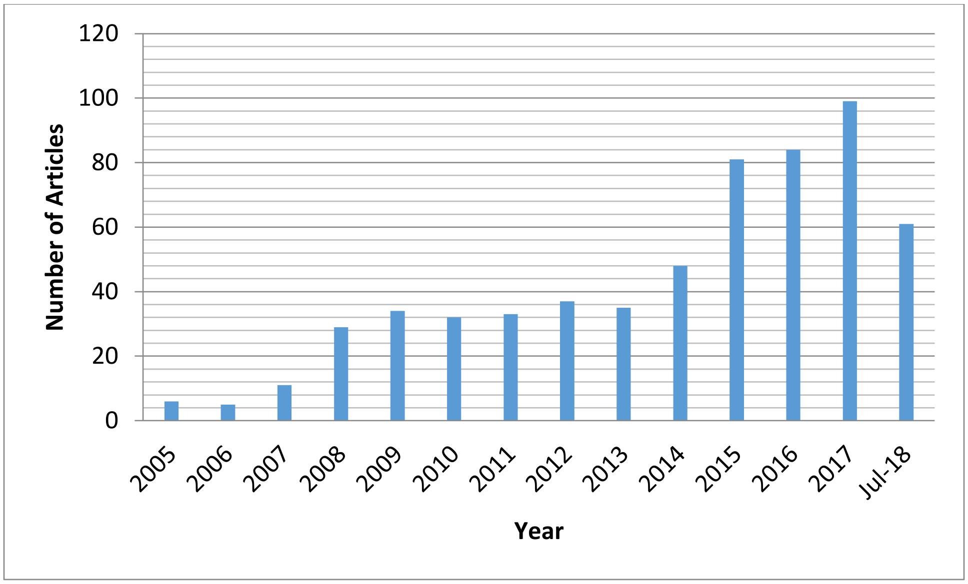

Figure 2.1 Number of publications in each year relevant to energy hubs.

As seen from Figure 2.1, the number of published studies relevant to energy hubs has significantly increased over the past decade. These publications comprise of journal articles, conference proceedings, dissertations and other forms of research media. Furthermore, the number of publications per year has almost doubled in the past few years. This substantial rise indicates the growing interest of researchers in this area of study and the wide application of this approach.

2.2.1 Planning & Operation

According to the classification of literature conducted in this study, there are more than 150 research papers addressing the issue of the planning and operation of energy hubs. When examining such issues for an energy hub or a network of energy hubs, there are several factors to consider including:

- The volume and scale of energy hubs;

- The conversion and storage technologies to implement within hubs; and,
- The control methodology of power flow within energy hubs.

These characteristics not only govern the overall operational efficiency of the energy system, in general, but also, they specifically determine the reliability of the system when subjected to the increasing load.

Energy hubs have the ability to increase the reliability of energy systems, because the coupling of multiple energy carriers increases the flexibility of energy systems in which the load demands are met. Geidl et al. [25] performed a case study for a standard small company and demonstrated that the projected load is supplied by the conversion of thermal or chemical energy to electricity via an energy hub concept for most of the day, week or season.

One of the earliest study, on operation planning of synergistic systems using energy hubs, is conducted by Unsihuay et al. [53]. The work aim at minimizing operation costs for an integrated hydrothermal and gas system. Another study, conduct by Robertson et al. [54], outline an energy infrastructure for the UK as it progresses towards a lower-carbon economy. It employs the energy hub approach to determine the framework that would allow the most effective conversion and transfer of energy. Galus and Andersson [55] carried out research work focusing on the planning integration of plug-in hybrids electric vehicles (PHEVs) into energy hub networks; driving behavior was simulated and different conditions pertaining to vehicle usage were tested for, on the proposed energy hub network.

2.2.1.1 Scheduling

Scheduling of energy hubs plays an important role in integrated energy systems in tackling with the energy shortage issues as well as the environmental impacts (Fan, Chen, Liu, Li, & Chen, 2016); It is also profitable in reducing operational costs [42], [56]. As multiple energy carriers enter an energy hub, deciding what type of source of energy used to meet the specific load can be challenging problem. If intermittent sources of energy are involved (commonly renewables), as in this research work, effective planning can aid in reducing operational costs and harmful greenhouse gas (GHG) emissions while ensuring reliability of the energy system.

Pazouki et al. conducted several studies on scheduling of energy hubs, including a case study on an urban area in North-West of Iran [42], [56]–[58]. Economic scheduling resulted in the reduction of the operational costs, an improvement in reliability, and a decrease in greenhouse gas emissions [42], [56]–[59]. In another study, Moghaddaam et al. [60] presented a comprehensive profit-based model that allow self-scheduling of energy hubs; the model was capable of adopting complex strategies, considering the cost of electricity and natural gas to maximize profit with great accuracy and the potential of the exchange of electricity with the grid. However, operation-scheduling entails various sources of uncertainties. Vaccaro et al. [61] state that these uncertainties arise from, but are not limited to, (i) unpredictable dynamics of energy prices, (ii) randomness of energy hub loads, and (iii) renewable energy converters. Nevertheless, the results obtain by Zidan et al. [59] showed significant enhancement because of the addition of renewable energy sources.

2.2.1.2 Control

Since hybrid energy systems are dynamic and susceptible to uncertainties, the need for communication and controllers arises to ensure an effective coordinated operation. These controllers are expected to adapt to changes in loads, based on the system dynamics and operational constraints [62]. Additionally, they keep these uncertainties within acceptable levels by using storage devices [63].

Intermittent renewable sources of energy are often found as energy vectors in the modeling of energy hubs [42], [50]. However, as these sources of energy fail to provide a steady amount of energy throughout the year, the energy imbalance is either met by purchasing electricity off the grid or by backup generators [63]. Thus, energy storage systems within hubs work as an asset that allows better control and, by extension, a more reliable cost effective energy system [62], [63].

2.2.2 Economic and Environmental Considerations

Economy improvement and greenhouse gas mitigations are significant intended outcomes of the future energy systems. The focus of several studies, from the literature surveyed, was an evaluation of an energy hub system based on economic and environmental aspects. The energy systems is modelled using the energy hub approach and the results were then compared to previous case studies.

2.2.2.1 Economics and Financials

In the economic assessment of multiple energy carrier systems, the cost of available energy resources is the one of the focal points of the study. Feasibility studies can be carried out to determine the viability of using a particular energy source, with or without an energy hub framework. Models have been developed in order to devise energy systems in an economic way whilst considering changes in energy prices and future energy demand.

Fabrizio et al. [43] carried out research to set economic and environmental objectives and investigated the trade-off between them for a hybrid energy system. In another study, by Fabrizio[64], the economic feasibility for applying the energy hub framework for health-care facilities in Italy was investigated in multiple scenarios. Schulze and Del Granado [65] evaluate the impact of implementing tariffs to promote renewable energy production; A model was developed to optimize the power supply through the energy system. The results indicated that feed-in tariffs is an effective methodology to increase overall benefits while satisfying energy demand [65]. A study, by Barsali et al. [66], investigates the viability of energy storage systems based on energy tariff changes over different hours of the day.

Kienzle [67] developed a model for optimizing a portfolio of energy investments by applying the mean variance portfolio theory to multiple energy carrier systems. Kienzle [68] also presented a method of valuating energy hubs under uncertainty. Instead of utilizing historical price data as the basis for financial analysis, a Monte Carlo approach was used to account for policy and technology changes. A methodology was proposed in which energy prices were modeled as random variables and applied the Monte Carlo approach by simulating a deterministic model with thousands of different prices paths. Kienzle et al. [69] extended the

Monte Carlo approach to incorporate Demand-Side Management (DSM) on loads.

The Monte Carlo methodology was applied in other energy hub studies. Maniyali et al. [70] formulated an energy hub model which incorporates nuclear energy and hydrogen storage in addition to wind, solar and biomass energy. The formulated model was used to determine the total power generated, the hydrogen storage, carbon emissions and revenue based on 200 scenarios of different technology combinations. Detailed analysis was conducted on the minimal cost scenario, minimal emissions scenario and hydrogen economy scenario. It was found that nuclear energy with electricity generation capacity close to the yearly average demand was most economical in terms of energy production. In terms of energy storage, underground hydrogen storage was deemed most economical for all scenarios.

Sharif et al. [71] adapted the energy hub model to use natural gas as the main energy source which is supplemented using wind and solar energy and hydrogen energy storage. They simulated the model using a Generic Algebraic Modelling Software (GAMS) with three main scenarios: a baseline single energy carrier scenario, a multi energy carrier scenario, and a multi energy carrier scenario with energy storage; the final scenario produced the lowest cost and emissions.

2.2.2.2 Emissions

Energy hubs have the capability of reducing emissions related to energy production and transmission due to the capability of integrating multiple renewable energy carriers. Orehounig et al. [72] investigated the integration of renewable energies into a small village in Switzerland. The energy carriers and transform technologies included are grid electricity, oil, photovoltaic, wind, small hydro, and wood chips and was in the scale of MWh. They used the energy hub concept to simulate a set of future scenarios with regards to the amount of energy available from each energy carrier, and found that the best performing scenario could reduce carbon emissions by 38%. Orehounig et al. conducted further studies on the implementation of energy systems on the same village, which include retrofitting of buildings and neighborhood-level energy management. Similar to their previous study, they simulated a set of scenarios and found that the best performing scenario had a 86% reduction in carbon emissions [72].

Chicco and Mancarella focused on the energy and environmental evaluation of polygeneration systems, powered by natural gas [73]. A polygeneration CO_2 emission reduction (PCO2ER) indicator was developed that could be used as a tool to assess environmentally the energy systems. Galus et al. [74] designed a framework for plug-in hybrid electric vehicles (PHEVs) using energy hub approach to forecast region-wide CO_2 emission decrease.

Del Real et al. [45] conducted a study on the power dispatch of energy hub networks by considering the cost of environmental impacts as a part of an objective function. Morvaj et al. investigated the impact on energy systems by mitigating carbon emissions from the electricity grid [75]. Several scenarios were simulated using the energy hub framework and a Pareto front was constructed for each. These Pareto fronts showed a decrease in carbon emissions resulting in an increase in the cost associated with the increasing share of renewables in the generation of power. Nevertheless, it was found that only when the grid was completely fueled by renewable energy sources, a carbon neutral economy would be attainable [75].

2.2.3 Applications

The energy hub approach has opened up a wide spectrum of possibilities for people and various energy load or demands within in energy hub. Based on the literature reviewed, this approach has been perceived as a significant approach towards future energy systems. Moreover, the transition to future energy systems involves utilizing Distributed Energy Systems (DES), green or zero emission vehicles (ZEV) as well as building a hydrogen economy. An ‘hydrogen economy’ is where hydrogen is generated via emission free nuclear and renewable technologies, and then used as an energy vector to store, distribute energy, and most importantly power transportation applications. As evident from the literature surveyed above, the energy hub approach is well-established. Based on the theme of this research work, literature based on applications on distributed energy systems and electric vehicles has been presented here.

2.2.3.1 Distributed Energy Systems (DES)

Distributed Energy Systems commonly refer to decentralized power generation systems, usually onsite, as opposed to centralized power plants, often located in remote or ‘off grid’ areas, providing energy to a specific region. These include, but not limited to, microgrids, diesel generators, solar panels, wind turbines, combined heat and power (CHP), micro turbines and energy storage systems [76].

With the Geidl and Andersson proposed methodology, DES can be easily modeled using the energy hub approach [30].

In a study, Hemmes et al. [77] explored the potential of multiple energy carriers by demonstrating 5 applications of energy hubs as distributed energy systems; the applications involve multiple energy carriers with CHP, production of hydrogen and electricity by a fuel cell with and without fluctuating renewable energy and the integration of fuel cells in a natural gas network [78]. On another hand, Schulze et al. [78] applied the energy hub model with the aim of optimizing energy flow, using renewables. Franziska applied the energy hub approach to examine optimal power supply for a larger region with increasing renewable demand [79]. A multiple-level model was introduced in determining the optimal power supply strategy in an area with varying power generation levels and various energy carriers. This study considered the impact of renewable energy power plants and storage systems from various sizes and costs, deciding which energy conversion and storage technologies can employ and where to place them whilst minimizing the dependency on centralized power plants [79]. Maroufmashat et al. [80] developed an energy hub network, modeling a distributed energy system, considering combined heat and power (CHP) systems and solar energy; the study demonstrated the cost reduction due to the proposed energy network and potential to mitigate carbon emissions.

Del Real [81] carried an optimization study on a solar-hydrogen energy system, conceptualized through the energy hub approach, used for residential purpose. The model was able to determine the optimal power flow and hydrogen storage through the year, considering seasonal changes [81]. Anastasiadis et al. [82] examined the power losses in low-voltage micro-grids, using energy hubs. Highest annual energy losses were observed in scenarios where no DES were considered. Moreover, independently operated DES including wind turbines, solar photovoltaic (PV), and combined heat and power (CHP) technologies showed about 59% less annual power loss than the former case (i.e. no DES) [81], [82].

In a review study, Chicco and Mancarella described energy hubs as one of the emerging approaches towards decentralized and multi-generation systems in addition to micro-grids and virtual power plants [83]. On the contrary, Buehler studied the integration of renewables into these energy systems and discussed how the energy hub approach should be used to enhance virtual power plants and micro-grids [50]. In a study conducted by Schule and Crespo Del Granado, three storage systems with intermittent renewable energy sources were optimized using the energy hub model. Moreover, an optimization tool was developed, based on the optimization models, which aided in reducing computation time [84]. Robertson et al. developed a simulation tool called Hybrid Energy System Analysis (HESA), based on the energy hub model, to investigate the DES impact on the existing energy infrastructure. Results showed that the tool was capable of simulating DES systems of various levels and sizes [85].

2.2.3.2 Plug-in Hybrid Electric Vehicles (PHEVs) and Battery Electric Vehicles (BEVs)

Several studies have been conducted, demonstrating the modeling and optimization research on Plug-in Hybrid Electric Vehicles (PHEVs) and battery electric vehicle (BEVs), charging infrastructure and integration into current system, using energy hubs. Since BEVs and PHEVs draw electrical power from the grid or energy hub and store it on-board the vehicle to provide emission free charge, the vehicle can be used in an 'grid to vehicle' (G2V), or vehicle to grid (V2G) model. BEVs receive all of their onboard energy from a charging station, while a PHEVs has some charge depletion range from rechargeable batteries and some from an onboard range extender internal combustion engine (so a PHEV is not a zero emissions vehicle, but has some zero emission range)[86]. This is considered when conducting the study on energy infrastructure, presented in Chapter 6.

Galus and Andersson applied the methodology to demonstrate the potential of this approach for implementation of PHEVs in different applications [55], [87]. Different operating states such as driving, charging, refueling, and regulation services to the electricity network can be easily modeled using the proposed framework [87]. In addition to easily extending the model with various other architectures, the energy hub model allows extensive space for optimization.

Prior to implementing EVs on a large scale, a reliable infrastructure needs to be provided for it to be effective. Andrade et al. modeled a parking lot that served as a charging stations for electric vehicles [88]. Three different scenarios (i.e. early morning, morning and afternoon) were examined to analyze power flow in the electric parking lot, using MATLAB Simulink. It was observed that the electricity consumption by the electric vehicles was much higher than the daily consumption. Thus, a bigger transformer and an effective energy management system was required [88]. Another study, by Damavandi et al., considers the parking lot as a storage system [89]. Results denoted that the operation of energy hubs was very flexible and allowed changes to meet energy demand [89]. In addition to parking lots, Rastegar and Fotuhi-Firuzabad were able to determine optimal charge scheduling for PHEVs at home, using the EH model, based on time-differentiated pricing of electricity [90].

Integration of PHEVs with smart grid, modeled by 4 energy hubs, was studied by Waraich et al. [88]. Energy demand of PHEVs was simulated using an agent-based traffic demand model and various charging policies were tested. The proposed approach was successful in determining whether a particular energy infrastructure was capable of handling a certain penetration of PHEVs [88]. Using the EH approach, Morvaj et al. was able to develop a framework successfully to minimize carbon emissions while meeting energy demand for electric vehicles and buildings in a residential area [91]. Haghifam et al. integrated PHEVs and renewable energy sources with the gas and electricity infrastructure, using the energy hub approach [92]. Operational costs were observed to decrease as less electricity was purchased from the grid [92].

2.3 Modeling

Energy hubs, in addition to being optimal multi-energy carrier systems, have also been identified as interfaces between different energy generation and loads, as depicted in Figure 2.2[25], [93]. The unit commonly is comprised of three types of elements: direct connections, converters and storage. The connections include the different energy carriers (i.e., electricity grid, natural gas, etc.) that enter the system as well as the outputs to the consumer. Within the energy hub, there exist a set of conversion technologies to condition into the desired form. Additionally, energy storage systems can be considered in the hub for scheduled dispatch of various forms of energy.

Among the various pros of this methodology, added reliability, load flexibility, and enhanced performance of the system are some of the notable ones [30]. Using the energy hub approach, a wide spectrum of energy-related problems can be addressed throughout the residential, commercial, and industrial areas [94].

Geidl et al. worked on defining a model for multiple energy carrier systems with energy hubs. Initially, they expressed the energy hub model in terms of only energy conversion. However, in later works, energy storage was incorporated into the model[30]. Geidl et al. emphasized that the proposed formulation of the energy hub leaves significant room for optimization since the coupling matrix is usually non invertible due to the presence of more energy carriers than users or vice versa.

As illustrated in Figure 2.2, the energy from carrier 1 is split between energy conversion technologies A and B. In contrast, energy from carrier 2 is split into two further energy vectors after passing through the conversion technology C. D and E are other components for further conversion. For example, in the case where C may be a co-generation system, E may represent a chiller cascaded with to meet the demand of Load 2, which is cooling load.

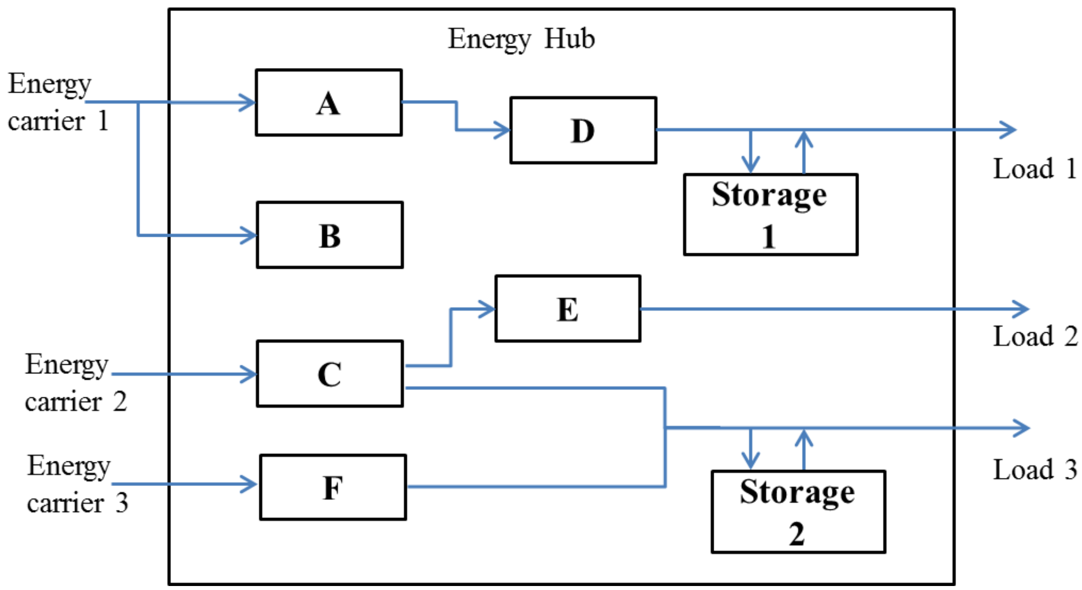

Figure 2.2 Illustration of a simple energy hub (Adopted from [94]**)**

<u>2.3.1 Generic Framework</u>

One of the main aims of the future energy system projects [28] was to develop a generic modeling and analysis framework in which the economical, ecological and technical effects concerning energy systems could be studied. This generic structure would allow high flexibility in modeling without posing any constraint on the size of the system. Hence, to model the energy conversion of each technology, as described in the previous section, Geidl et al. [95] proposed to use a coupling matrix C that would transform the input energy to the required energy vectors. Maroufmashat et al. [144] modified this formulation as shown in the following equation. Eqn. 2.1 shows a mathematical expression used to define the overall energy mapping process.

$$\overbrace{\begin{bmatrix} L_1 \\ L_2 \\ . \\ L_i \\ . \\ L_I \end{bmatrix}}^{L(t)} = \overbrace{\begin{bmatrix} C_{11} & C_{12} & .. & C_{1j} \\ C_{21} & C_{22} & .. & C_{2j} \\ . & . & . & . \\ . & . & C_{ij} & . & . \\ . & . & . & . \\ C_{I1} & . & . & . & C_{IJ} \end{bmatrix}_{I\times J}}^{C(t)} .\mathrm{I}_{J\times J}.\mathrm{b}. \overbrace{\begin{bmatrix} P_1 \\ P_2 \\ . \\ P_j \\ . \\ P_J \end{bmatrix}_{J\times 1}}^{P(t)} \tag{2.1}$$

L and **P**, in the above equation, denote the load demand and the input energy carrier *i j*, respectively. *b* is a vector that converts the units of energy from the input to power, being consistent with that of the load. $\mathrm{I}_{J\times J}$ is inserted in the equation to allow uniformity for matrix multiplication. The entities of the coupling matrix C represent the efficiency with which energy is converted. If a particular entity within the coupling matrix is zero, it depicts that no conversion of energy is taking place. If a single conversion technology is utilized, the efficiency of that conversion process is considered as the coupling factor. Additionally, if load demand is as the result of one or more energy conversion technologies, the product of the efficiencies is considered as the coupling factor. On the other hand, the input energy carriers may possess certain operational limits, based on their capacity. Thus, their power needs to constrained by lower and upper boundaries (i.e. min/max), as expressed by Eqn. 2.2.

$$P^{min} \leq P(t) \leq P^{max} \tag{2.2}$$

Overall, this simple model can either be utilized under the steady state conditions or further developed to tackle dynamic systems with control strategies, while including energy storage and losses. Moreover, unidirectional as well as bidirectional flow of power can be considered based on energy hub configuration [78]. For example, an electrical transformer would be able to realize reverse power flow whilst a turbine may not [30]. Based on this generic structure, the model opens a wide range of possibilities for optimization [77]–[79]. Stochastic models can be collated alongside for planning and operation of energy sources [81]–[83]. In addition, interactions between the energy carriers can be studied to assess reliability and performance [84], [85].

2.3.2 Energy Storage Modeling

Energy storage is one of the key elements of the energy hub considered by Geidl et al [25], [28], [30]. More than half of the publications, adhering to multi-energy systems, have incorporated energy storage within their models. It is essential to account time dependency when energy storage is considered as energy accumulates over a certain period. Hence, the conversion technologies are perceived as discrete temporal systems [94].

$$\dot{M}_q = \alpha_q^{ch} Q_q^{ch} - \frac{1}{\alpha_q^{dis}} Q_q^{dis} \tag{2.3}$$

Eqn. 2.3 shows energy balance on the storage technology, accounting for energy entering the storage system (i.e. charging) and leaving it (i.e. discharging). $\mathrm{Q_q^{ch}}$ represents the power in-flow through the storage technology q at an efficiency $\mathrm{\alpha_q^{ch}}$,while $\mathrm{Q_q^{dis}}$ represents the power flowing out of it at an efficiency of $\mathrm{\alpha_q^{dis}}$.

As mentioned earlier, dynamic modelling is required when considering storage systems. Thus, the storage function needs to discretized into separate time periods. This has been done using the forward difference formula, as seen in Eqn. 2.4.

$$\dot{M}_q = M_q(t) - M_q(t-1) + M_q^{stdby} \qquad (2.4)$$

$\mathrm{M_q(t)}$ and $\mathrm{M_q(t-1)}$ represent the energy stored time periods (t) and (t-1), respectively. In order to account for losses, the $\mathrm{M_q^{stdby}}$ term is added to the expression to express energy loss when the storage system is in its standby state. By compiling Eqns. 2.3 and 2.4, the overall equation for the qth storage device at time period (t) can be written as illustrated in Eqn. 2.5.

$$\mathrm{M_q(t) = M_q(t-1) + \alpha_q^{ch} Q_q^{ch}(t) - \frac{1}{\alpha_q^{dis}} Q_q^{dis}(t) - M_q^{stdby}} \quad \forall q, \forall t \qquad (2.5)$$

In matrix representation, Eqn. 5 may be expressed as Eqn. 6.

$$\mathrm{M(t) = M(t-1) + A^{ch} Q^{ch}(t) - A^{dis} Q^{dis}(t) - M^{stdby}} \qquad \forall t \qquad (2.6)$$

As written, $\mathrm{A^{ch}}$ and $\mathrm{A^{dis}}$, in Eqn. 2.6, are diagonal matrices representing charging and dis-charging efficiencies to allow matrix multiplication. In addition to the above model equations, technical constraints need to be structured to define the limitations of the storage technology. For instance, simultaneous charging and discharging of a storage system is not possible. Hence, Eqn. 2.7 comprises of two binary variables $\delta_q^{dis}(t)$ and $\delta_q^{ch}(t)$ are introduced for each storing technology at each time period t to define the situation.

$$\delta_q^{dis}(t) + \delta_q^{ch}(t) \leq 1 \qquad \forall q. \forall t \tag{2.7}$$

Eqn. 2.8 shows the additional limitations on the capacity and exchange energy of each storage system.

$$M_q^{min} \leq M_q(t) \leq M_q^{max} \qquad \forall q. \forall t \tag{2.8}$$

$$\delta_q^{ch}(t). Q_q^{ch,min} \leq Q_q^{ch}(t) \leq \delta_q^{ch}(t). Q_q^{ch.max}$$

$$\delta_q^{dis}(t). Q_q^{dis,min} \leq Q_q^{dis}(t) \leq \delta_q^{dis}(t). Q_q^{dis.max}$$

$\mathrm{M_q^{min}}$ and $\mathrm{M_q^{max}}$ represent the minimum and the maximum level of energy stored in the q^{th} storage system. Moreover, $Q_q^{ch.min}, Q_q^{dis.min}, Q_q^{ch.max},$ and $Q_q^{dis.max}$ represent the minimum and maximum energy that can flow through the q^{th} storage technology during the energy charging and discharging process.

2.3.3 Network Modeling

In many cases, a single energy hub model suffices to represent the entire energy system. Yet, for large-scale planning and operational problems, a network of energy hubs is considered [87], [88], [93], [94]. These energy hubs are interconnected, facilitating energy transfer between each other.

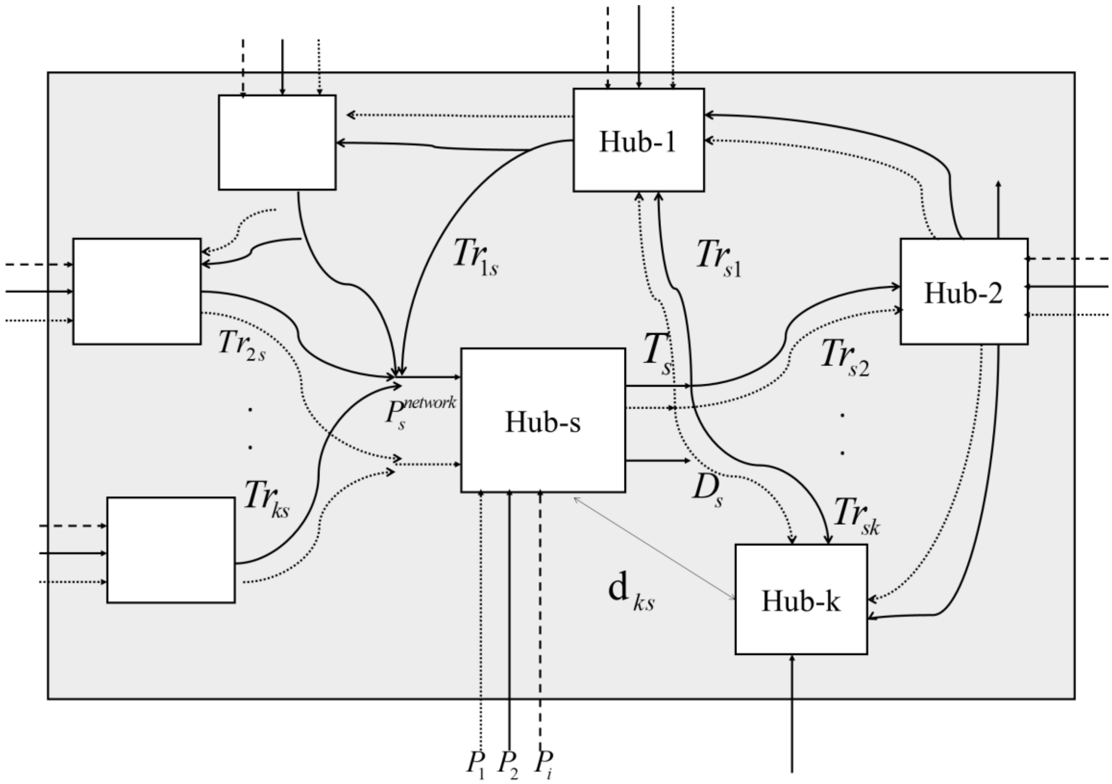

Figure 2.3 Diagram depicting the interconnected energy hubs with energy hubs [94]**.**

Figure 2.3 shows a network of energy hubs with the focus on energy hub *s*. Each energy hub within the network either receives energy from outside the network (i.e. grid, renewable energy sources, etc.) as denoted by P_i or from other energy hubs in the network (i.e. Tr_{sk}). Likewise, each energy hub produces energy to meet energy demand within the energy hub or supply to other interconnected energy hubs. As evident in Figure 2.3, three energy carriers have a flow of power into energy hub *s*. The total energy from hub *s* supplied to other connected energy hubs is represented by T_s. This total is the summation of individual energy output, Tr_{sk}, to each connected energy hub, *k*, from energy hub *s*. This relationship can be expressed mathematically in the following way:

$$T_s = \sum_{k \in S-\{s\}} Tr_{sk} \tag{2.9}$$

Similar to the coupling factors in the coupling matrix as well as energy storage efficiencies, a coefficient may be multiplied by Tr_{sk} to account for the losses due to the transmission of energy from energy hubs *s* to *k*. All the energy vectors that exist between the interconnected energy hubs can be written in the matrix form, as shown below.

$$\begin{bmatrix} T_1 \\ T_2 \\ \cdot \\ \cdot \\ \cdot \\ T_s \\ \cdot \\ \cdot \\ Ts \end{bmatrix}_{S\times 1} = \begin{bmatrix} 0 & Tr_{12} & Tr_{13} & \cdots & Tr_{1k} \\ Tr_{21} & 0 & Tr_{23} & \cdots & Tr_{2k} \\ \cdot & \cdot & \cdots & & \\ \cdot & \cdot & \cdots & & \\ \cdot & \cdot & \cdots & & \\ Tr_{s1} & Tr_{s2} & \cdots & & Tr_{sk} \\ \cdot & & & & \\ \cdot & & & & \\ Tr & & \cdots & & 0 \end{bmatrix}_{S\times S} \cdot \begin{bmatrix} 1 \\ 1 \\ \cdot \\ \cdot \\ \cdot \\ 1 \\ \cdot \\ \cdot \\ 1 \end{bmatrix}_{S\times 1} \tag{2.10}$$

The first column vector contains the sum of all energy vectors leaving a particular energy hub (i.e. T_s). The *Tr* matrix contains each vector that leaves a particular energy hub *s* and enter energy hub *k*. The column vector on the right hand side of the expression is a vector with each element equal to 1 to allow matrix multiplication.

In theory, the proposed approach is flexible in levels and sizes. Also, it possesses extensive room for optimization. Issues hindering its execution may be matters pertaining to problem complexity such as mixed integer non-linear formulations. Moreover, strategies that would need to be implemented to combat large-scale problems in reasonable execution time.

Chapter 3 Model Framework

This chapter discusses the development of the general framework for optimally integrating renewable energy within a process industry/energy infrastructure. Furthermore, it defines several different constraints based on technical, economic and environmental considerations.

3.1 Superstructure

Figure 3.1 shows the general superstructure for integrating renewable energy within the process industry and/or energy infrastructure, posed as a network of energy hubs.

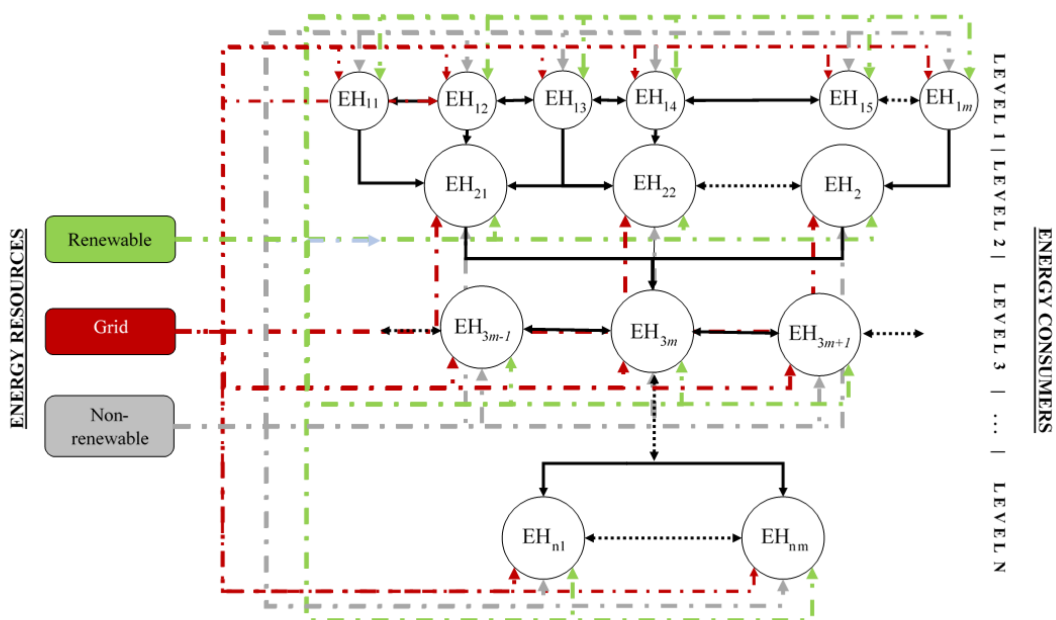

Figure 3.1 Superstructure depicting the energy consumers and resources

EH_{nm} represents an energy hub representing the m^{th} unit at the n^{th} level within the process/energy network. Each of these energy hubs are interconnected with each other in order to facilitate energy transfer. Moreover, as shown in the superstructure, each of the energy hubs have access to energy resources that help meet effective demand of each unit.

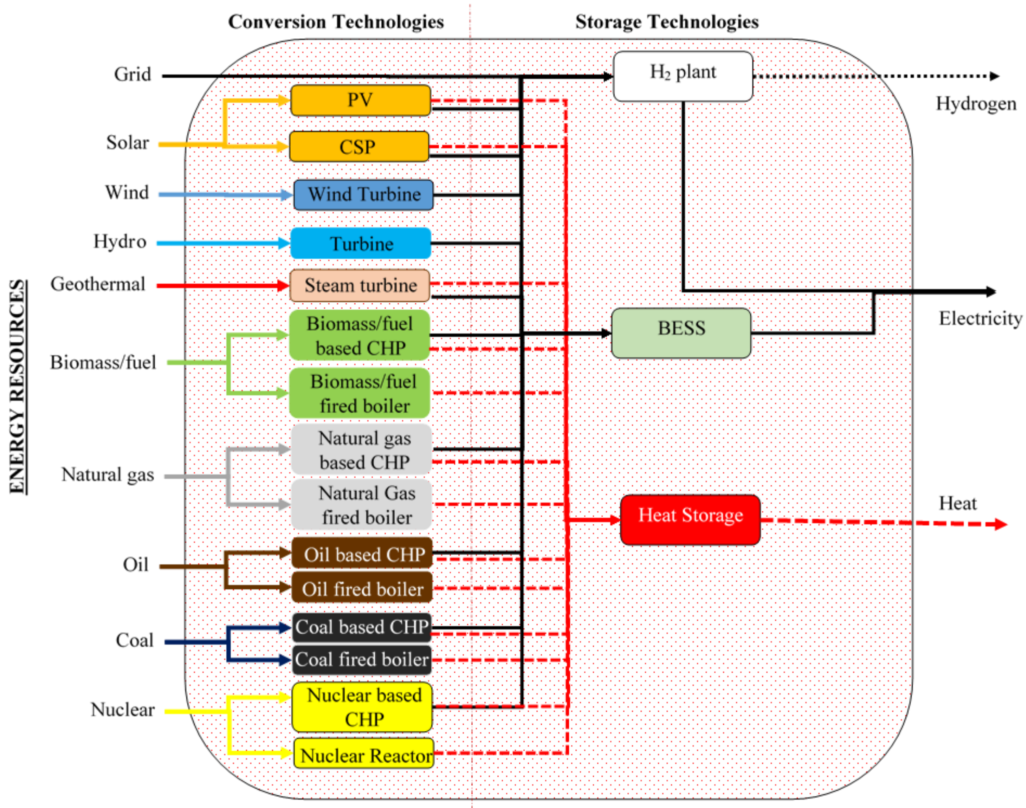

Figure 3.2 Schematic of proposed energy hub with storage technologies

Figure 3.2 illustrates the proposed energy hub, considering all possible energy vectors and respective technologies. These include all possible sources of energy, renewable and non-renewable. Grid represents the grid-connected electricity purchased. Two types of solar technologies, Photovoltaic (PV) and Concentrated Solar Power (CSP), are considered that can generate electricity and/or heat, based on the respective configuration. Wind and hydro energy is harnessed using wind and hydro turbines, respectively, to generate electricity. Geothermal energy, extracted in the form of steam, may be used for electricity generation or heating purposes. Biomass along with the fossil fuels (i.e. natural gas, oil and coal) may be used solely for heating using a boiler to meet heat requirements. On the contrary, respective Combined Heat and Power (CHP) systems may be utilized to generate electricity and heat, as proven effective in several studies [96]–[101]. Finally, nuclear technology may also be considered that may generate heat through reactors and/or yield electricity through nuclear based CHP systems. It is important to understand that energy hubs may be physical units where all energy conversion, storage technologies are housed. On the other hand, they may represent system boundaries that include these elements. Nevertheless, the approach to modeling would be same in both cases which is the within the scope of this study.

Electricity may either be stored using Battery Energy Storage System (BESS) or sent to the Hydrogen plant. The H_2 plant comprises of an electrolyzer, a hydrogen storage tank, and a fuel cell. The electrolyzer converts water into hydrogen and oxygen gases, using the electricity. This hydrogen gas can be converted back to electricity using a fuel cell for the consumption by the unit. Additionally, it may be exchanged and consumed as hydrogen wherever necessary. Both electricity storage technologies (i.e. BESS and H_2 plant) have been included as there are various factors and limitations that affect that the technical and economic feasibility of each of the two types of storage technology[102]. Moreover, much research work is being carried out in the area of hydrogen infrastructure as it is considered an integral part of future energy systems[103]. Heat storage systems have also been incorporated within the model, as evident from Figure 3.2.

3.2 Objective Function

A multi-objective function was developed that assigned varying weights, ω, to the total cost (z_1) and carbon dioxide emissions (z_2) objective functions, as shown in the equations below. The model may be optimized with respect to either the multi-objective function or to each of the other single objective functions, z_1 and z_2, individually, to minimize total economic costs or carbon dioxide emissions, respectively.

$$z_1 = Cost^T_{energy} + Cost^T_{storage} + Cost^T_{CCS} \tag{3.1}$$

$$z_2 = \sum_t \sum_s \left(\sum_j P_{s,j,t} CO2_{s,j} + \sum_i D_{s,i,t} CO2_{s,i} \right) \tag{3.2}$$

The total cost objective function (z_1) comprises of the cost of energy resources utilized by the process/energy infrastructure, the cost of storage technologies employed as well as the cost of carbon capture and storage techniques applied. On the other hand, carbon dioxide emissions objective function (z_2) contains emissions generated from utilizing the energy resource and from significant emissions sources independent of the type of energy resource employed. For a process network, this may be dependent on the volume of production and respective energy requirement, as seen in Eqn. 3.2. In an energy infrastructure problem, latter part of the second objective function may not be necessary to include unless there exists a specific significant source of emissions, independent of the energy resource.

3.3 Energy Supply

The total cost of energy, $Cost_{energy}^{T}$, comprises of the total capital costs and total operating costs of conversion technologies as well as total fuel costs needed for the operation of these energy resources. This is expressed mathematically by Eqn. 3.3.

$$Cost_{energy}^{T} = Cost_{cap}^{T} + Cost_{op}^{T} + Cost_{fuel}^{T} \tag{3.3}$$

The total capital cost, $Cost_{cap}^{T}$, is mainly the cost of the energy generation plant based on its capacity. For small-scale commercial projects, it may only include the cost of all the equipment needed. Moreover, this information may be readily available and provided by the retailers and/or manufacturers. For example, the capital cost for a residential system may comprise of the cost of the PV modules, DC-AC inverter, battery and other equipment costs. For large-scale projects, the capital costs may also include the cost of land and/or construction costs. In this case, data pertaining to the cost of existing plants may be obtained and scaled based on the plant capacity. Such data is often available in literature in the public domain. On the other hand, capital cost is also reported in several research studies as a unit of power rating[9], [104]–[106]. In this case, capital cost per power rating, C_{j}^{cap}, (e.g. $/kW) can be multiplied by the maximum plant capacity, $P_{s,j}^{max}$, as seen in Eqn. 3.4.

$$Cost_{cap}^{T} = \sum_{s}\sum_{j} P_{s,j}^{max} C_{j}^{cap} \tag{3.4}$$

For large-scale energy generation plants, this cost tends to be high and payments are made in installments over a period of time rather than upfront at the beginning of the project. The total capital cost may be multiplied with the Capital Recovery Factor (CRF) to calculate these cash flows, based on the number of payments, *Np*, and the discount rate, *D* (aka interest rate). Commonly, the number of payments is linked and made equal to the lifetime of the project. The CRF can be calculated using Eqn. 3.5. In addition to that, the tax rate paid on these payments as well as depreciation of capital are other factors that may also considered.

$$CRF = \frac{D\,(1+D)^{Np}}{(1+D)^{Np}-1} \tag{3.5}$$

Similar to capital cost, fixed capital costs are also reported as $ per unit of power whereas variable costs are reported as $ per unit of energy produced. The total operating costs may be calculated using Eqn. 3.6. For each energy resource *j*, as the name suggests, the variable costs may change over a time period, *t*. However, it is also a common practice to consider an average value for these variable costs for simplicity.

$$Cost_{op}^{T} = \sum_t \sum_s \sum_j (P_{s,j,t} C_{j,t}^{var} + P_{s,j}^{cap} C_j^{fixed}) \tag{3.6}$$

Lastly, the total cost of the fuel utilized by the particular energy generation technology, $Cost_{fuel}^{T}$, is calculated using Eqn. 3.7.

$$\sum_t \sum_s \sum_j P_{s,j,t} C_{j,t}^{fuel} \tag{3.7}$$

$$\sum_t \sum_s \sum_j m_{s,j,t}^{fuel} C_{j,t}^{fuel} \tag{3.8}$$

$$\sum_t \sum_s \sum_j V_{s,j,t}^{fuel} C_{j,t}^{fuel} \tag{3.9}$$

The cost of fuel, $C_{j,t}^{fuel}$, as expressed in the above equations, may be expressed as cost per unit energy, per unit volume, or per unit mass, based on availability of data. Thus, it is multiplied with either the amount of energy, mass ($m_{s,j,t}^{fuel}$) or volume ($V_{s,j,t}^{fuel}$) of fuel needed to generate desired energy from energy vector *j* from energy hub *s* at time *t*. Referring back to Eqn. 3.7, for grid, it refers to the price of electricity available for purchase from the grid. This price may be different at different times of the day (i.e. on-peak, mid-peak, off-peak); hence, giving additional flexibility to the model when alternate sources of energy and/or storage are considered. For non-renewable energies, nuclear and biomass/biogas, prices of respective fuels per unit of energy need to be known. Similar to grid-connected electricity, prices of these commodities may or may not change with time. Depending on the scope of a particular study, changes in these fuel prices may be considered. For renewable energies such as wind and solar, there is no evident fuel required and no associated cost is reported. However, there is significant operational water consumption per unit of energy reported for almost all energy generation technologies (i.e. renewable, non-renewable)[107]. This detail may also be included as fuel cost depending on the scope of the study.

Another methodology for calculating cost of energy is by using the Levelized Cost of Energy (LCOE) aka Levelized Energy Cost (LEC), as seen in the following equation:

$$Cost_{energy}^{T} = \sum_t \sum_s \sum_j P_{s,j,t} LEC_j \tag{3.10}$$

LEC is the cost of energy generated from a particular source of energy over the lifetime of the system. It is calculated by dividing the total cost (i.e. sum of all costs incurred during the lifetime of the system) by the lifetime expected power output [108], [109]. LEC has been widely used by researchers in their respective studies to estimate power generation costs[109]. It generally includes all of the cost elements discussed above. The general simplified LEC formulation for each type of energy resource can be seen in Eqn. 3.11.

$$LEC_j = \frac{C_j^{cap}\ CRF_j(1-D_{PV})}{h \times CF_j(1-T)} + \frac{C_j^{fixed\ O\&M}}{h \times CF_j} + C_j^{var\ O\&M} + C_{j,t}^{fuel} \qquad (3.11)$$

In addition to the cost elements discussed previously, depreciation (D_{PV}), tax rate (T) and capacity factor of energy technology j (CF_j) are included in Eqn. 3.11. Several other studies have been developed with similar formulations of the LCOE, varying on the level of detail or specific to a particular energy source[106], [108]–[110].

3.4 Energy Demand

The total energy required by the proposed energy hub network is calculated using the following equation.

$$D^T = \sum_t \sum_s \sum_i D_{s,i,t} \qquad (3.12)$$

where $D_{s,i,t}$ refers to the energy demanded by hub s as energy vector i at time period t in MJ. For the process industry, volume of production, $Prod_t$, and energy requirement of the process energy hub per product, $E_{s,i,t}$, may prove to be crucial in determining the energy demand, $D_{s,i,t}$. This can be calculated using Eqn. 3.13.

$$D_{s,i,t} = E_{s,i,t} Prod_t \tag{3.13}$$

Moreover, a constraint may be placed on the volume of production, based on the process capacity, as seen in the following equation.

$$Prod_t^{min} \leq Prod_t \leq Prod_t^{max} \tag{3.14}$$

3.5 Storage

The total cost of storage, in Eqn. 3.1, comprises of similar components (i.e. capital and operating costs of relevant technologies) as the cost of energy does, in Eqn. 3.3, as seen in the equation below. In addition, the cost of replacement, $Cost_{Rep}^{T}$, of replaceable energy storage systems (e.g. batteries) need to be considered in order to accommodate storage technology for the lifetime of the energy generation plant.

$$Cost_{storage}^{T} = Cost_{st-cap}^{T} + Cost_{st-op}^{T} + Cost_{Rep}^{T} \tag{3.15}$$

Costs associated with recycle and disposal of storage technology elements are often neglected in studies. However, it is another item that can be included within the total cost of storage[111]. The capital and operating costs for storage technologies can be calculated using Eqn. 3.16 and 3.17.

$$Cost_{st-cap}^{T} = \sum_s \sum_q \sum_i M_{s,q,i}^{max} \, C_q^{st-cap} \tag{3.16}$$

$$Cost_{st-op}^{T} = \sum_t \sum_s \sum_j (M_{s,q,i,t} C_{q,t}^{st-var} + M_{s,q,i}^{max} C_q^{st-fixed}) \tag{3.17}$$

The capital cost for storage technologies are reported per unit energy and needs to be multiplied with the maximum storage capacity ($M_{s,q,i}^{max}$) in order to determine the total storage capital costs. This capital cost may include costs associated with Power Conversion Systems (PCS), storage section and Balance of Plant (BOP). PCS may be necessary in cases where input energy form may be different than that it is being stored in (e.g. electricity to hydrogen). The storage section costs may comprise of containment vessel costs, construction and excavation costs and other related costs. BOP costs include all other costs related to utilities, protective devices, monitoring and control systems. For the calculation variable operating costs, knowledge of the energy level within a storage technology ($M_{s,q,i,t}$) at each time period, *t*, is required.

On the contrary, the total cost of energy storage, in Eqn. 3.1, may also be calculated using Eqn. 3.18.

$$Cost_{storage}^{T} = \sum_t \sum_s \sum_q \sum_i M_{s,q,i,t} LCOS_q \qquad (3.18)$$

The Levelized Cost of Storage, $LCOS_q$, was calculated using the methodology developed by Zakeri and Syri[111], as seen in the following equations. All cost elements were annualized so that energy storage costs may be calculated for the lifetime of the energy generation plant. Additionally, all of these costs were reported as cost per unit of energy.

$$LCOS_q = \frac{C_q^{LCC,a}}{n \cdot h} - \frac{LEC_j}{\eta_q} \qquad (3.19)$$

Annual life-cycle costs, $C_q^{LCC,a}$, was divided by yearly operating hours (h) of the storage technology and the number of discharge cycles (n) the storage technology undergoes in a year, as seen in Eqn. 3.19. The cost of energy used to charge the storage technology was subtracted from this ratio as well as overall storage technology efficiency (η_q) was considered.

In the study [111], the life-cycle cost of the storage technologies comprised of the capital cost, operating costs, replacement costs and, disposal and recycling costs, as shown in Eqn. 3.20.

$$C_q^{LCC,a} = C_q^{st-cap,a} + \left(C_q^{fixed,a} + \left(C_{q,t}^{var,a}\, nh_{yr}\right)\right) + C_q^{Rep,a} + C_q^{DR,a} \quad (3.20)$$

The annual replacement cost ($C_q^{Rep,a}$), in addition to previously discussed factors, considered number of replacements (r) and the replacement period (t^{rep}).

$$C_q^{Rep,a} = CRF \sum_{k=1}^{r} (1+D)^{-kt^{rep}} \left(\frac{C_q^{Rep} h}{\eta_q}\right) \quad (3.21)$$

Finally, the disposal and recycling costs of the storage technology was annualized using Eqn. 3.22.

$$C_q^{DR,a} = C_q^{DR} \left(\frac{D}{(1+D)^N} - 1\right) \quad (3.22)$$

3.6 Carbon Capture and Storage (CCS)

The total cost of carbon capture and storage (CCS) is calculated by the difference between the sum of CCS costs ($Cost_{s,t}^{CCS}$) for each energy hub over all periods of time and revenue generated from carbon emissions trade (C_{trade}), as evident from using Eqn. 3.23.

$$Cost_{CCS}^{T} = \left(\sum_t \sum_s Cost_{s,t}^{CCS}\right) - C_{trade} \quad (3.23)$$

The CCS cost for each energy hub arises from the cost of capturing CO_2 emissions ($Cost_{s,t}^{capture}$) from it, cost of storing them ($Cost_{s,t}^{storage}$) and cost of transporting ($Cost_{s,t}^{transport}$) them from the energy hub to the storage site, as seen in Eqn. 3.24.

$$Cost_{s,t}^{CCS} = Cost_{s,t}^{capture} + Cost_{s,t}^{storage} + Cost_{s,t}^{transport} \quad (3.24)$$

The cost of each of these stages in CCS is calculated by multiplying the carbon dioxide emissions, in gCO_2, undergoing the technology and cost of respective technology employed per gCO_2, as expressed by the following equations. The cost of employing different CCS technologies at each stage has been reported in literature[112].

$$Cost_{s,t}^{capture} = \sum_x Car_x^{cap} C_x^{cap} \quad (3.25)$$

$$Cost_{s,t}^{transport} = \sum_y Car_y^{trans} C_y^{trans} \quad (3.26)$$

$$Cost_{s,t}^{storage} = \sum_z Car_z^{stor} C_z^{stor} \quad (3.27)$$

All carbon emissions from the energy hub network are subjected to a particular technology at each stage within the CCS process, as demonstrated in Eqn. 3.28.

$$\sum_x Car_x^{cap} = \sum_y Car_y^{trans} = \sum_z Car_z^{stor} \quad (3.28)$$

$$= \sum_j P_{s,j,t} CO2_{s,j} + \sum_i D_{s,i,t} CO2_{s,i}$$

Revenue generated from carbon emissions trade can be calculated by multiplying the amount of carbon emissions traded ($CO2_{trade}$) with the price at which these emissions may be traded ($CO2_{credit}$), as shown in Eqn. 3.29. $CO2_{trade}$may be positive or negative depending on whether carbon emissions were below or above the defined limit, respectively, set by the governing authorities.

$$C_{trade} = CO2_{trade}CO2_{credit} \tag{3.29}$$

3.7 Energy Hub

Energy hubs, as illustrated by Geidl et al.[30], can be modeled using the following equation.

$$L_{s,i,t} = C_{i,j}P_{s,j,t} \tag{3.30}$$

It is possible that the output load ($L_{s,i,t}$) and input energy carriers ($P_{s,j,t}$) are expressed in different units and may require multiplication with conversion units. However, as seen in the later section, conversion is carried out while calculating $P_{s,j,t}$ for each energy carrier, j. $C_{i,j}$ is known as the coupling matrix that contains the efficiencies of conversion from energy input j to energy output i.

3.7.1 Energy Storage

The proposed energy hub, seen in Figure 3.2, shows different storage technologies. Thus, the governing energy hub model can be modified to Eqn. 3.31 that includes the amount of energy flowing in (i.e. charging,$Q^{ch}_{s,q,i,t}$) and out (i.e. discharging,$Q^{dis}_{s,q,i,t}$) of the storage technology.

$$L_{s,i,t} = \left(C_{i,j}P_{s,j,t}\right) + \sum_q Q^{dis}_{s,q,i,t} - Q^{ch}_{s,q,i,t} \tag{3.31}$$

Moreover, an energy balance on the storage technology would yield the following equation[94]. α^{ch}_q and α^{dis}_q is the charging and discharging efficiency of the storage technology q whereas $M_{s,q,i,t}^{loss}$ accounts for any energy loss within the storage system.

$$M_{s,q,i,t} = M_{s,q,i,t-1} + \alpha_q^{ch} Q_{s,q,i,t}^{ch} - \alpha_q^{dis} Q_{s,q,i,t}^{dis} - M_{s,q,i,t}^{loss} \qquad (3.32)$$

Limitations on the amount energy stored by each technology q need to be defined, as illustrated in Eqn. 3.33. $\varepsilon_{s,q,i,t}$ is a binary variable which is 1 when the particular storage system is being used.

$$\varepsilon_{s,q,i,t} M_{s,q,i,t}^{min} \leq M_{s,q,i,t} \leq \varepsilon_{s,q,i,t} M_{s,q,i,t}^{max} \qquad (3.33)$$

Also, the charging and discharging limits of each storage technology need to be incorporated. These are expressed in the following equations. $\delta_{s,q,i,t}^{ch}$ and $\delta_{s,q,i,t}^{dis}$ are binary variables which equal to 1 when the storage system is being charged or discharged, respectively.

$$\delta_{s,q,i,t}^{ch} Q_{s,q,i,t_{min}}^{ch} \leq Q_{s,q,i,t}^{ch} \leq \delta_{s,q,i,t}^{ch} Q_{s,q,i,t_{max}}^{ch} \qquad (3.34)$$

$$\delta_{s,q,i,t}^{dis} Q_{s,q,i,t_{min}}^{dis} \leq Q_{s,q,i,t}^{dis} \leq \delta_{s,q,i,t}^{dis} Q_{s,q,i,t_{max}}^{dis} \qquad (3.35)$$

$$\delta_{s,q,i,t}^{ch} + \delta_{s,q,i,t}^{dis} \leq 1 \qquad (3.36)$$

The total number of storage technologies may also be restricted, as shown in Eqn. 3.37.

$$N_{storage}^{min} \leq \sum_q \varepsilon_{s,q,i,t} \leq N_{storage}^{max} \qquad (3.37)$$

3.7.2 Network

In the superstructure, shown in Figure 3.1, a network of energy hubs is depicted. This can be modeled using Eqn. 3.38 to allow exchange of energy between energy hubs. $T_{s,b,i,t}$ is energy transferred from energy hub *s* to *b* if a connection, $\beta_{s,b}$, exists between them.

$$L_{s,i,t} = D_{s,i,t} + \sum_{b \in S-s} T_{s,b,i,t}\beta_{s,b} \tag{3.38}$$

Using Eqn. 3.39, simultaneous bi-directional flow between energy hubs may be restricted. Hence, the amount received by one energy hub is equivalent to the amount sent by the other energy hub at particular time period *t*.

$$T_{s,b,i,t} = -T_{b,s,i,t} \tag{3.39}$$

Eqn. 3.40 defines the limits of energy that can be transferred from one energy hub to another.

$$T_{s,b,i,t}^{min} \leq T_{s,b,i,t} \leq T_{s,b,i,t}^{max} \tag{3.40}$$

Power losses in network may also be incorporated into the model. These mainly arise from power transmission over distances between energy hubs and can be accounted by multiplying with a coefficient of energy loss as a function of distance between the two energy hubs, as illustrated by Maroufmashat et al.[94].

3.8 Constraints

Different constraints have been imposed onto the model based on the limitations of energy resources, storage technologies as well as energy transfer between energy hubs. The underlying principle constraint for capacity of energy generation by each resource can be expressed as follows:

$$\gamma_{s,j,t} P_{s,j,t}^{min} \leq P_{s,j,t} \leq \gamma_{s,j,t} P_{s,j,t}^{max} \tag{3.41}$$

$$N_{tech}^{min} \leq \sum_j \gamma_{s,j,t} \leq N_{tech}^{max} \tag{3.42}$$

The minimum ($P_{s,j,t}^{min}$) and maximum ($P_{s,j,t}^{max}$) capacities are multiplied by a binary variable γ_j that can be used to limit the technologies available within each energy hub. This may be beneficial when assessing the impact of integrating a particular energy source or a number of energy sources within the energy hub and/or network. Almost all formulations of energy potential, presented in this work, are multiplied with an efficiency factor that is incorporated within the coupling matrix ($C_{i,j}$), present in Eqn. 3.30. These conversion efficiencies also differ based on the type of energy vector they are converted in (i.e. heat, electricity).

3.8.1 Grid

Electricity purchased from the grid is also subject to limits, based on quantity made available by grid-connected energy supplier(s) for the particular application and whether power grid connection exists in that energy hub *s*. This is expressed as follows:

$$\gamma_{s,grid,t} P_{s,j,t}^{min} \leq P_{s,grid,t} \leq \gamma_{s,grid,t} P_{s,grid,t}^{max} \tag{3.43}$$

3.8.2 Solar

In this framework, two types of solar technologies are considered: (i) solar photovoltaic (PV) and Concentrated Solar Power (CSP) parabolic trough technologies. Eqn. 3.44 and Eqn. 3.45 can be used to determine the energy generated from solar PV technology, based on available solar energy within the region and technical limitations. Eqn. 3.46 defines the areas occupied by the solar PV technology.

$$P_{s,PV,t} \leq Land_{s,PV} GHI_t PR_{PV} \tag{3.44}$$

$$\sum_t P_{s,PV,t} = N_{s,PV-module} CF_{PV} Power_{PV-module} PR_{PV} h_{PV} \tag{3.45}$$

$$Land_{s,PV} = 1.5 Area_{PV-module} N_{s,PV-module} \tag{3.46}$$

Similarly, Eqn. 3.46 and Eqn. 3.47 can be used to determine the energy generated from solar CSP parabolic trough technology, based on its limitations.

$$P_{s,CSP,t} \leq Land_{s,CSP} DNI_t PR_{CSP} \tag{3.47}$$

$$\sum_t P_{s,CSP,t} = N_{s,CSP-SCA} CF_{CSP} Power_{CSP-SCA} PR_{CSP} h_{CSP} \tag{3.48}$$

$$Land_{s,CSP} = 4 \times Aperture_{SCA} length_{SCA} N_{s,CSP-SCA} \tag{3.49}$$

In studies assessing PV and CSP potential, the energy potential calculation from these solar technologies includes a conversion efficiency term (often denoted by η)[113]–[117]. In this framework, as stated earlier, all conversion efficiencies are incorporated within the coupling matrix ($C_{i,j}$), presented in Eqn. 3.30. For Photovoltaic (PV) systems, $Land_{s,PV}$ denotes the total area covered by PV modules (i.e. area of each module multiplied with the number of modules installed) in a particular energy hub *s*. $GHI_{PV,t}$, refers to the Global Horizontal Irradiance amount falling per horizontal surface area in time period *t*, often expressed in kWh/m^2. Lastly, the Performance Ratio of PV system (PR_{PV}), as defined by Mahtta, Joshi and Jindal[114], is the ratio of field performance of the system to its performance in standard test conditions (i.e. 1000 W/m^2 solar radiation, 25^{o}C module temperature, and 1.5 air mass). Hence, accounting for losses due to temperature, inverter, AC and DC cables, weak radiation, dust, and all other types of losses.

In the case of Concentrated Solar Power (CSP) parabolic trough systems, $Land_{s,CSP}$ denotes the total solar field aperture area (i.e. the number of solar collector assemblies (SCA) multiplied by aperture area of each SCA) that may either include the reflective area and gaps, or the reflective area only[118]. DNI_t refers to the Direct Normal Irradiation (DNI) the CSP system is exposed to over a period of time *t*.

3.8.3 Wind

The electrical energy generated from n wind turbines (WT) in a year, in Wh, either onshore or offshore, can be determined using Eqn. 3.50 – 3.52[71], [119]:

$$P_{s,WT,t} \leq N_{s,WT} 0.5 \rho_{air} A_{swept} ws_{s,t}^3 h \qquad (3.50)$$

$$\sum_t P_{s,WT,t} = N_{s,WT} CF_{WT} Power_{WT} h_{WT} \qquad (3.51)$$

$$Land_{s,WT} = 5 N_{s,WT} {rotor_{WT}}^2 \qquad (3.52)$$

Onshore and offshore wind farms may differ in the wind speed ($ws_{s,t}^3$), in m/s, turbines are exposed to and the area swept (A_{swept}) by these installed turbines. This area, expressed in m^2, depends on the blade length of the turbine. In addition to that, the power coefficient that accounts for the maximum power captured by these wind turbines (CF_{WT}), all affect the wind energy potential [71], [120]. ρ_{air} represents the density of air, in kg/m^3, and h_{WT} represents the number of operating hours by the wind turbine in a time period *t*. The total amount of electrical energy generated from the wind turbines can be determined using the number of wind turbines installed, power rating of each wind turbines and its operating hours, as seen shown in Eqn. 3.51. $Land_{s,WT}$ represents the land occupied by the wind turbines, signifying each wind turbine needs to be placed approximately 5 rotor diameter apart, in order to avoid the wake effect.

The total land area occupied by the renewable energy technologies can be constrained based on the available area at the energy hub *s*, using the following equation.

$$\sum_s Land_{s,PV} + Land_{s,CSP} + Land_{s,WT} \leq Area_s^{max} \quad (3.53)$$

3.8.4 Hydro

Electrical energy generated from large or small hydro plants, in Joules, may be calculated using Eqn. 3.54[121].

$$P_{s,hydro,t} = \rho_{water} g head_{hydro,t} v_{hydro,t} h \quad (3.54)$$

ρ_{water} represents the density of water, in kg/m3, while g is the acceleration due to gravity, in m/s^2. $head_{hydro,t}$ and $v_{hydro,t}$ refers to the pressure head, in m, (i.e. distance the water will fall on its way to the turbine-generator) and flow of water stream, in m^3, respectively.

3.8.5 Geothermal

Geothermal power plants are relatively less efficient compared to other fossil fuel-based and nuclear power stations[122]. However, fluctuating oil prices and increasing carbon emissions has increased significantly in the last decade[123]. Generally, there are two basic approaches in using geothermal: (i) hydro-geothermal and (ii) hot dry rock[124]. In the former approach, hot water is present within reservoirs and heat is extracted from it. In the latter case, water is pumped into hot plutonic rocks under high pressure which is heated underground[124]. It is, then, returned through a second bore for the energy transfer process. Geothermal maps are available that contain data regarding geothermal power potential, in W/m^2. It may be multiplied by the area of the geothermal field from which energy is extracted. Eqn. 3.55 serves as a basic equation in order to estimate the geothermal energy flow, in kWh, from a particular field[122], [123], [125]. Other complex methods exist in literature that use data pertaining to rock properties (e.g. porosity, permeability, etc.) in order to calculate the geothermal energy flow[126].

$$P_{s,geothermal,t} = \dot{m}_t \Delta H_t h \qquad (3.55)$$

m_t is the mass flow rate of the heat transfer fluid, in kg/s, and ΔH_t is the change in enthalpy, in kJ/kg, during time period *t*. The generated power may be subtracted with any parasitic load within the process (e.g. pump) to calculate the net energy. For calculation of heat and/or electricity generation potential via geothermal energy, the change in enthalpies across a condenser and/or turbine need to be considered, respectively.

3.8.6 Biomass/fuel, fossil fuel and nuclear energy

For different biomass and fossil fuel based energy generation plants, the available energy in period *t* from energy hub *s* may be calculated using the heating value of the fuel for energy source j, usually the lowest heating value (LHV_j), and the quantity of fuel available, mass or volume, as seen in Eqn. 3.56 and Eqn. 3.57, respectively[94].

$$P_{s,j,t} = m_{s,j,t}^{fuel}\text{LHV}_j \quad \forall j = Biomass, Coal, Nuclear \quad (3.56)$$

$$P_{s,j,t} = V_{s,j,t}^{fuel}\text{LHV}_j \quad \forall j = Natural\ gas, Oil \quad (3.57)$$

These fuels are consumed by either CHP to produce electricity and heat or by the boiler(s) for heat production only for consumption by processes within energy hub *s*. The coupling matrix ($C_{i,j}$) includes efficiencies based on the type of technology involved. On the other hand, the amount of the fuel consumed may be limited based on its supply to an energy hub *s* at time period *t*. Hence, Eqn. 3.58 and Eqn. 3.59 may be used to define these limits.

$$\gamma_{s,j.t} m_{s,j,t\ min}^{fuel} \leq m_{s,j,t}^{fuel} \leq \gamma_{s,j.t} m_{s,j,t\ max}^{fuel} \quad \forall j = Biomass, Coal, Nuclear \quad (3.58)$$

$$\gamma_{s,j.t} V_{s,j,t\ min}^{fuel} \leq V_{s,j,t}^{fuel} \leq \gamma_{s,j.t} V_{s,j,t\ max}^{fuel} \quad \forall j = Natural\ gas, Oil \quad (3.59)$$

It is possible that both technologies (i.e. CHP and boiler) are considered for optimization purposes; thus, Eqn. 3.60 may be used to constraint the total amount of energy available.

$$P_{s,j,t}^{CHP} + P_{s,j,t}^{boiler} \leq P_{s,j,t}^{max} \ \forall j = biomass, natural\ gas, coal, oil, nuclear \quad (3.60)$$

Chapter 4 Optimal Renewable Energy Integration within the Upstream Oil Supply Chain (USOSC) Network[3]

4.1 Introduction

Crude oil has been contributing to about 40% of global energy since 1980 [127]. Despite the advancement in technology, a persistent decline has been observed in the energy return on energy invested (EROEI) for crude oil and other fossil based fuels [21]. Consequently, resulting in increasing emissions of greenhouse gases (GHG) that have adverse effects on human health and the environment [2].

A study on Abu Dhabi, one of the world's largest energy producer through fossil fuels, showed that more than 55% of its energy was consumed by the industry sector in 2010[20], [128]. More than 30% of that grid-connected energy was expended by Abu Dhabi National Oil Company (ADNOC). Furthermore, it has been forecasted to exceed 2000 GWh/year by 2020 [20]. Yet, this does not include energy consumption through off-grid energy sources. Since the most abundant and 'cleanest' renewables are intermittent sources of energy (i.e. solar, wind), a major challenge that exists in integrating these renewables into the electricity grid is maintaining grid reliability [129]. Yet, there exist possibilities of integrating renewable energy sources to existing energy-related industries that require enormous amounts of energy to generate them (i.e. oil and gas) [8].

[3] A variant of this chapter is submitted for publication: S. Taqvi, A. Elkamel, A. Almansoori, "Optimal Renewable Energy Integration within the Upstream Oil Supply Chain (USOSC) Network: A Case Study on Abu Dhabi, UAE".

Therefore, a need arises for developing a model for optimally integrating potential renewable energy sources into the upstream oil supply chain (USOSC).

Different comprehensive review studies have been conducted on multi-energy systems (MES), outlining various strategies for modelling MES including Virtual Power Plants (VPP), micro-grids, integrated energy systems, energy hubs (EH), intelligent power grids and various others [50], [83], [130]–[132]. Among the above mentioned strategies, the energy hub approach, introduced by Geidl and Andersson[30], was regarded as "the most elegant way to describe energy flows in a synthetic way"[130]. Mancarella[130] also stated its ability to model other aggregation concepts such as VPP and micro-grids through it. Buehler studied the integration of renewables into these energy systems and discussed how the energy hub approach should be used to enhance virtual power plants and micro-grids[50].

From the literature surveyed, a study was found, presenting different renewable energy systems that have been installed in the oil and gas industry in various parts of the world[133]. However, a research gap was identified in the area of modelling and optimization for renewable energy integration within the oil or gas supply chain. Thus, this paper aims at developing a generic framework for the optimal integration of renewable energy within the upstream oil supply chain (USOSC) whilst considering economic and environmental gains, using the multi-energy hub approach. In addition, a case study on Abu Dhabi is carried out to demonstrate the application of the developed model.

4.2 Upstream Oil Supply Chain (USOSC)

Oil sector deals with exploration and production of petroleum, refining of petroleum, and distribution of petroleum products. Upstream operations involve crude petroleum extraction through oil wells, oilfield processing and pipeline transportation of crude oil to refineries and/or shipping terminals. All the previously mentioned operations exhaust remarkable amount of energy and contribute significantly to GHG emissions through different mechanisms[19], [134]. Information related to each oilfield is often classified as confidential and is challenging to acquire. However, several studies have been carried out in order to assess the energy expended in each sector in the USOSC. These studies have reported the Energy Return on Energy Investment (EROEI or EROI) which, as the name implies, is a ratio of the total energy input to the total energy output, for a particular process/industry. According to Gagon et al., the global EROEI reported in 2006 for crude oil was 18 [21]. However, EROEI of oil producing countries has been reported to be much greater. For example, the EROEI value reported for Saudi crude was 40[135], [136]. In addition, it was found that 68% of the expended energy was used in the crude oil extraction whilst the remaining was used for oilfield processing [21]. In all, energy consumption within the USOSC can be classified by sectors: extraction, processing and transport.

4.2.1 Crude Petroleum Extraction

According to statistics, global onshore petroleum production was 1.7 times greater than offshore production in 2010[137]. Onshore and offshore facilities act similarly as onshore gathering stations exist where crude petroleum is collected from each of these platforms and processed before transporting it to an onshore processing facility[138]. However, offshore production is much more challenging than onshore due to its remote nature and relatively harsh environment[138]. A platform needs to be installed above sea level with adequate utilities (i.e. electricity, water) to support operations as well as meeting staff requirements. In addition, due to the limited space available and in cases of no direct pipeline connection, crude oil is often stored in the base and tankers are employed for the transportation of crude oil[138]. The entire offshore structure is also exposed to a more corrosive environment. On the other hand, onshore sites often have access to utilities, ample storage space and/or pipelines that can transport extracted petroleum to a central processing facility via collection platforms (CP).

The design and types of operations that occur on the wellhead are dictated by the geographical location of the well and the production flow rate[139]. If there are several wells together in the same field, production may be beneficial through a gathering system to a central processing facility. Otherwise, each well may have its own wellhead processing facility[139]. For offshore platforms, it is favorable to do as little processing onsite due to the limited platform facilities as well as high cost associated with it[139]. However, minimal processing needs to be carried out, separating water and solids from petroleum crude, to prevent fouling in process equipment and/or pipeline[138]. There are, though, presence of large ships with processing facilities on board, known as floating production system (FPS), being used since 1970s[138]. They are capable of separating crude oil from water and solids, for transportation and further processing. Innovative technologies, over time, have improved the economics of these offshore operations[138]. High power electric submersible pumps (ESPs), effective heat management systems and compact separation systems have contributed positively towards economic oil production[138].

4.2.2 Oilfield processing

There are several processes that take place after oil has been extracted from the petroleum reservoirs. Figure 4.1 outlines all the major processes that take place in the USOSC. As stated earlier, these processes may take place at the wellhead or may be carried out at a central processing facility, depending on the nature of the process and the availability of resources at the wellhead. Yet, crude needs to undergo sufficient treatment, after extraction from the well, for effective transportation.

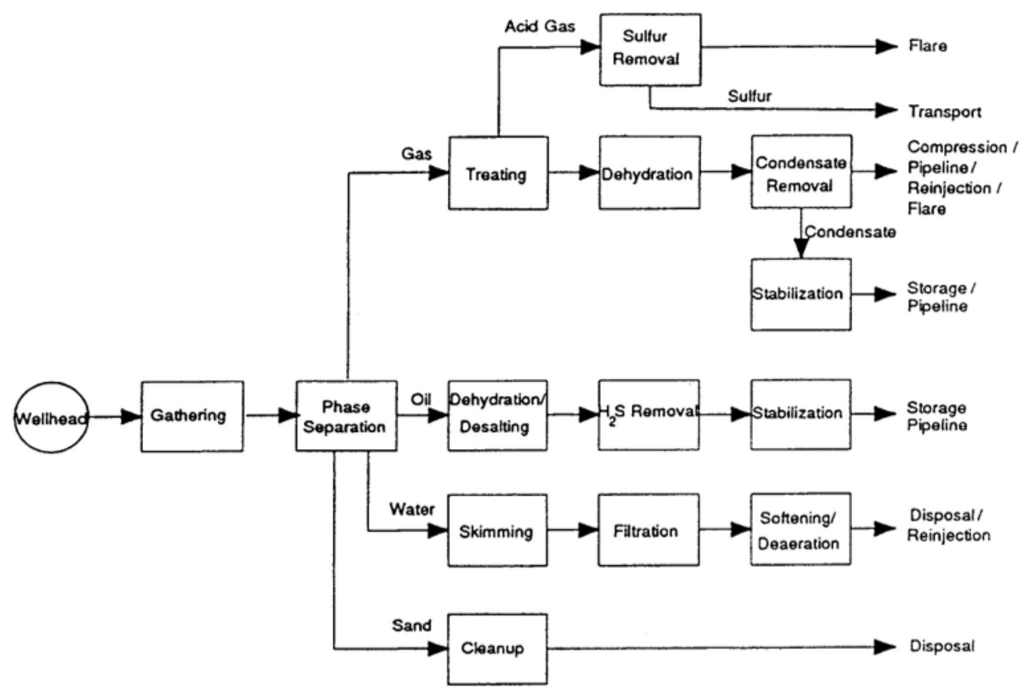

Figure 4.1 Typical oilfield processing scheme in the upstream supply chain (Adopted from Manning and Thompson[139]**)**

4.2.3 Transportation

Transportation of crude oil, after processing, is mainly done through pipelines. Tankers (offshore) and/or diesel trucks (onshore) are used in the case where no pipeline connection exists, as stated earlier. Crude oil is either transported to the local refinery for domestic use and/or to shipping terminals to be exported to other countries. For transportation via pipelines, pumping stations are strategically built at specific locations between the crude oil processing facility and the refinery/shipping terminal.

4.2.4 CO_2 emissions in USOSC

According to a study, CO_2 emissions generated in Upstream Oil Supply Chain (USOSC) processes account up to 20-30% of total emissions[140]. There are mainly two sources of GHG emissions in the upstream operations of the oil industry. These include combustion and non-combustion sources along the operation chain. Fossil fuels such as diesel and fuel oil in combustion engines represent the first category as major emitters of CO_2. They are used extensively to operate internal combustion engines, process heaters, and to produce steam. Additionally, diesel fuel is used for off-road transportation. Flaring, as a continuous operation or as an emergency measure to control the pressure within equipment, is another source of CO_2 emissions.

A study conducted on Arab Medium crude oil found that processes in the drilling sector, such as water re-injection, lifting, gas re-injection, and flaring, emit 2.19 g of CO_2 per MJ of energy[141]. The processing (also referred to as production) sector emits 1.04 gCO_2/MJ while the emission from the transport sector is about 0.475 gCO_2/MJ[141]. Moreover, the emissions due to losses in the USOSC are 0.14 g CO_2/MJ[141]. The overall emissions due to drilling, processing, transportation and losses within the USOSC are 57%, 27%, 12.5% and 3.5% respectively[140]. It needs be emphasized that the multi-pollutants emissions generated from oil operation demands a comprehensive engineering approach since estimating these emissions is very challenging. The challenges include limited availability of data and high uncertainty associated with the methodologies used in calculations[19].

Even though the oil industry is one of major emitters of carbon dioxide, it is also the major consumer of it. More than 62% of CO_2 captured from large point sources is consumed for Enhanced Oil Recovery (EOR) purposes [142]. There are several different on-going and completed projects that aim to employ Carbon Capture and Storage (CCS) technologies and pump captured carbon dioxide into oil reservoirs to increase produced oil[143]. Other modern approaches exist that suggest to increase storage of CO_2 within these oil reservoirs to yield positive economic and environmental outcomes, increasing profit and mitigating carbon emissions, respectively[144].

4.3 Model Framework

The proposed model framework, for integrating renewable energy within the upstream oil supply chain, is based on the general superstructure, as seen in Figure 3.1. The oil supply chain is modeled as a standard pooling problem to allow changes in flowrate, based on the optimization criteria. All nodes within the supply chain network are modelled as energy hubs. EH_{nm} represents an energy hub representing the m^{th} unit at the n^{th} level within a supply chain. In the USOSC problem, level 1 energy hubs (sources) represent the crude oil production platforms, onshore and offshore. Energy hubs within level 2 (pools) represent collection platforms that gather crude oil coming from different production platforms. Level 3 energy hubs represent onshore treatment facilities (terminal) where crude oil processing takes place. Further levels may be defined that include pumping stations, refineries and/or shipping terminals. Energy hubs may be interconnected with each other in order to facilitate energy transfer. Moreover, as shown in the superstructure, each of the energy hubs have access to energy resources that help meet effective demand of each unit.

4.3.1 Objective Function

The optimization criteria considered in this study is the economic profit and the carbon dioxide emissions. Thus, the objective functions are formulated based on these standards, maximizing profit and minimizing emissions. The total economic profit (z) is defined as:

$$z = Revenue - (CE^T + CS^T + C_{CCS}^T + C_{CC\&T}^T) \quad (4,1)$$

The total economic profit is the difference between the revenue generated from the sale of crude oil and total costs incurred. Since the price of crude oil ($Price_t$) fluctuates with time, the revenue generated is calculated by the summation of the product of price of crude oil and flowrate ($Flow_t$) across all time intervals, as expressed by Eqn. 4.2.

$$Revenue = \sum_t Flow_t Price_t \quad (4.2)$$

The costs, in the profit objective function include the total cost of energy (CE^T), the total cost of energy storage (CS^T), the total cost of carbon capture and injection to the oil reservoir (C_{CCS}^T) and the total cost of carbon trade ($C_{CC\&T}^T$). CE^T may either be formulated as the sum of capital costs, operating costs and fuel costs, or in terms of levelized cost of energy (LCOE), aka levelized energy cost (LEC) which encompasses all these factors. Data pertaining to these factors are often reported in literature as a unit of energy or power [9], [104]–[106]. Different formulation for LCOE, varying on the level of detail or specific to a particular energy source, can also be found in literature [106], [108]–[110]. CS^Tcan be calculated in a similar manner, either using individual cost elements or using a levelized formulation[111].

The total CCS cost (C_{CCS}^{T}) comprises of costs related to the capture, transport and injection of carbon emissions into the reservoir. Different carbon capture technologies exist that vary in terms of the amount of carbon emissions they capture and their costs [112]. Moreover, transport costs depend on the volume of CO_2 and the distance over which it is transported. In this study, captured emissions are injected into the reservoir for EOR; thus, there are associated injection costs and no storage costs. It is possible though, CO_2 is temporarily stored on-site before injection. Therefore, that cost may also be considered.

The total cost of carbon trade ($C_{CC\&T}^{T}$) is the profit realized or the cost incurred by selling or buying carbon dioxide emissions, respectively. It can be expressed using Eqn. 4.3.

$$C_{CC\&T}^{T} = \sum_{t} Ctrade_t Price_t^{carbon} \tag{4.3}$$

The amount of carbon emissions traded ($Ctrade_t$) can be determined, using Eqn. 4.4, by the difference between the carbon emissions and the limit set by regulating authorities, at time t. $Ctrade_t$ may either be positive or negative depending on whether carbon emissions were below or above the defined limit , respectively, set by the governing authorities

$$Ctrade_t = Lim_t^{carbon} - g_t \tag{4.4}$$

On the other hand, the total amount of carbon dioxide emissions, expressed by Eqn.4.5, accounts for emissions from energy generation sources (i.e. $CO2_{s,j}$), in the form of energy vector j, as well as emissions from processes within the USOSC (i.e. $CO2_{s,i}$).

$$g^T = \sum_t g_t = \sum_t \sum_s \left(\sum_j P_{s,j,t} CO2_{s,j} + \sum_i OE_{s,i,t} CO2_{s,i} \right) \qquad (4.5)$$

In different scenarios involving carbon cap-and-trade (CC&T) and carbon capture and injection, multi-objective analysis is conducted using modified epsilon constraint method; where economic profit is posed as the governing objective function and CO_2 emissions, as the constraint.

4.3.2 Constraints

The proposed objective function is subjected to several constraints pertaining to the standard pooling problem and the energy hub formulation. Constraints related to energy generation technologies, energy hub storage and networking, CC&T and CCS, discussed earlier, are also included in this model.

4.3.2.1 Pooling

In this study, the upstream oil supply chain (USOSC) is posed as a standard pooling problem where no flow between pools is considered. Complexity of the pooling problem may be increased when considering pool-pool flows; converting the MILP to an MINLP problem.

The mass balance between the sources (i.e. production platforms) and the pools (i.e. collection platforms) can be expressed in the following manner:

$$FPT_{pool,terminal,comp,t} = \sum_{source} (1 + EOR_{source,t}) FSP_{source,pool,t} VS_{source,comp} \tag{4.6}$$

$FPT_{pool,terminal,comp,t}$, in Eqn.4.6, represents the flow from the collection platforms to the treatment facility with a particular composition, $comp$, in a particular time period, t. Whereas, $FSP_{source,pool,t}$ represents the flow from the production platforms to the collections platforms in a particular time period t. $VS_{source,comp}$ represents the quality or composition of the crude oil at the production platform while EOR is the ratio of incremental oil produced to the total flow, as a result of CO_2 injection, for each source at time, t.

The supply of crude oil from production platforms, onshore or offshore, can be constrained by the limitations of their reserves. This can be expressed by Eqn. 4.7.

$$Source^{min} \leq (1 + EOR_{source,t}) FSP_{source,pool,t} \leq Source^{max} \tag{4.7}$$

Additionally, the flow between the sources and pools is also subjected to the limitations of the existing infrastructure (i.e. pipeline capacity), as seen in Eqn. 4.8.

$$FSP^{min} \leq (1 + EOR_{source,t}) FSP_{source,pool,t} \leq FSP^{max} \tag{4.8}$$

In order to ensure that crude oil, reaching the terminal, meets the terminals' requirements, Eqn.4.9 presents the respective constraint. The terminal may be a treatment facility which can handle crude oil of a certain composition, dictated by its technological limitation. On the other hand, if adequate oil processing is considered at each individual production platform, the terminal may represent client requirements (i.e. refinery, export oil quality). In either case, the following constraint will suffice.

$$\sum_{pool}\sum_{comp} FPT_{pool,terminal,comp,t} VT_{terminal,comp} \geq \sum_{pool} FPT_{pool,terminal,comp,t} \tag{4.9}$$

Furthermore, the total crude oil production is subjected to the minimum and maximum demand, as expressed in Eqn. 4.10.

$$Demand_t^{Min} \leq \sum_{pool}\sum_{terminal}\sum_{comp} FPT_{pool,terminal,comp,t} \leq Demand_t^{Max} \tag{4.10}$$

4.3.2.2 Energy Hub

Energy hubs, in this study, can be modeled using the following equation.

$$L_{s,i,t} = \left(C_{i,j} P_{s,j,t}\right) + \sum_q Q^{dis}_{s,q,i,t} - Q^{ch}_{s,q,i,t} \tag{4.11}$$

$L_{s,i,t}$ represents the output load (i.e. energy demand) at the energy hub site, $P_{s,j,t}$ represents the energy generated by different conversion technologies and $Q^{ch}_{s,q,i,t}$ and $Q^{dis}_{s,q,i,t}$ represent the energy stored and utilized from the storage technologies, within the energy hub.

In order to satisfy the required energy demand and allow energy transfer within energy hubs, the following constraint is formulated. The '=' sign may be replaced with '≥' sign to allow for the production of excess energy. This may prove to be useful in cases where a particular technology may generate more than one *i* energy vectors (i.e. CHP) and producing excess energy may be found to be optimal, based on the optimization criteria.

$$L_{s,i,t} = OE_{s,i,t} + \sum_{b \in S-s} T_{s,b,i,t} \alpha_{s,b} \quad (4.12)$$

$OE_{s,i,t}$ represents the energy demand by energy hub *s* in the form of energy vector *i* at time *t*. This energy demand is expressed for energy hubs for sources, pools and terminals by Eqns. 4.13, 4.14 and 4.15, respectively.

$$OE_{source,i,t} = \frac{Dem_{source,i,t} FSP_{source,pool,t} CV}{EROI} \quad (4.13)$$

$$OE_{pool,i,t} = \frac{Dem_{pool,i,t} \sum_{comp} FPT_{pool,terminal,comp,t} CV}{EROI} \quad (4.14)$$

$$OE_{terminal,i,t} = \frac{Dem_{terminal,i,t} \sum_{comp} FPT_{pool,terminal,comp,t} CV}{EROI} \quad (4.15)$$

$Dem_{s,i,t}$ represents the energy demand by each site (i.e. source, pool, terminal) in the form of energy vector *i* at time *t*. CV, the energy content within a barrel of crude oil, is used for conversion purposes.

$T_{s,b,i,t}$ is energy transferred from energy hub *s* to *b* if a connection, $\alpha_{s,b}$, exists between them. Eqn. 4.16 may be used to define limits of energy that can be transferred from one energy hub to another.

$$T_{s,b,i,t}^{min} \leq T_{s,b,i,t} \leq T_{s,b,i,t}^{max} \quad (4.16)$$

4.4 Abu Dhabi Case Study

In order to assess the applicability of the proposed multi-energy hub model, it is applied to a case study on a USOSC problem in Abu Dhabi. 10 production platforms (P: 8 onshore/ 2 offshore), 4 collection platforms (CP), 1 central treatment facility (F), and two pumping stations (PS) were considered. These nodes and assumed existing connections between them are depicted in Figure 4.2.

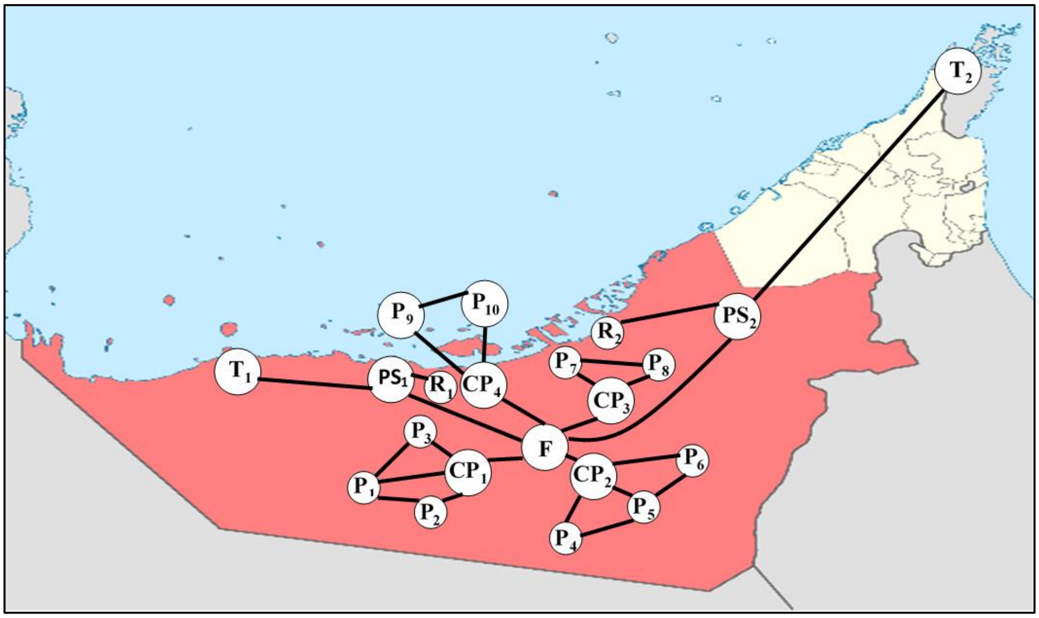

Figure 4.2 USOSC network considered for Abu Dhabi Case Study

Figure 4.3 shows the superstructure for the renewable energy integration application to this Upstream Oil Supply Chain (USOSC) problem. Solar and wind are the only renewable sources considered in this case study. For this case study, 300W Suntech Hypro monocrystalline 60-cell modules were considered for solar PV technology whereas Abengoa Solar Astro collectors with Flabeg RP3 parabolic trough mirror were considered for solar CSP technology. These models were selected since they have already been employed in PV and CSP plants in Abu Dhabi[145], [146]. For generating electricity from wind energy, Honeywell WT6500 small wind turbines were considered due to low wind speed in the region. On the other hand, the available land for the installation of renewable energy technology was assumed to be 5% of each site area.

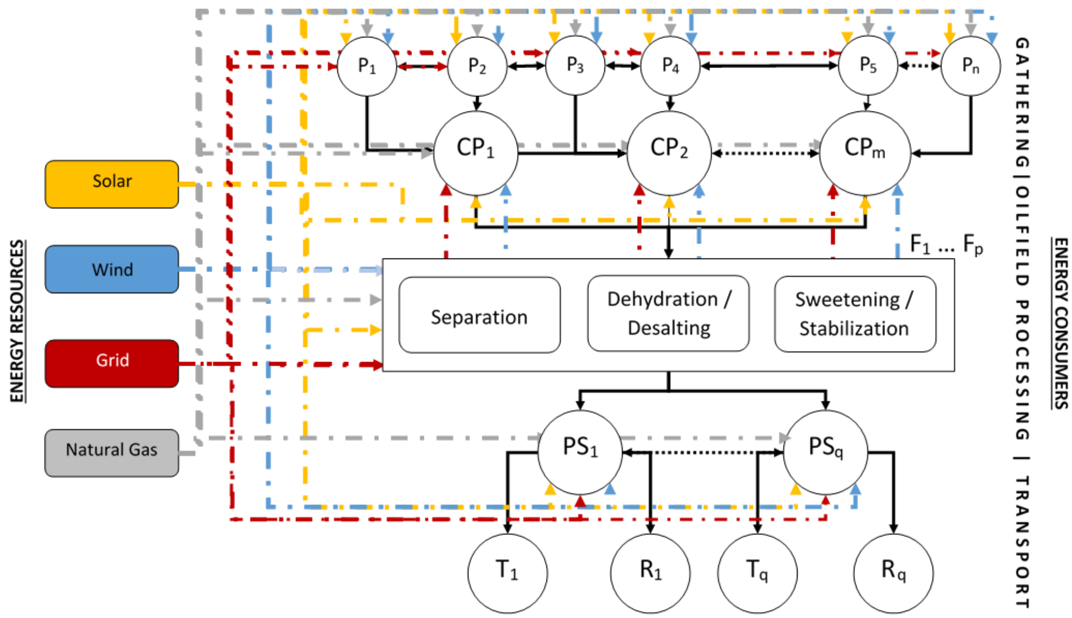

Figure 4.3 General superstructure depicting the energy consumers within the USOSC and potential energy resources

P represents the production platforms that extract crude oil from the reservoirs. These platforms could be onshore or offshore, depending on the oil field. CP represents a collection platform where crude oil is gathered and transported to the treatment facility, F. After crude oil has been treated (i.e. separation, dehydration/desalting, sweetening/stabilization), it is sent to pumping stations, PS. These pumping stations transport the treated crude oil to shipping terminals (T) and refineries (R). Crude oil transported to the shipping terminals are stored on-site until exported to other countries. On the other hand, crude oil sent to refineries for further processing for local consumption. However, this falls under the downstream oil sector and not within the scope of this study. Hence, there are no connections of energy transfer between T and R, and energy producers.

Each unit (i.e. P, CP, UN, PS, R, T) requires energy in order to carry out the particular processes and pose as energy consumers. The energy suppliers are the represented by the shaded shapes in Figure 4.3. These include all possible sources of energy, renewable and non-renewable, which can be analyzed in this study. Solar PV and Solar CSP represent electricity generated through solar energy, collected using photovoltaic and concentrated solar power technologies, respectively. Wind includes energy provided from onshore and offshore wind fields. Grid is the electricity provided to the energy consumers through the power stations or through on-site generators. These grid connected energy generation sources are commonly fueled by fossil fuels, namely natural gas and diesel, as assumed in this study.

Figure 4.4 shows the proposed energy hub to represent the nodes (i.e. P, CP, F, PS), as outlined in the superstructure.

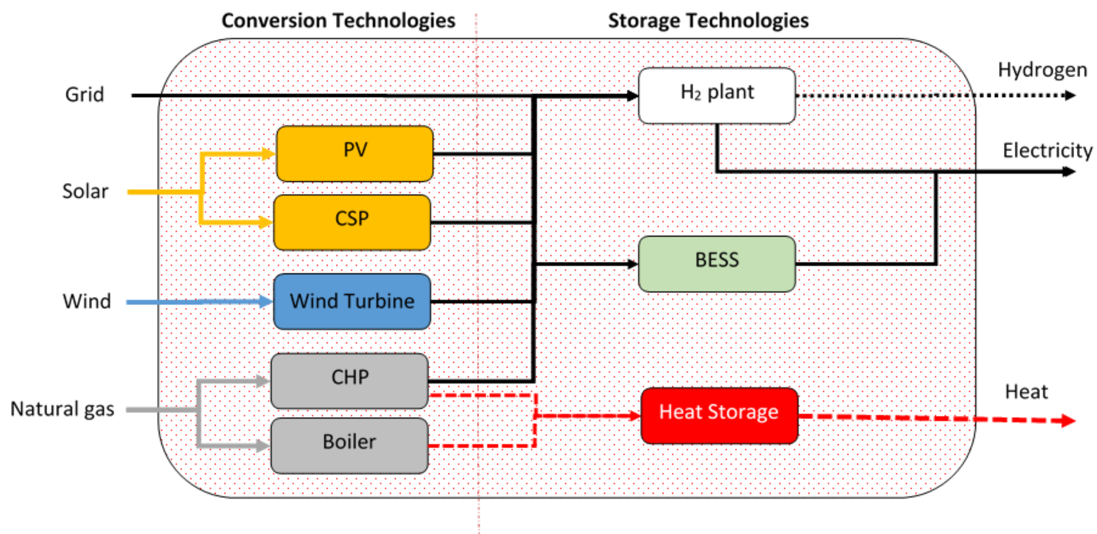

Figure 4.4 Proposed energy hub to represent energy nodes within the Upstream Oil Supply Chain problem

As seen in Figure 4.4, multiple renewable and non-renewable energy vectors enter the energy hub and are converted to electricity and/or heat using respective conversion technologies. Photovoltaic (PV) and Concentrated Solar Power (CSP) are considered for generation of electricity using solar energy. In addition, Combined Heat and Power (CHP) technology, exists within the proposed energy hub, to produce electricity and heat from natural gas. In this study, no energy storage technologies are considered.

4.5 Results and Discussion

Different scenarios were considered in this case study. The following sections discusses of each of these scenarios and presents the major findings from them.

4.5.1 Energy generation

In this scenario, different energy technologies were considered, based on availability within the region, for maximizing profit and minimizing carbon dioxide emissions. These results, along with the required number of equipment for each case, are shown in Figure 4.5 and Table 4.1, respectively. Figure 4.6 presents the profit and carbon emissions seen for different crude oil production. Additionally, Table 4.2 shows the total land utilized by RE technologies for each case.

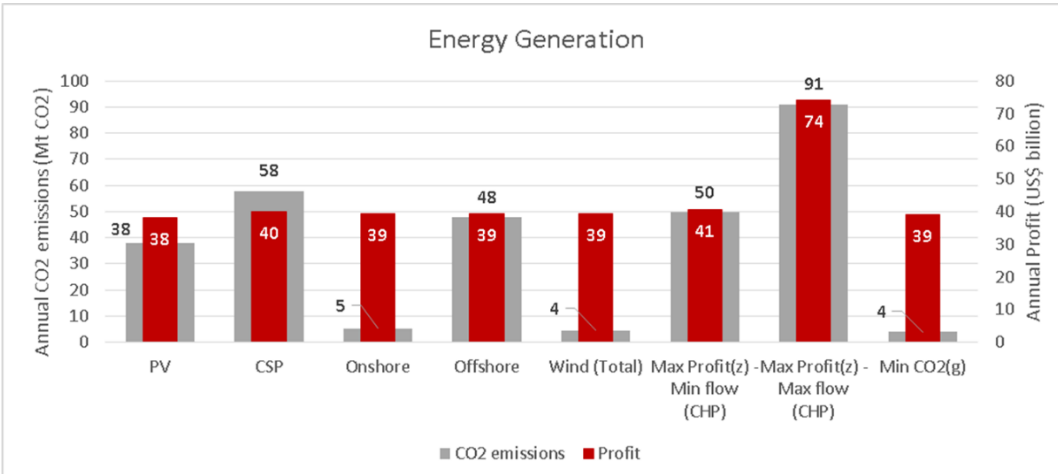

Figure 4.5 Profit and CO_2 emissions observed annually for each of the energy generation technology configurations

Table 4.1 Energy distribution for each of the different energy generation technologies configuration shown in Figure 4.5

Case	PV	CSP	Wind	CHP El.	CHP Heat	Grid	Boiler	PV Mod	SCA	WT	Natural Gas
	TWh										bcf
Minimum Flow Rate = 1.5 MMbbl/d											
Max Profit	0.00	0.00	0.00	5.78	8.25	18.47	0.00	0	0	0	144.33
Min CO_2	5.19	~0	13.28	5.78	8.25	0.00	0.00	113825200	1	7487928	144.33
PV	10.68	0.00	0.00	0.00	0.00	13.57	8.25	234076200	0	0	102.56
CSP	0.00	2.65	0.00	0.00	0.00	21.60	8.25	0	163850	0	102.56
Wind (Onshore)	0.00	0.00	23.89	0.00	0.00	0.36	8.25	0	0	13468430	102.56
Wind (Offshore)	0.00	0.00	7.07	0.00	0.00	17.18	8.25	0	0	3985025	102.56

Wind (Total)	0.00	0.00	24.25	0.00	0.00	~0	8.25	0	0	13670580	102.56
CHP	0.00	0.00	0.00	5.78	8.25	18.47	0.00	0	0	0	144.33
Maximum Flow Rate = 2.7 MMbbl/d											
Max Profit	0.00	0.00	0.00	10.60	15.15	33.88	0.00	0	0	0	265.00
Min CO_2	4.70	0.00	29.18	10.60	15.15	~0	0.00	103069400	0	16448140	265.00
PV	10.68	0.00	0.00	0.00	0.00	33.80	15.15	234076200	0	0	188.26
CSP	0.00	2.65	0.00	0.00	0.00	41.83	15.15	0	163850	0	188.26
Wind (Onshore)	0.00	0.00	37.31	0.00	0.00	7.17	15.15	0	0	21031820	188.26
Wind (Offshore)	0.00	0.00	7.07	0.00	0.00	37.41	15.15	0	0	3985025	188.26
Wind (Total)	0.00	0.00	44.38	0.00	0.00	0.10	15.15	0	0	25016740	188.26
CHP	0.00	0.00	0.00	10.60	15.15	33.88	0.00	0	0	0	265.00

The least amount of CO_2 was emitted, in the presence of all technologies, when *g* (i.e. CO_2 emissions objective function) is minimized. The model does this by increasing the use of renewables and reducing the crude oil flow rate. As less crude oil is produced, less energy is required by the industrial processes and less energy demand needs to be met by the energy sources. Thus, for this case, no grid-connected electricity was consumed. The renewable energy share observed was about 76%, of which 21% was contributed by solar PV technology and the remainder by onshore (53%) and offshore (2%) wind farms. In addition, the annual profit accumulated was about $39.8 billion, as evident from Table 4.1, for an average daily production of about 1.5 million barrels of crude oil. For this level of production, about 65% of available sites area was occupied by RE technologies. The utilized of land increased to about 88% when the daily production of crude oil increased to 2.73 MMbbl, yielding a profit of $71.3 billion. The increase in the amount of CO_2, due to this increase in production, was 3.27 Mt.

On the contrary, for the maximum profit case, all energy consumption resulted from fossil-based sources, namely grid and CHP, yielding the highest amount of CO_2 emissions. CHP was found to meet the entire heat requirement by the upstream oil supply chain, as evident from Table 4.1. Since the production of excess energy was restricted in this study, CHP partially fulfills electricity demand by the USOSC. The annual profit was observed to be $40.63 billion for an average daily production of 1.50 MMbbl. As the daily production increases to 2.73 MMbbl, the annual profit increased by about $33 billion. Furthermore, the additional volume of natural gas consumed, in order to meet this change in energy demand, is 121 bcf. The increase in CO_2 emissions, due to this increase in production, was 41.14 Mt, as evident from Figure 4.6.

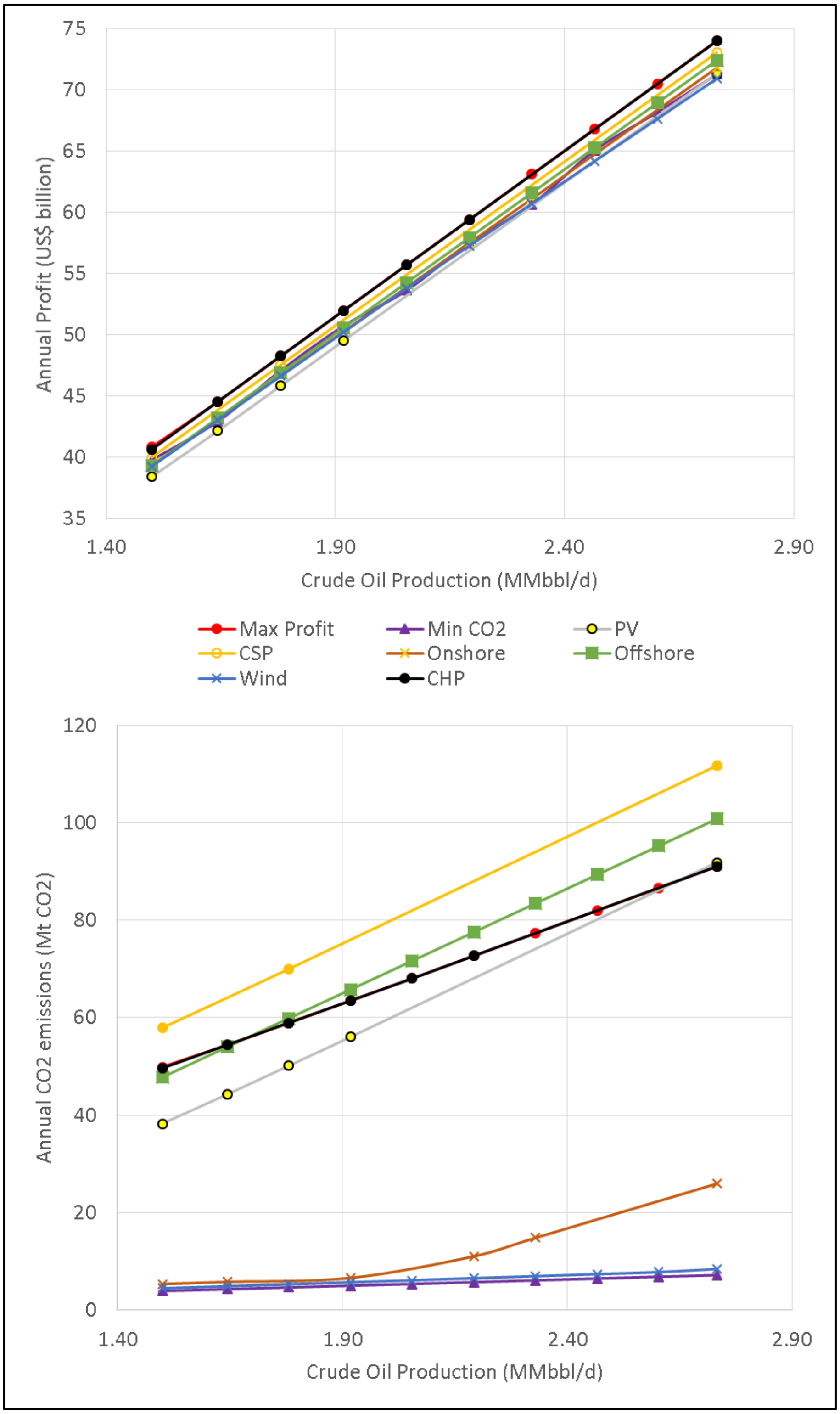

Figure 4.6 Annual profit and CO_2 emissions observed for different crude oil production

For the renewable energy (RE) cases within this scenario, the CO_2 emissions objective function was minimized while isolating each particular RE technology. The least carbon emissions were observed when small wind turbine technology was utilized. In this case, about 99% of electricity was met by onshore wind farms. As seen from Table 4.2, about 40% of available land (i.e. reserved for installation of RE technology) was utilized by 13.5 million onshore small wind turbines. The profit realized for this configuration was recorded to be about $39 billion for an average crude oil production of 1.5 MMbbl/d. In contrast, for an average daily production of 2.73 million barrels of crude oil, whilst utilizing onshore farms, the profit is found to be $71.8 billion while emitting about 26 Mt of CO_2. Moreover, about 62.5% of available land is occupied by 21 million small wind turbines. Observing the change in profit and emissions of onshore wind farm in Figure 4.6, it can be seen that there is a steady increase in profit with an increase in crude oil production. However, carbon emissions experience a sudden rise once crude oil production goes beyond 1.90 MMbbl/d. This increase results from the increase in the contribution of electricity by grid-connected energy, resulting in a higher volume of carbon emissions, also seen in Table 4.1.

For the remaining renewable technologies (i.e. solar PV, CSP and offshore wind), there is no additional occupancy land observed with an increase in crude oil production. This is because these technologies had reached their maximum potential, given the limitations that have been defined. For example, in the case of solar PV and CSP, it must be understood that these installations are sufficient to meet the hourly demand of the USOSC only when solar energy is available. In order to maximize their utilization, energy storage technologies need to be considered. As evident from Table 4.1, the electricity generated by these sources has been the same, at minimum and maximum crude oil production. The remainder electricity demand is met by grid-connected energy. For all these remaining technologies, the increase in profit and emissions is about $33 billion and about 53 Mt, respectively, when crude oil production increases from 1.5 MMbbl/d to 2.73 MMbbl/d.

Table 4.2 Land occupied by renewable energy technology configurations

Case	**Min Flow Rate**		**Max Flow Rate**	
	Area (km2)	**% Used**	**Area (km2)**	**% Used**
PV	491.56	88.16	491.56	88.16
CSP	491.55	88.16	491.56	88.16
Wind (Onshore)	223.06	40.01	348.33	62.47
Wind (Offshore)	66.00	11.84	66.00	11.84
Wind (Total)	226.41	40.61	414.33	74.31
Min CO2 (g)	363.05	65.11	488.86	87.67

Table 4.2 shows the land utilized when employing renewable energy technology configurations to meet refinery energy requirements. As stated earlier, the available land onsite for installation of renewable technology was 6 km^2. However, we see that a maximum of about 12% was utilized; implying additional land is available to meet increased demand.

4.5.2 Carbon Capture and Storage

The CCS scenario was considered to investigate the impact of employing a carbon capture and storage (CCS) technology on annual profit and emissions. As discussed in the earlier sections, captured CO2 emission were injected into the oil reservoir for EOR. Figure 4.7 presents the annual profit and carbon emissions that result from carbon capture and injection.

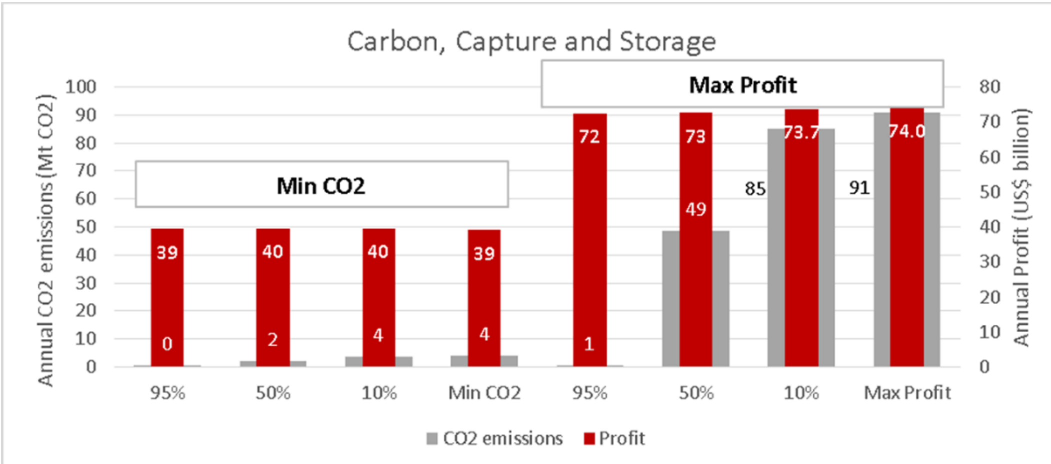

Figure 4.7 Profit and carbon dioxide emissions resulting annually from different amounts of CCS

For the maximum profit cases, also the maximum crude oil production (i.e 2.73 MMbbl/d), the highest profit was realized when no CCS technology is employed. As more carbon emissions are captured and injected into the reservoir, a higher cost is observed, resulting to a decrease in profit by about $281 million whilst capturing and injecting 5.93 Mt of CO_2. For these cases, the total cost of carbon capture, transport and injection are higher than the profit gained due to the incremental production of EOR. However, for the minimum CO_2 cases (i.e. 1.5 mmbbl/d crude oil production), the lowest profit was observed for the case where no CCS technology was employed. In contrast, the highest profit was observed when 10% of carbon emissions were captured and injected into the oil reservoir. Comparing both cases, 10% CCS mitigated 0.25 Mt of CO_2 whilst increasing the profit by $0.44 billion. Comparing 95% CCS with the case where no CCS is employed, the former captured and injected 3.58 Mt of CO_2 whilst increasing the profit by $0.34 billion. These results indicate that employing CCS technology with the integration of renewable energy can lead to further gains.

4.5.3 Carbon Cap & Trade

Carbon cap and trade systems and carbon tax programs are policies introduced by economies to mitigate greenhouse gas emissions. In contrast to direct regulations, such as mandated technologies or performance standards, “carbon cap and trade” and carbon tax approaches have the potential to achieve emissions reduction at lower costs[147]. However, carbon tax, in comparison to the cap and trade program, does not guarantee that emissions will be kept within the given limit. Thus, the impact of carbon cap and trade policy on refinery energy generation configurations was investigated in this scenario. Outcomes of such an analysis can aid in decision making whether to invest in ‘clean’ energy generation or comply with the carbon cap-and-trade program. For this analysis, the annual carbon emissions cap for the USOSC was set to 68.3 Mt of CO_2 (i.e. 75% of the maximum). Moreover, the impact of different carbon credit values on annual profit and emissions was studied.

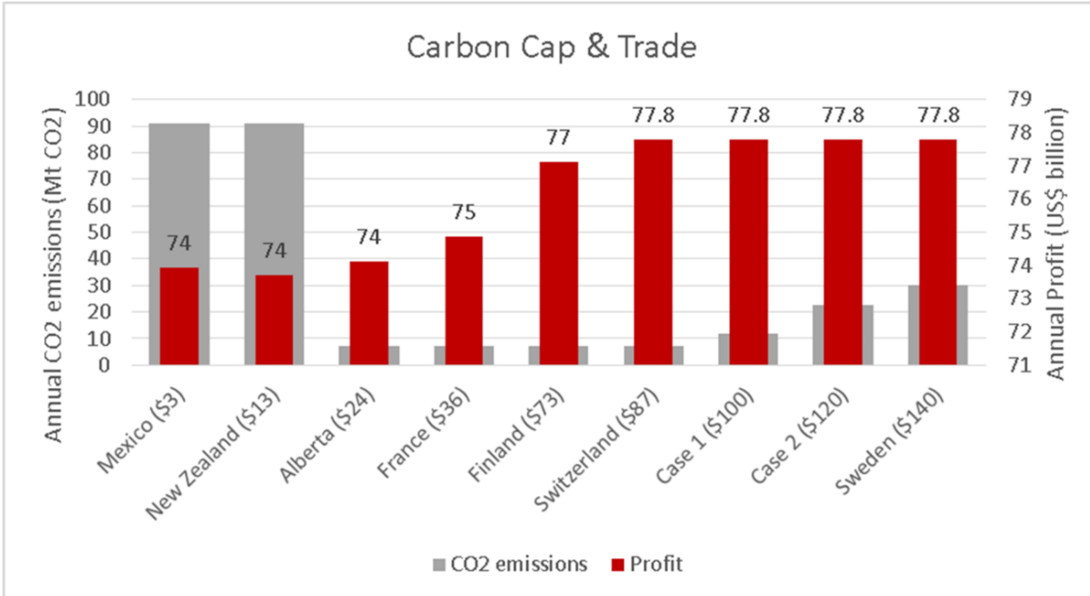

Figure 4.8 Results of carbon cap-and-trade for different carbon credit values

As seen in Figure 4.8, as carbon credit value increases, the value of annual profit increases. However, it can be seen annual carbon emissions are significantly higher for Mexico and New Zealand. As carbon credit value increases to that of Alberta (i.e. \$24/tCO_2), it falls significantly from 91 Mt CO_2 to 7 Mt CO_2. This is because the carbon credit values of Mexico and New Zealand are considerably low that it is profitable to buy emissions allowance from other countries rather than investing in RE technologies, as evident from Table 4.3. The maximum profit of \$78 billion is observed for carbon credit value of Switzerland and higher. Beyond this carbon credit value (i.e. \$87), carbon emissions are observed to increase whilst experiencing no change in the annual profit. Thus, in this scenario, the carbon credit value of Switzerland can be regarded as optimal, resulting in the least carbon emissions and highest profit, annually.

Table 4.3 Energy distribution for each for different energy generation technologies configuration shown in Figure 4.8.

Case	PV	CSP	Wind	CHP El.	CHP heat	Grid	Boiler	PV Mod	SCA	WT	Natural Gas	Ctrade
	TWh										bcf	Mt
Mexico	0.00	0.00	0.00	10.60	15.15	33.88	0.00	0	0	0	265.00	-22.77
New Zealand	0.00	0.00	0.00	10.60	15.15	33.88	0.00	0	0	0	265.00	-22.77
Alberta	0.00	0.00	33.88	10.60	15.15	~0	0.00	0	0	19098400	265.00	61.07
France	0.00	0.00	33.88	10.60	15.15	~0	0.00	0	0	19098400	265.00	61.07
Finland	0.00	0.00	33.88	10.60	15.15	~0	0.00	0	0	19098400	265.00	61.07
Switzerland	0.00	0.00	33.88	10.60	15.15	0.00	0.00	0	0	19098400	265.00	61.07
Case 1	0.00	0.00	32.03	10.60	15.15	1.85	0.00	0	0	18056480	265.00	56.50
Case 2	0.00	~0	27.64	10.60	15.15	6.24	0.00	0	5	15579020	265.00	45.62
Sweden	0.00	~0	24.66	10.60	15.15	9.22	0.00	0	4	13901460	265.00	38.25

4.5.4 Multi-objective

Multi-objective optimization was carried out using the epsilon constraint method, employing CPLEX 11.1.1 solver in the GAMS 22.8.1 environment. A plot of annual profit versus annual CO_2 emissions was constructed to observe the impact of different annual cost and resulting carbon dioxide emissions, as shown in Figure 4.9.

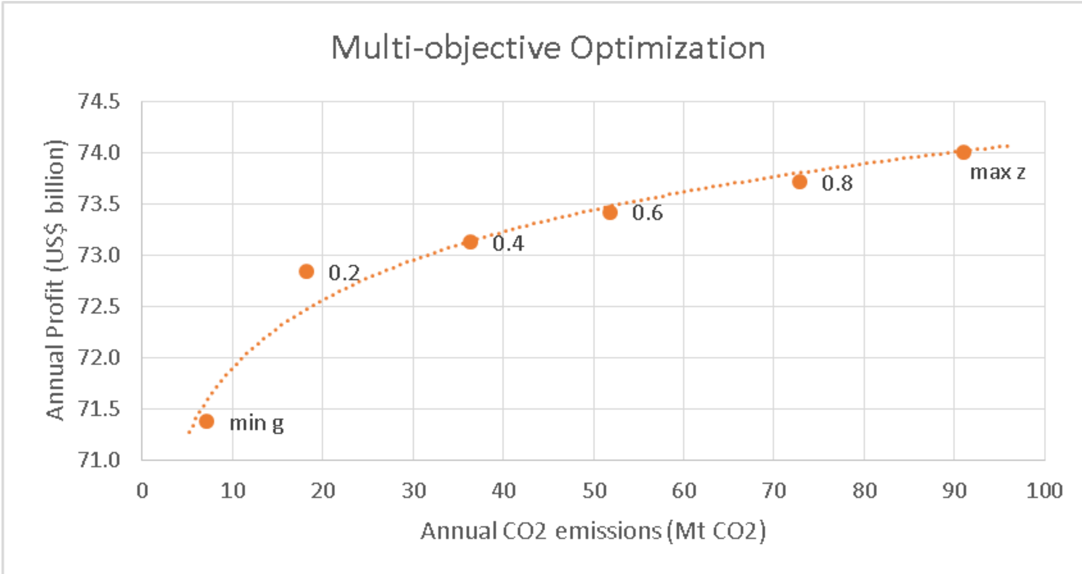

Figure 4.9 Annual profit vs annual carbon emissions results generated using epsilon constraint method

As stated earlier, multi-objective optimization can be performed, using the modified epsilon constraint method, where the annual profit is the governing objective function and the carbon emissions expression is posed as a constraint. It can be seen from Figure 4.9, as more carbon emissions are allowed (i.e. utilizing non-renewable technologies), a higher profit is attained. Also, a higher increase (i.e. slope) in profit is observed at lower emissions than at higher emissions. This is due to the fact that RE can significantly reduce carbon footprint; but at a relatively high cost. Referring to Table 4.4, for the case where emissions are minimized, solar PV technology is utilized. However, once the weight index goes to 0.2, solar PV technology is no longer pursued; rather grid-connected energy is used to meet the electricity demand. The RE share decreases as the weight as higher indices are studied.

Table 4.4 Energy distribution for each for different energy generation technologies configuration shown in Figure 4.9

Case	PV	CSP	Wind	CHP El.	CHP Heat	Grid	Boiler	PV Mod	SCA	WT	Natural Gas
	TWh										bcf
Min CO_2	4.70	0.00	29.18	10.60	15.15	~0	0.00	103069400	0	16448140	265.00
0.2	0.00	0.00	29.42	10.60	15.15	4.46	0.00	0	0	16587250	265.00
0.4	0.00	0.00	22.07	10.60	15.15	11.81	0.00	0	3	12440440	265.00
0.6	0.00	2.33	13.50	10.60	15.15	18.05	0.00	0	143850	7607775	265.00
0.8	0.00	0.00	7.36	10.60	15.15	26.52	0.00	0	0	4146810	265.00
Max Profit	0.00	0.00	0.00	10.60	15.15	33.88	0.00	0	0	0	265.00

4.5.5 EROEI

In this scenario, the effect of EROEI on annual profit and annual carbon emissions is studied and the results are presented in Figure 4.10.

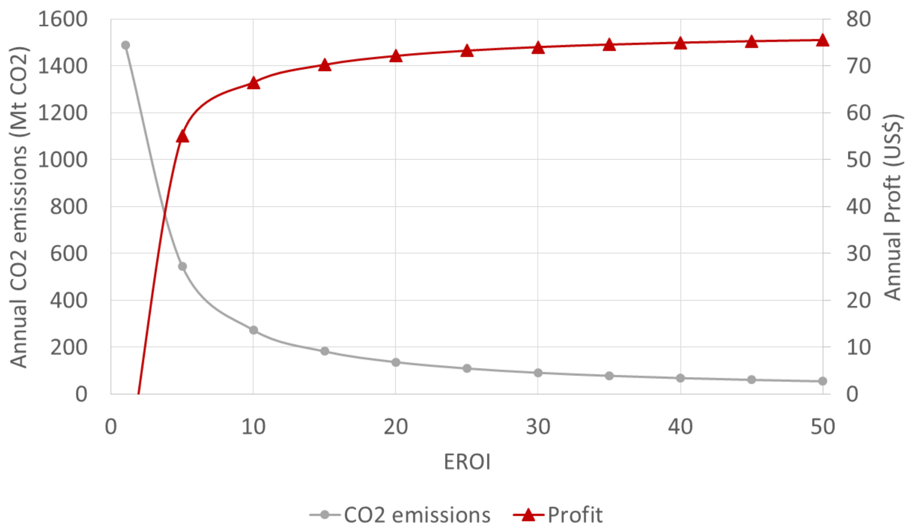

Figure 4.10Annual profit and CO2 emissions observed for varying EROI values

As stated earlier, the oil and gas study have been experiencing a continual overall decline in the EROI value. Certain short periods were observed where a rise was observed whenever innovative technology was implemented in order to recover more crude oil from the reservoirs. However, in all, the ratio of energy input per output is generally decreasing. Thus, it is more reasonable to analyze these results with decreasing EROI values. Thus, as observed from Figure 4.10, a decrease in EROI value decreases the annual profit and increases annual CO_2 emissions. In a study by Brandt et al.[136] in 2015, the EROI value for a field in Abu Dhabi was reported to be about 30 (also considered in this study). Considering it as the current value and the declining trend, soon a very steep decrease is expected with a steep increase in emissions, once the EROI value falls below 10.

4.5.6 Overall

In this section, all obtained results from the different scenarios are presented and are discussed in comparison to each other. The graphical representation, seen in Figure 4.11, shows how different techniques and technologies influence the annual profit and carbon emissions as compared to other techniques. For example, the results obtained from the carbon cap-and-trade scenario yielded the highest annual profit values. Carbon capture and injection, with minimum flow rate and RE technologies, yielded the lowest carbon emissions.

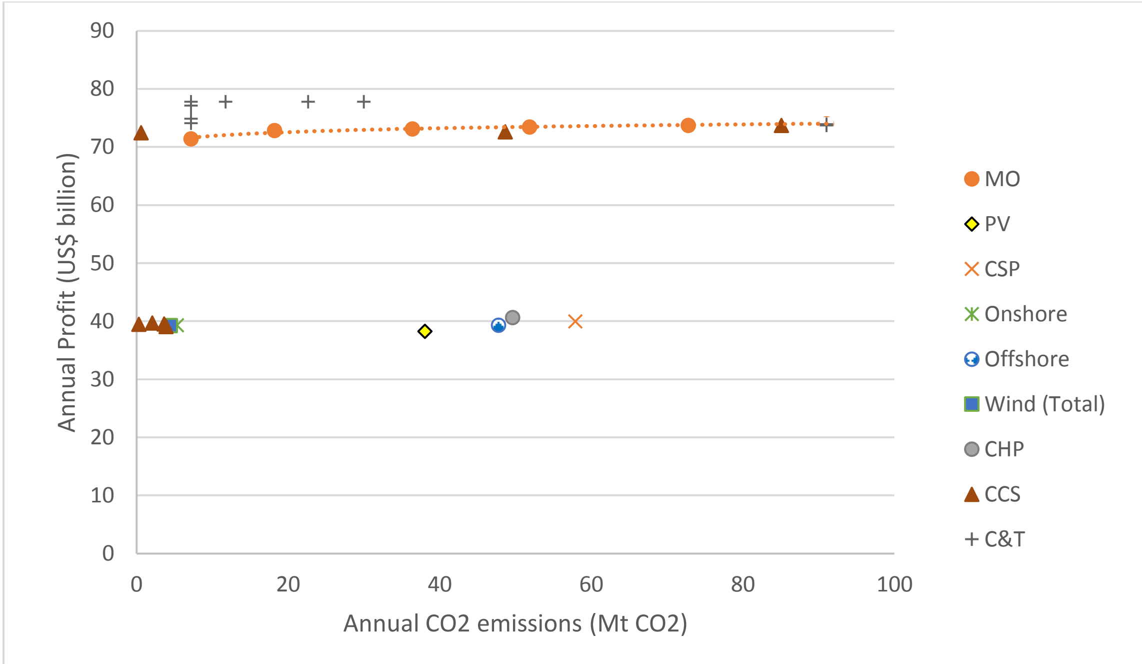

Figure 4.11 Results from all scenarios considered in this study

4.6 Conclusion and Future Work

In this study, a generic framework was developed to optimally integrate renewable energy technologies into the upstream oil supply chain (USOSC) with economic and environmental considerations. A case study on Abu Dhabi was conducted in order to examine the applicability of the proposed model. Different scenarios considering various energy generation and capture technologies as well as impact of policies were studied. Options exist that allow the optimal integration of various renewable energy technologies within the USOSC with significant economic and environmental gains. Based on the EROI discussion, there is a strong need in order to invest in renewable energy to optimally integrate these technologies within the current infrastructure. Moreover, with the advancement of technology, less dependence on fossil fuels can be experienced; resulting in less carbon footprint and sustainable energy.

Storage systems and hydrogen vector was not considered in this study. However, they are known to have an impact on the economic and environmental aspects. For example, with the utilization of storage systems, excess energy can be stored for future utilization. Moreover, the CHP excess case (i.e. allowing the CHP to produce excess energy) was not studied. If excess heat is obtained and thermoelectric systems are considered, further economic gains can be realized. The USOSC network was posed as a standard pooling problem. Interaction between pools can be considered to observe its impact on future energy planning. Various stochastic parameters such as crude oil prices may be introduced to this model to investigate its impact on the performance of the model. In all, the proposed model is flexible and can be further developed and/or used for applications, in greater detail.

Chapter 5 Refinery-wide optimal renewable energy integration using Solar and Wind technologies

5.1 Introduction

Refining of crude oil is one of the most complex stages within the oil industry. Tremendous amounts of energy is consumed by refineries to produce desired petroleum products. According to Hall et al., up to 27% of total energy invested in the oil industry, from extraction to transport, is expended on refining of crude oil[148]. This energy comprises of direct heat (i.e. furnace), indirect heat (i.e. steam) and electricity from co-generation plants[149]. Additionally, a substantial amount of carbon dioxide (CO_2) emissions is associated with this invested energy[149]. These emissions arise from the refinery processes as well as from energy generation sources responsible for meeting the energy demand of these processes. Several measures have been taken globally to mitigate carbon emissions in almost all industries. Integration of renewable energy within energy intensive industries is one of such measures that may considerably reduce CO_2 emissions.

Crude oil undergoes several different processes in a petroleum refinery before it is distributed to the end user. These processes mainly comprise of distillation, conversion (i.e. decomposition, unification, reforming), treatment and blending. Since no two crude oils are the same, each refinery is unique and its configuration evolves with time[150]. Nevertheless, Figure 5.1 shows the layout of a refinery.

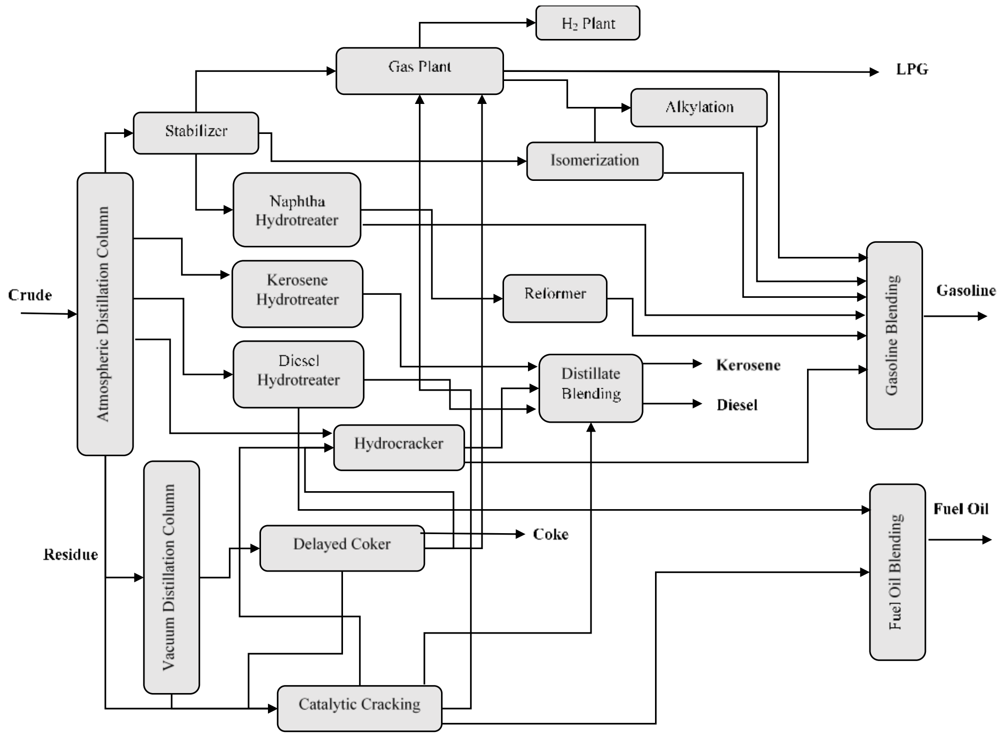

Figure 5.1 Schematic diagram depicting process units within a refinery

5.1.1 Distillation

Crude oil enters an atmospheric distillation column where it is separated into different crude oil fractions such as hydrocarbon gases, naphtha, kerosene, diesel, gas oil and topped crude (i.e. residue)[150]. This separation occurs based on the different boiling points of the components. Typical furnace temperatures for the distillation process range from 315^{o}C to 370^{o}C[150]. Lighter fractions of oil (i.e. hydrocarbon gases and naphtha) emerge from the top of the column and are sent to a stabilizer column which separates gases from liquid naphtha[151]. Other petroleum products, such as kerosene and diesel, are withdrawn from different stages of the atmospheric distillation column. All these products undergo treatment processes before they may be sent to storage. Vacuum distillation columns are commonly used in refineries which are fed with a part of the residue from the atmospheric distillation column, to extract further petroleum products out of this heavier fraction of crude oil.

5.1.2 Conversion

Several conversion processes occur within the refinery to enhance product properties, adding value to these petroleum products. Alkylation is one such process that converts isobutene and low molecular weight alkenes to alkylate, commonly using hydrofluoric acid (HF) or sulfuric acid (H_2SO_4). Isomerization is another conversion process that converts linear molecules into branched molecules. N-butane molecules may be isomerized and may be sent to the alkylation unit. Reforming units are employed, in refineries, to convert naphtha into branched alkanes and napthenes. Products recovered from all these processes are high-octane petroleum products, usually treated as stocks in blending processes.

Cracking processes such as hydrocracking, catalytic cracking, thermal cracking, are examples of other conversion processes that break down long chain hydrocarbon molecules into smaller ones. As their names suggest, they may use hydrogen, a particular catalyst or simply heat to decompose these molecules.

5.1.3 Treatment

Petroleum products, distilled from the atmospheric distillation column, such as naphtha, kerosene, diesel, are sent to their respective hydrotreaters to have impurities removed (i.e. nitrogen, sulfur, aromatics) from them whilst enhancing their properties. Other treatment processes within the refinery include desalting, hydrodesulfurization, solvent refining, sweetening, solvent extraction and dewaxing.

5.1.4 Blending

Blending is the process of combining hydrocarbon fractions and additives to produce end-user petroleum products. Through blending, product demands and specifications may be met. For example, different grade of gasoline products with varying octane level may be produced based on market forces.

5.1.5 Other processes

Refineries may include other processes based on economic and environmental requirements. These include, but are not limited to, sulfur recovery, acid gas treatment, wastewater treatment and hydrogen production[150].

5.2 Methodology

5.2.1 Superstructure

For this study, Figure 5.2 shows the superstructure for the renewable energy integration application to the refinery units. The acronyms used in this superstructure are defined in Table 5.1. Since this study focuses on a refinery in the Middle East, the energy sources listed in the superstructure are considered due to their availability.

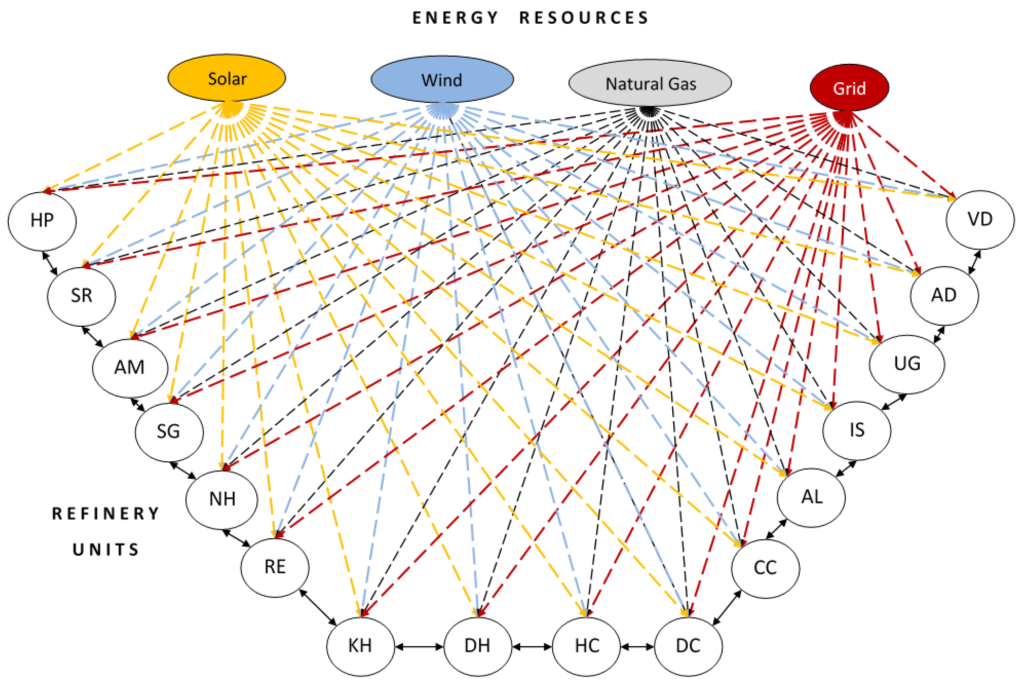

Figure 5.2 Superstructure depicting the refinery process units and potential energy resources

Table 5.1 List of acronyms used in refinery superstructure

Refinery Unit	Acronym
Hydrogen Production Plant	HP
Sulfur Recovery Unit	SR
Amine Sweetening Unit	AM
Saturated Gas Plant	SG
Naphtha Hydrotreater	NH
Reformer	RE
Kerosene Hydrotreating Unit	KH
Diesel Hydrotreating Unit	DH
Hydrocracker	HC
Delayed Coker	DC
Catalytic Cracking Unit	CC
Alkylation Unit	AL
Isomerization Unit	IS
Unsaturated Gas Plant	UG
Atmospheric Distillation Column	AD
Vacuum Distillation Column	VD

5.2.2 Simulation

In order to determine the energy requirements of the refinery units, Aspen HYSYS V8.4 was used to simulate the refinery operations. Figure 5.3 shows the Process Flow Diagram (PFD) of the simulated refinery. As shown, two streams of crude oil, sweet and sour, were considered with flow rates of 160,000 and 240,000 barrels per day, respectively. The power and heat requirements of this refinery are initially assumed to be met through grid-distributed electricity and natural gas boilers, respectively. Additionally, a 6 km^2 land area is assumed to be available on-site that can be utilized towards renewable energy generation technology installation.

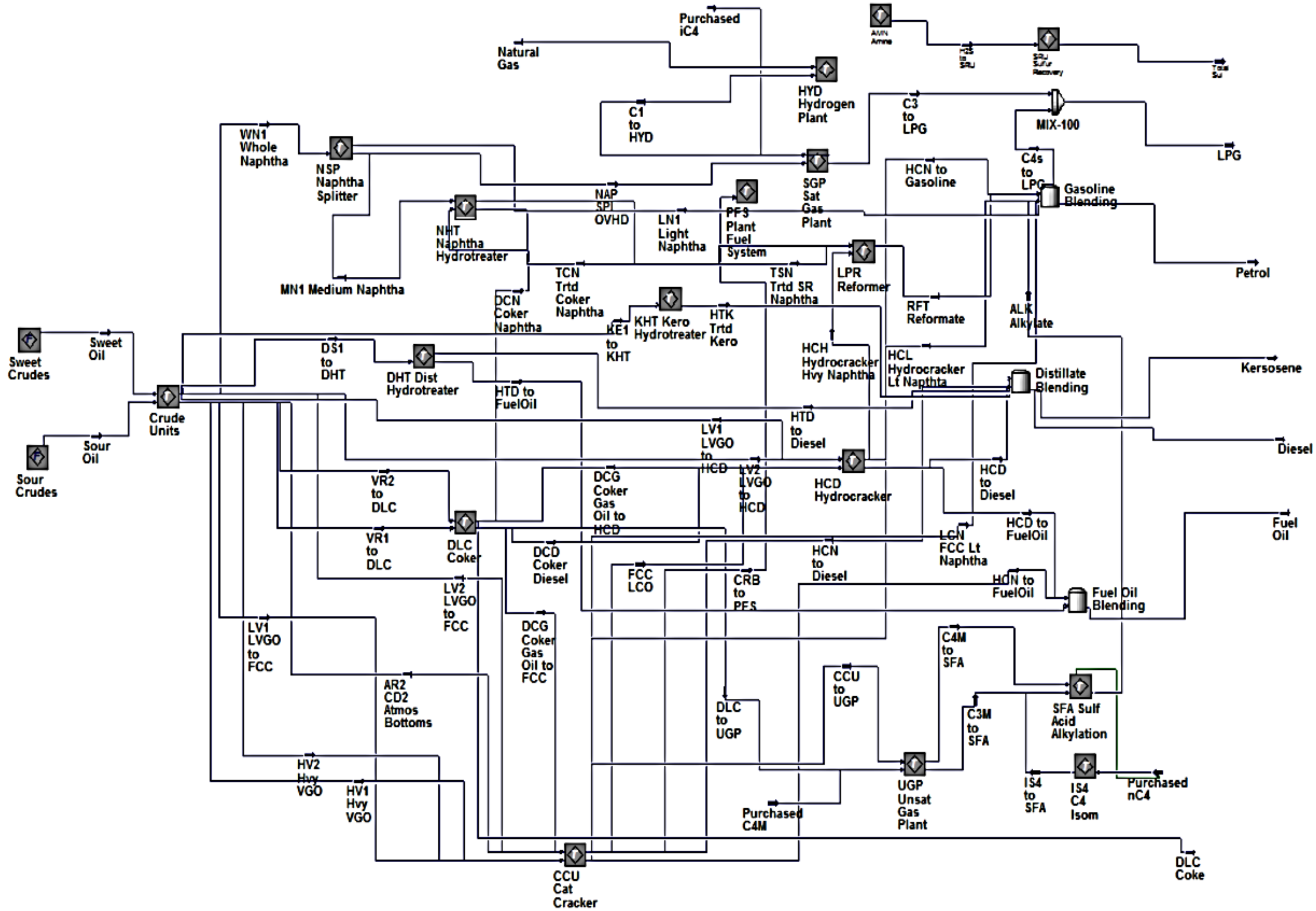

Figure 5.3 Process flowsheet of the refinery simulated using Aspen HYSYS

5.3 Results and Discussion

After obtained the required energy demand from the simulation, the CPLEX 11.1.1 was used to solve the model in GAMS environment to obtain optimal solution. Different scenarios were considered in this case study. This section presents the results generated from each of these scenarios and discusses each of them in detail.

5.3.1 Energy generation without storage

In this scenario, different energy technologies were considered, based on availability within the region, for minimizing cost and carbon dioxide emissions, in the absence of storage technologies. These results along with the required number of equipment for each configuration are shown in Figure 5.4 and Table 5.2, respectively.

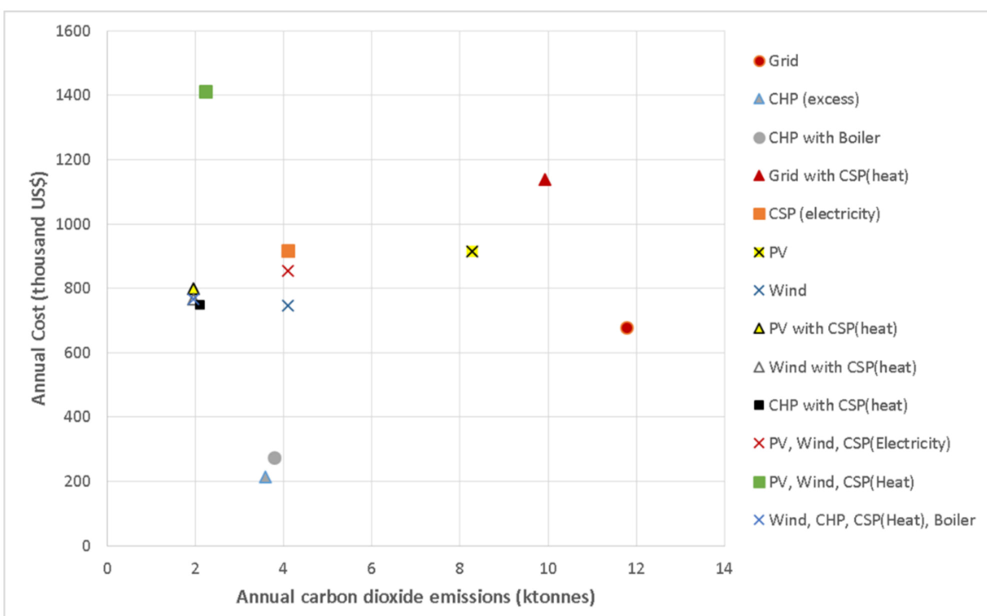

Figure 5.4 Cost incurred and CO_2 emissions annually for each of the energy generation technology configurations

Table 5.2 Energy distribution for each of the different energy generation technologies configuration shown in Figure 4.5

Configuration	PV	CSP	Wind	CHP El.	CHP Heat	Grid	Boiler	PV Mod	SCA	WT	Natural Gas
	GWh										mmscf
Grid	0.00	0.00	0.00	0.00	0.00	3.11	7.59	0	0	0	94.4
CHP (excess)	0.00	0.00	0.00	5.31	7.59	0.00	0.00	0	0	0	133
CHP with Boiler	0.00	0.00	0.00	3.11	4.44	0.00	3.15	0	0	0	117
Grid with CSP(heat)	0.00	3.46	0.00	0.00	0.00	3.11	4.13	0	214	0	51.3
CSP (electricity)	0.00	3.11	0.00	0.00	0.00	0.001	7.59	0	192	0	94.4
PV	0.00	0.00	0.00	0.00	0.00	1.69	7.59	31136	0	0	94.4
Wind	0.00	0.00	3.11	0.00	0.00	0.002	7.59	0	0	1752	94.4
PV with CSP(heat)	0.22	3.46	0.00	2.89	4.12	0.00	0.00	4921	214	0	77.7
Wind with CSP(heat)	0.00	3.46	0.22	2.89	4.13	0.00	0.00	0	214	125	77.7
CHP with CSP(heat)	0.00	3.46	0.00	3.11	4.44	0.00	0.00	0	214	0	77.7
PV, Wind, CSP(Electricity)	0.38	0.94	1.79	0.00	0.00	0.00	7.59	8398	58	1008	94.4
PV, Wind, CSP(Heat)	1.42	3.46	1.69	0.00	0.00	0.00	4.13	31136	214	953	51.3
PV, CHP, CSP(Heat)	1.32	3.46	0.00	2.89	4.13	0.00	0.00	28950	214	0	72.2
Wind, CHP, CSP(Heat), Boiler	0.00	3.46	0.23	2.89	4.12	0.00	0.004	0	214	127	72.2

As evident from Figure 4.5, the lowest carbon emissions are obtained when wind turbines or solar PV technology are coupled with CSP parabolic trough SCA for electricity and heat generation, respectively. However, the lowest cost observed among these relatively low CO_2 emitting configurations was that of the Wind, CHP, CSP(Heat), Boiler scheme. Even though a small amount of thermal energy is produced by the boiler, as seen in Table 4.1, the cost decreases by US$ 11,680 annually for a difference of 251 kg in CO_2 emissions, as compared to the configuration without the boiler. Moreover, wind coupled with CSP without boiler, in comparison to PV with CSP(heat), results in being about US$ 32,936 cheaper whilst reducing 172 kg of more CO_2 emissions, annually. In all, the total reduction in annual CO_2 emissions by these configurations, as compared to the assumed case (i.e. grid), is recorded to be about 9.8 ktonnes at an annual cost of about $88,000.

The option of utilizing CSP to generate electricity was also explored when considering employment of these renewable technologies individually and collectively. In individual scenarios, wind and solar CSP were able to meet most of power demand; thus, reducing 4.18 ktonnes more CO_2 emissions than solar PV. Comparing the annual cost, wind technology was found to be the cheapest while solar CSP was found to be the most expensive option for electricity generation. In the collective scenario, annual carbon emissions were similar to those of CSP and PV when considered individually. In addition, the annual cost incurred was about $854,149. In the collective scenario, solar CSP technology was also considered as a source of heat generation. The carbon dioxide emissions were 1.86 ktonnes lower but at a higher cost of about $558,924.

The lowest cost incurred, amongst all configurations, when a Combined Heat and Power (CHP) system was employed. Two cases were studied with this configuration; with and without allowing excess electricity generation. In the latter case, boiler was used to make up for shortfall in heat generation, as evident from Table 4.1. In the case where excess electricity was allowed, the annual cost and carbon dioxide emission were observed to lower by $60,156 and 209 tonnes of CO_2, respectively. However, options for selling this electricity to the grid or surrounding dwellings was not explored. This may help generate revenue for the refinery and help lower its costs.

Table 5.3 Land occupied by renewable energy technology configurations

	Area (km2)	% Used
Grid with CSP(heat)	0.642	10.70
CSP (electricity)	0.576	9.60
PV	0.065	1.09
Wind	0.029	0.48
PV with CSP(heat)	0.652	10.87
Wind with CSP(heat)	0.644	10.73
CHP with CSP(heat)	0.642	10.7
PV, Wind, CSP(Electricity)	0.208	3.47
PV, Wind, CSP(Heat)	0.723	12.05
Wind, CHP, CSP(Heat), Boiler	0.644	10.74

Table 4.2 shows the land utilized when employing renewable energy technology configurations to meet refinery energy requirements. As stated earlier, the available land onsite for installation of renewable technology was 6 km^2. However, we see that a maximum of about 12% was utilized; implying additional land is available to meet increased demand. For the case of solar PV and CSP, it appears that land was not utilized even though these technologies individually are not able to meet demand. It must be understood that these installations are sufficient to meet the hourly demand of the refinery only when solar energy is available. In order to maximize their utilization, energy storage technologies need to be considered.

5.3.2 Energy generation with storage

In this scenario, sodium-sulfur (NaS) and hot water systems were considered for electrical and thermal energy storage, respectively. NaS batteries are one of the most established storage technologies in MW scale with a relatively high overall efficiency[111], [152]. Similarly, hot water storage systems can be up to 90% efficient in MW scale applications at a relatively low cost[153]. The impact of different energy storage capacity constraints on annual cost and carbon dioxide emissions was studied, while minimizing the latter. This 'allowed' energy storage capacity does not refer to an addition of energy storage technology, rather poses as a constraint to limit maximum energy storage. The results generated for this case are presented in Figure 5.5. The solid lines represent the annual cost whereas the dashed lines with identical markers represent the corresponding annual carbon dioxide emissions.

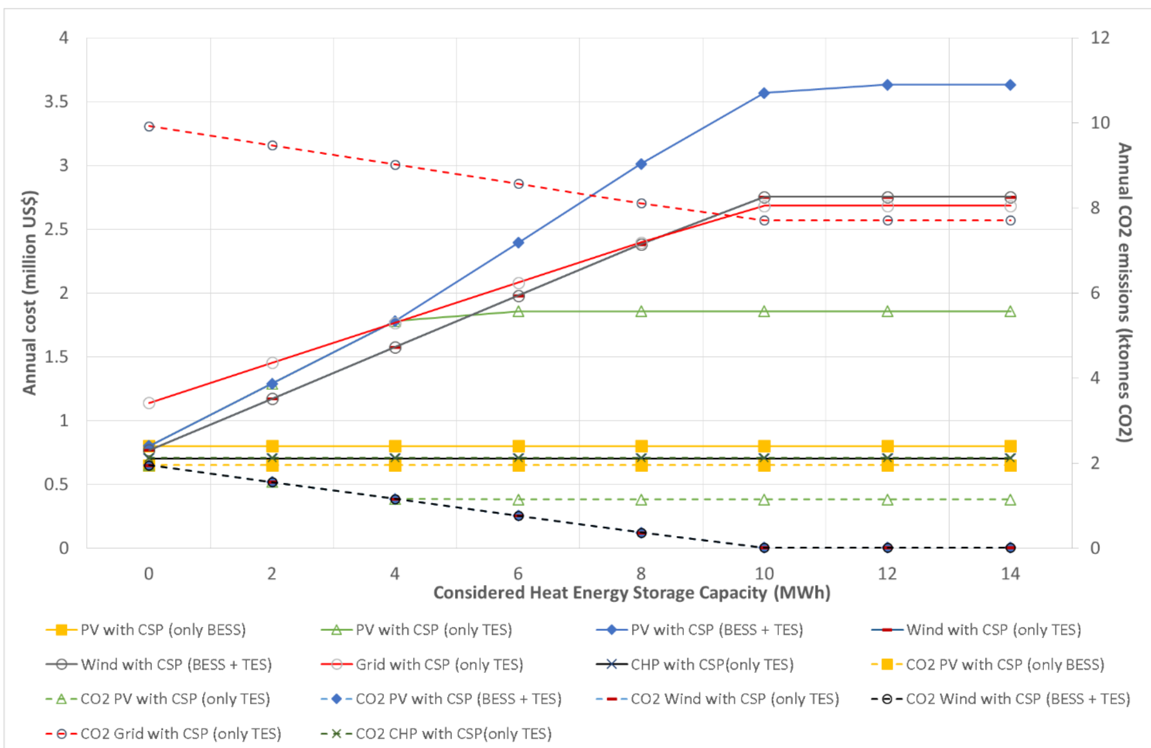

Figure 5.5 Annual cost and carbon dioxide emissions for different electrical and thermal energy storage capacities

Table 5.4 shows the energy generated by each technology for each scenario presented in Figure 5.5. Moreover, it shows the number of modules/SCA/turbines that need to be installed and volume of natural gas consumed, in order to provide the required energy.

Table 5.4 Energy distribution for each for different energy generation technologies configuration shown in Figure 5.5

Configuration	Allowed Heat Capacity	Optimal Heat/El Capacity	PV	CSP	Wind	CHP El.	CHP Heat	Grid	Boiler	PV Mod	SCA	WT
	MWh		GWh									
PV with CSP (only BESS)	0+	0/0	0.22	3.46	0.00	2.89	4.12	0.00	0.00	4921	214	0
PV with CSP (only TES)	0	0/0	0.22	3.46	0.00	2.89	4.12	0.00	0.00	4921	214	0
	2	2/0	0.81	4.31	0.00	2.30	3.28	0.00	0.00	17850	266	0
	4	4/0	1.40	5.15	0.00	1.71	2.44	0.00	0.00	30779	318	0
	6+	4.41/0	1.42	5.33	0.00	1.69	2.41	0.00	0.00	31136	329	0
PV with CSP (BESS+ TES)	0	0/0	0.22	3.46	0.00	2.89	4.12	0.00	0.00	4921	214	0
	2	2/0	0.81	4.31	0.00	2.30	3.28	0.00	0.00	17850	266	0
	4	4/0	1.40	5.15	0.00	1.71	2.44	0.00	0.00	30779	318	0
	6	6/0.558	1.99	5.99	0.00	1.12	1.60	0.00	0.00	43708	370	0
	8	8/1.13	2.58	6.83	0.00	0.53	0.75	0.00	0.00	56636	422	0
	10	9.79/1.64	3.11	7.61	0.00	0.00	0.00	0.00	0.00	68171	470	0
	12+	10.18/1.64	3.11	7.75	0.00	0.00	0.00	0.00	0.00	68172	479	0
Wind with CSP (only BESS)	0+	0/0	0.00	3.46	0.23	2.89	4.12	0.00	0.00	0	214	127
Wind with CSP (only TES) + Wind with CSP (BESS+TES)	0	0/0	0.00	3.46	0.23	2.89	4.12	0.00	0.00	0	214	127
	2	2/0	0.00	4.31	0.81	2.30	3.28	0.00	0.00	0	266	459
	4	4/0	0.00	5.15	1.40	1.71	2.44	0.00	0.00	0	318	791
	6	6/0	0.00	5.99	1.99	1.12	1.60	0.00	0.00	0	370	1124
	8	8/0	0.00	6.83	2.58	0.53	0.75	0.00	0.00	0	422	1457
	10+	9.8/0	0.00	7.61	3.11	0.00	0.00	0.00	0.00	0	470	1753
Grid with CSP (only TES)	0	0/0	0.00	3.46	0.00	0.00	0.00	3.11	4.13	0	214	0
	2	2/0	0.00	4.31	0.00	0.00	0.00	3.11	3.28	0	266	0
	4	4/0	0.00	5.15	0.00	0.00	0.00	3.11	2.44	0	318	0
	6	6/0	0.00	5.99	0.00	0.00	0.00	3.11	1.60	0	370	0
	8	8/0	0.00	6.83	0.00	0.00	0.00	3.11	0.76	0	422	0
	10+	9.9/0	0.00	7.61	0.00	0.00	0.00	3.11	0.00	0	470	0

CHP with CSP(only TES)	0+	0/0	0.00	3.19	0.00	3.10	4.42	0.01	0.00	0	197	0

PV with CSP (only BESS) denotes the case where only electrical storage was considered. As observed, adding Battery Energy Storage System (BESS) of different capacities does not affect the annual carbon emissions. This occurs because CSP technology, without energy storage, is unable to meet heat demand by the refinery. Thus, heat demand is supplemented with thermal energy produced from CHP technology through natural gas consumption. As a result, electricity is also generated that is utilized to meet the electricity demand of the refinery, as evident from Table 5.4.

On the contrary, when only thermal storage is considered for CSP technology (i.e. no BESS for PV), the annual carbon dioxide emissions further reduces from 1.95 ktonnes to 1.14 ktonnes of CO_2 when 4.41 MWh TES is considered. Additional TES does not lead to further emission reduction. This reduction in emissions occurs at an additional annual cost of about $ 1.06 million. Since no BESS is employed, electricity demand is met by utilizing PV and CHP technologies, as seen in Table 5.4. In comparison to the former configuration (i.e. only BESS), it can be seen that TES allows for more electricity and heat generation by PV and CSP technologies, respectively.

When considering both storage technologies (i.e. BESS and TES) for PV coupled with CSP, a maximum reduction in annual carbon dioxide emissions of about 1.94 ktonnes is observed. The optimal BESS and TES capacities in this configuration are 10.18 and 1.64, respectively, as shown in Table 5.4. In this configuration, annual cost increases steadily with decreasing carbon emissions until a TES capacity of 9.79 MWh is employed. Up till this point, energy (i.e. electricity and heat) is generated from renewable and non-renewable sources. However, at BESS and TES capacities of 1.64 MWh and 10.18 MWh, respectively, energy is generated completely from renewable energy sources.

For this case study, wind energy generates sufficient electricity to meet the electricity demand, without the need of any BESS. Thus, both configurations, ‘Wind with CSP (only TES)’ and ‘Wind with CSP (BESS +TES)’, yields similar results. This is due to sufficient hourly wind speed that allows continuous electricity generation through small wind turbines. Furthermore, it reduces a similar volume of carbon emissions as PV with CSP(heat), but at a significantly lower cost. On the other hand, due to the intermittent nature of solar energy, CSP technology requires TES to meet heat demand via renewables. The optimal TES capacity needed, in order to meet this demand, is 9.8 MWh. Moreover, 470 solar PV modules and 1753 solar collector assemblies need to be installed. The annual carbon emission reduction observed for this configuration is 1.94 ktonnes against an annual cost of $275,000.

5.3.3 Carbon Cap & Trade

As stated earlier, carbon cap and trade systems and carbon tax programs are policies introduced by economies to mitigate greenhouse gas emissions. In contrast to direct regulations, such as mandated technologies or performance standards, “carbon cap and trade” and carbon tax approaches have the potential to achieve emissions reduction at lower costs[147]. However, carbon tax, in comparison to the cap and trade program, does not guarantee emissions will be kept within the given limit. Thus, the impact of carbon cap and trade policy on refinery energy generation configurations was investigated in this scenario. Outcomes of such an analysis can aid in decision making whether to invest in ‘clean’ energy generation or comply with the carbon cap-and-trade program. For this analysis, the carbon emissions cap for the refinery was set to 2 ktonnes of CO_2 annually. Moreover, the impact of a low, mid and high carbon credit was investigated. These were carbon values of \$0.000002 gCO_2^{-1}, \$0.000024 gCO_2^{-1}, and \$0.00014 gCO_2^{-1}, imposed in Estonia, Alberta and Sweden, respectively. Different cases with these carbon credit values were solved for minimizing annual costs (z) and carbon emissions (g), as seen in Figure 5.6.

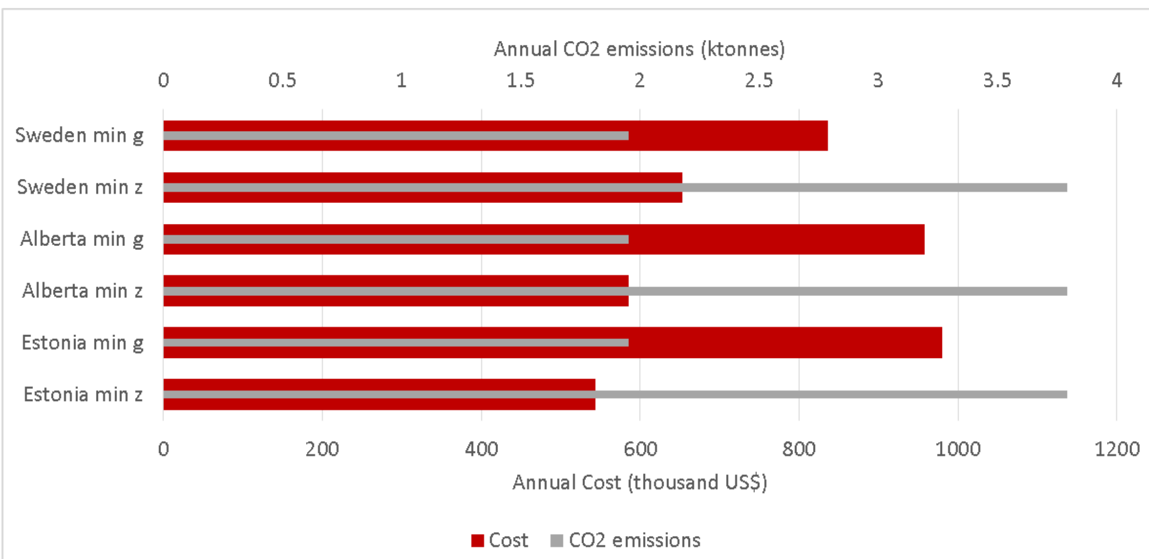

Figure 5.6 Results of carbon cap-and-trade analysis for different carbon credit values

Table 5.5 Energy distribution for each for different energy generation technologies configuration shown in Figure 5.6

Case	PV	CSP	Wind	CHP El.	CHP heat	Boiler	PV Mod	SCA	WT	Natural Gas
	GWh									mmscf
Estonia min z	0.00	0.00	0.00	3.11	4.44	3.15	0.00	0.00	0.00	117
Estonia min g	0.00	3.46	0.23	2.89	4.12	0.00	0.00	214.00	127.00	72.2
Alberta min z	0.00	0.00	0.00	3.11	4.44	3.15	0.00	0.00	0.00	117
Alberta min g	0.00	3.46	0.23	2.89	4.12	0.00	0.00	214.00	127.00	72.2
Sweden min z	0.00	0.00	0.00	3.11	4.44	3.15	0.00	0.00	0.00	117
Sweden min g	0.00	3.46	0.23	2.89	4.12	0.00	0.00	214.00	127.00	72.2

As seen from Figure 5.6, when minimizing annual CO_2 emissions, the lowest annual cost resulted from the high carbon credit value case of \$ $1.4x10^{-4}$ gCO_2^{-1}, imposed in Sweden. The amount of CO_2 emissions allowance 'traded' was 1.05 ktonnes, generating a revenue of about \$147,000. The Wind, CHP, CSP(Heat), Boiler configuration yielded these results, employing 214 SCA and 127 wind turbines along with the total consumption of 72.2 mmscf of natural gas. This result is in agreement with observations recorded in Figure 4.5 and Table 4.1.

On the other hand, the minimum annual cost was observed for the credit value imposed in Estonia. 0.79 ktonnes of CO_2 emissions allowance was bought at a credit value of \$ $2.0x10^{-6}$ gCO_2^{-1}. The CHP coupled with boiler was observed to be the configuration yielding this low annual cost. In contrast to results of CHP (excess) in Figure 4.5, the formerly mentioned configuration yielded a lower annual cost, consuming 117 mmscf of natural gas. The above analysis was repeated for a lower carbon emissions limit of 1 metric ktonnes of CO_2. A similar trend in results was observed with higher trading of emissions. Yet, regarding the same configuration as optimal.

5.3.4 Carbon Capture and Storage

Another scenario was considered to investigate the impact of employing a carbon capture and storage (CCS) technology. As the name suggests, CCS commonly refers to the process of capturing greenhouse gas emissions from point source and/or ambient air and transporting to a storage facility. Moreover, it covers a broad range of technologies; thus, a wide range of cost is associated with such a technology[112]. This captured CO_2 can also be sold to industries that need in their processes, such as CO_2 injection for Enhanced Oil Recovery (EOR). In this study, CCS cost along with carbon selling price was considered and the model was solved to minimize overall annual costs.

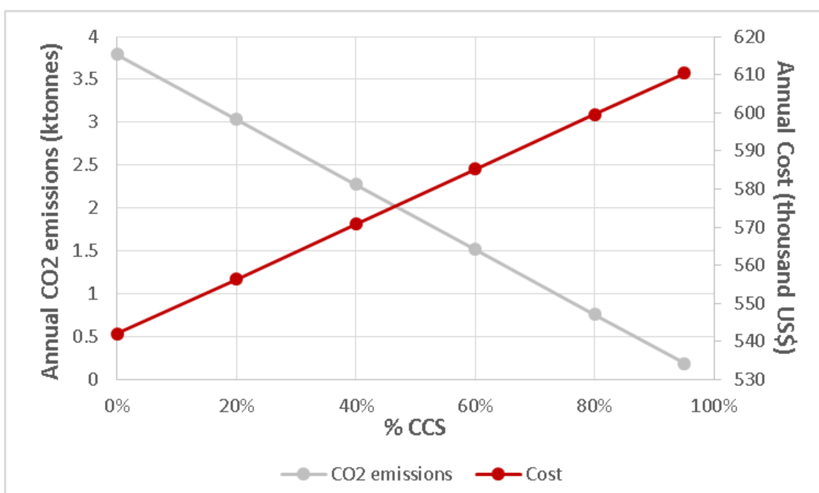

Figure 5.7 Annual cost and carbon dioxide emissions resulting from different amounts of CCS

As expected, annual cost increases as more carbon emissions are captured and stored. Even though excess CHP was observed to meet power and heat requirements at the lowest annual cost, as seen in Figure 4.5, CHP coupled with boiler results in the lowest costs. Moreover, this configuration was the optimal at each percentage of CCS. Thus, implying that investing in 'clean' energy is a less economical option at the assumed carbon price (i.e.$35/ton CO_2) and CCS cost (i.e. $54/ton CO_2). Further analysis on varying carbon price and CCS cost can be carried out to investigate the limit beyond which refinery would be economically forced to invest in renewable energy technologies. With advancement of technology, the assumed cost of CCS may be expected to decrease whereas CO_2 selling price may increase, based on market demand. For example, in the case of CO_2 injection for EOR, demand for CO_2 would increase as more oil is being recovered from the reservoirs. Nevertheless, CCS involves storage and transport costs which may increase or decrease with time as opposed to capture costs. Moreover, it can be understood that the values themselves may not affect the suggested configuration but rather the difference between these values. Hence, analysis is carried out by fixing the same carbon price and varying the CCS cost at 70% CCS, as shown in Figure 5.8.

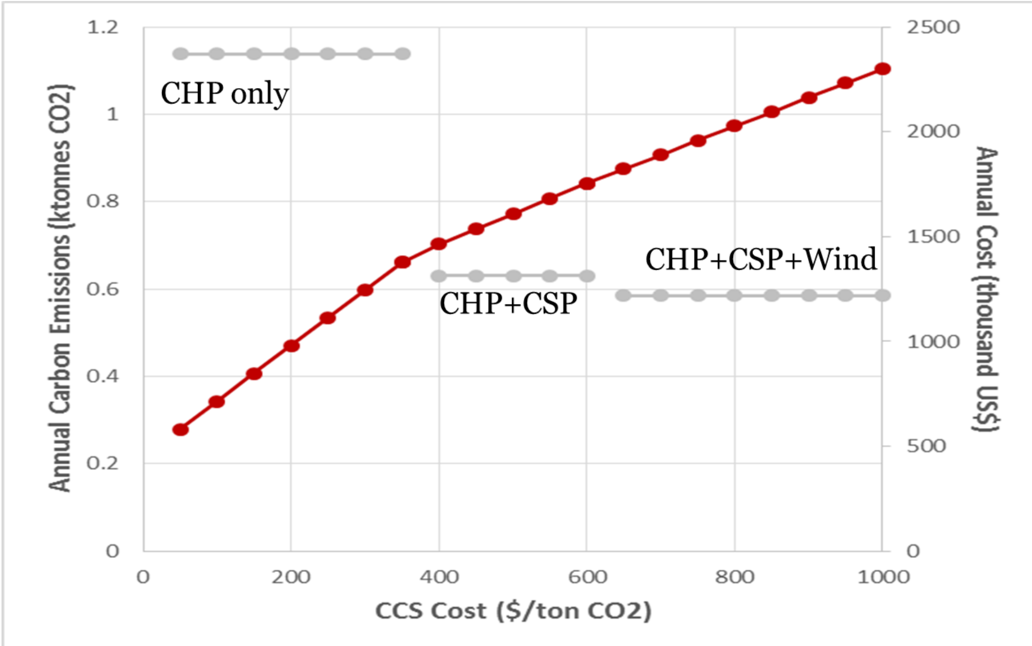

Figure 5.8 Annual carbon emissions and cost with varying CCS cost

As observed from the figure above, the preferred configuration switches from CHP with boiler to CHP with CSP(heat) between the CCS cost of \$350/ton CO_2 and \$450/ton CO_2, employing about 195 CSP-SCA. At this point, the amount of carbon emissions to be captured falls significantly from 2.65 ktonnes of CO_2 to 1.47 ktonnes of CO_2. Moreover, the cost increases less steadily as compared to lower CCS cost cases. The second shift in preferred configuration occurs between \$600/ton CO_2 and \$650/ton CO_2. In this case, 214 SCA and 126 wind turbines are employed, reducing carbon emissions captured to 1.37 ktonnes. In all, a tremendous difference between CCS cost and carbon selling price of at least \$450/ton CO_2 would be required in order to economically motivate decision makers at the refinery to invest in clean energy, at the current technology advancement.

5.3.5 Pareto Front

A Pareto front was constructed to observe the impact of different annual cost and resulting carbon dioxide emissions, as shown in Figure 4.9.

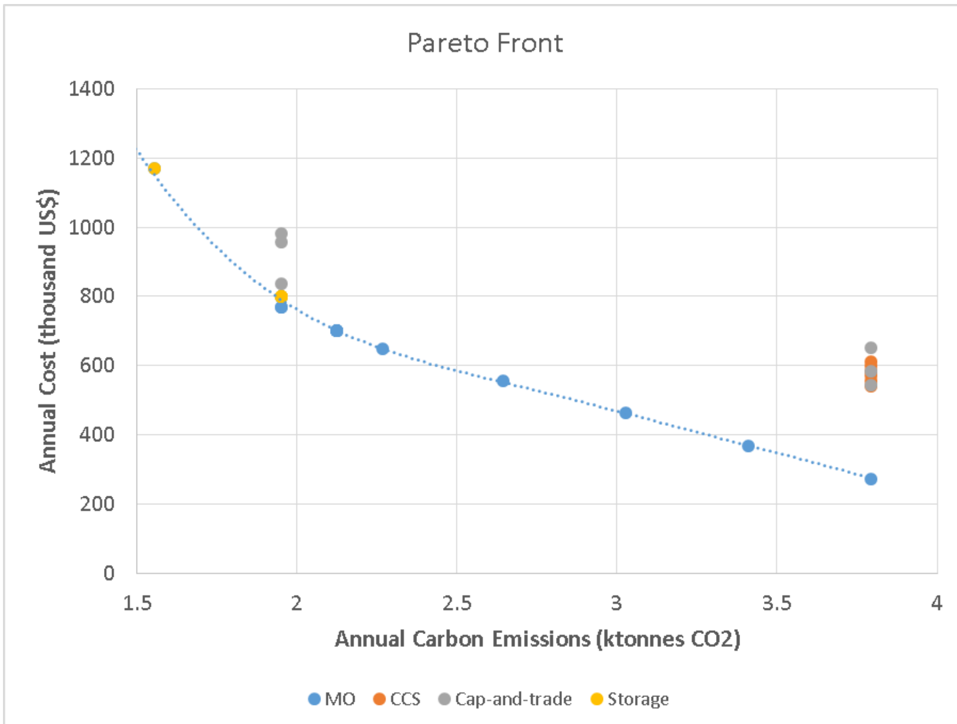

Figure 5.9 Pareto front constructed using the multi-objective function and storage technologies

As observed from earlier observations and Figure 4.9, annual carbon emissions have an inverse relationship with annual cost. As more investment in renewable energy and/or storage technologies is made, a higher carbon emissions reduction is observed.

5.4 Conclusion

In this study, the generic framework was applied to optimally integrate renewable energy technologies into the process industry with economic and environmental considerations. To investigate the applicability of the model, a refinery-wide case study was successfully examined. With the help of the developed model, the annual costs and carbon emissions resulting from different types of configurations of energy generation technologies were determined. Moreover, the developed model was able to calculate the number of modules/assemblies/turbines and/or volume of natural gas required to meet the power and heat requirement of a process industry. In addition, the model was able to determine the area of land occupied when utilizing the renewable energy generation technologies. Energy generation with and without electrochemical and thermal storage technologies were studied. It was found that further reduction in carbon emissions can be observed when utilizing storage systems. Other scenarios studied included the implementation of a carbon cap-and-trade program and employment of carbon capture and storage (CCS) technology. Though not demonstrated in the application, but evident from the model development, energy distribution to specific units within the refinery can also be optimally selected.

Chapter 6 Assessing Rooftop Renewable Energy in Abu Dhabi City for Electric Vehicle Charging and Energy Infrastructure

In this chapter, the last phase of the research work is presented where renewable energy is integrated into the energy infrastructure, focusing on reducing emissions generated from the transport sector by designing an electric vehicle charging infrastructure.

6.1 Introduction

One of the major challenges the electric vehicle industry faces, as opposed to internal combustion engine (ICE) vehicles, is the lack of infrastructure across many countries[24]. Historically speaking, the first ICE vehicle was driven by Karl Benz in 1886[154]. It was not until 1913 when the first filling station was built for such automobiles[155]. In contrast, the first electric vehicle was invented in the 1800s. Yet, it was not until December 2013 when an electric vehicle charging infrastructure was completed by Estonia with nationwide coverage[156]. Nevertheless, the first mass production of hybrid vehicles occurred in 1997[157].

On the other hand, Abu Dhabi, the capital of United Arab Emirates, is one of the largest producers of global energy. However, more than 99% of its electricity is generated from fossil-based fuels[1]. The government aims to increase its dependence on renewables up to 7% by 2020 as a step to mitigate carbon emissions[8]. The country has also promoted the use of electric vehicles (EV) by offering financial incentives in order to mitigate emissions from the transport sector[158], [159]. Coupled with rise in fuel prices, there exists potential for a significant shift to electric vehicles.

Within the past decade, several renewable energy projects have been initiated or completed, outside the Abu Dhabi (AD) city, such as Shams CSP, Masdar PV and Bani Yas Wind farm, to aid in meeting the AD 2020 target. Also, Abu Dhabi has been exploring rooftop RET deployment schemes since 2008[160]. Yet, these have been limited to policy-making stages and the idea of utilizing rooftop area of major structures within the metropolitan region towards renewable energy generation has not yet been studied. Thus, this study aims to assess the rooftop area of major structures within the Abu Dhabi city for electricity generation through RE technologies. This produced energy is used in planning of electric vehicle charging infrastructure as well towards meeting the Abu Dhabi electricity demand. Economic and environmental considerations are made in addition to technical limitations. Different scenarios have been analyzed to investigate the impact of various parameters on the total cost and overall carbon emission reduction.

6.2 Electric Vehicles (EVs)

There are mainly four types of electric vehicles: Battery Electric Vehicle (BEV), Plug-in Hybrid Electric Vehicle (PHEV), Hybrid Electric Vehicle (HEV) and Fuel-cell electric vehicle (FCEV) [24], [161]. BEVs, also referred to as EVs in this study, are completely powered by the battery and can be charged using an external source of electricity[161]. PHEVs and HEVs, in contrast, are equipped with both driving systems: internal combustion as well as electric drivetrain.

PHEVs rely highly on the battery and can be recharged using on-grid electricity whereas HEV battery is charged entirely by consuming gasoline. Fuel-cell electric vehicles generate power to operate its electric motor, using stored hydrogen and oxygen from the air. Since HEVs and FCEVs do not benefit from an EV charging infrastructure, these vehicles are not considered in this study.

6.2.1 Specifications

Several automobile manufacturers have invested in the EV industry and have produced vehicles that are already commercially available. Apart from the cost of the vehicle, another important factor in determining what EV to purchase is its range. Table 6.1 shows the range and prices of the some electric vehicles that are commercially available. It is observed that even the cheapest BEVs listed have a range of more than 100 km. FCEVs and HEVs have not been included as they cannot be charged with electricity. Hence, the scope of this study does not cater to their infrastructure.

Table 6.1 Specifications of some electric vehicles (EV) available on the market[162]–[165]

Model	Manufacturer	Range (km)	Price (USD)	Battery Size (kWh)	Type
A3 Sportback	Audi	25	39,500	8.8 (Li-ion)	PHEV
Model S	Tesla	435	69,500	85(Li-ion)	BEV
Leaf	Nissan	170	29,860	80 (Li-ion)	BEV
i-MiEV	Mitsubishi	100	23,485	16 (Li-ion)	BEV
Soul EV	Kia	150	32,800	30 (Li-ion)	BEV
Optima PHEV	Kia	47	35,000	9.8 (Li-ion)	PHEV
500e	Fiat	140	32,780	24 (Li-ion)	BEV
B250e	Mercedes Benz	140	42,375	36 (Li-ion)	BEV
GLE550e	Mercedes Benz	29	66,300	8.7 (Li-ion)	PHEV
e-Golf	Volkswagen	134	29,815	36 (Li-ion)	BEV
Spark EV	Chevrolet	132	25,995	19 (Li-ion)	BEV
Volt	Chevrolet	85	33,220	14 (Li-ion)	PHEV

Bolt	Chevrolet	383	37,496	60 (Li-ion)	BEV
Pacifica PHEV	Chrysler	52	43,090	16 (Li-ion)	PHEV
i3	BMW	181	42,275	33 (Li-ion)	BEV
i8	BMW	24	150,000	7.1 (Li-on)	PHEV
Focus Electric	Ford	122	29,995	23 (Li-ion)	BEV
Fusion Energi	Ford	34	31,995	7.6 (Li-ion)	PHEV
Electric Drive	Smart	110	25,750	16.5 (Li-ion)	BEV
Cayenne S E	Porsche	23	87,700	10.8 (Li-ion)	PHEV
Nexo	Hyundai	595	55,000	-	FCEV
Clarity Fuel Cell	Honda	589	60,000	-	FCEV

6.2.2 Chargers

There are generally three levels of chargers commercially available for electric vehicles (BEV and PHEV) [166]. Each charger is subjected to different technical limitations that affects the time it takes to charge EVs. For example, a level 1 (110V) charger may take up to 10 hours to fully charge a 20-kWh EV battery. Whereas, level 2 home chargers may fully charge a similar battery in about 5 hours. On the other hand, level 3 AC chargers may charge about 80% of 20-kWh battery in less than half an hour[167], [168].

Table 6.2 shows the specifications of the electric chargers commercially available. One significant element of information is the number of 20kWh charging cycles each charger can provide in a day. Super-fast DC public chargers have up to 288 cycles while level 2 AC public chargers have a maximum of 4 cycles. In contrast to charging, options exist where batteries may be swapped with fully charged ones to save time (i.e. 3 mins)[163]. However, this alternative requires stocking of batteries which may differ from one EV to the other[167]. Moreover, not all EVs are equipped with easily replaceable energy storage systems.

Table 6.2 EV chargers specifications [168]

	Level 3			Level 2		
	'Super-fast DC' public	DC public	AC public	AC public 3ϕ	AC public	AC home
Lifetime (years)	10	10-15	10-15	10-15	10-15	10-15
Load limit (V)	2000	500	400	230	230	230
Power limit (kW)	250	62.5	50	7.3	3.6	3.6
Duration of 20 kWh charge cycle (min)	5	19	24	164	333	333
Maximum number of 20kWh charging EV/day	288	75	60	8	4	1
Cost incl. installation (US$/kW)	585	1780	2100	1600	1624	325

6.2.3 Greenhouse Gas (GHG) emissions

Electric vehicles, in the past, faced several economic and technical challenges such as high cost and limited mileage. Due to these factors, they failed to compete with ICE vehicles and were not able to penetrate the market[157]. However, as evident from Table 6.1, these factors have now become relatively competitive to those of ICE vehicles. Moreover, the rise in environmental concerns, due to high CO_2 emissions, has driven governments to battle these issues by promoting 'cleaner' alternatives.

Electric cars may emit GHGs ranging from 0 g/km to 155 g/km, depending on the fuel type in use[169]. As mentioned earlier, BEVs run entirely on batteries; hence, do not emit any significant level of direct GHG emissions. However, a comprehensive life-cycle analysis may dictate significant emissions associated with these energy storage systems at the manufacturing stage. Measures may be taken during that process to mitigate or reduce harmful pollutants. A scenario within this study considers life-cycle emissions and depicts results based on these emissions. PHEVs and HEVs, on the contrary, are equipped with internal combustion engines that could emit about 50 to 130 g/km of direct CO_2 emissions, assuming various ratios of electricity and petrol consumption [169].

6.2.4 Rooftop Assessment

A study was conducted that identified strategies to aid in effective implementation of rooftop solar PV in the United Arab Emirates[160]. However, no research work had been conducted, to date, with regard to those strategies.

6.3 Methodology

6.3.1 Superstructure

Figure 6.1 shows the superstructure that outlines the renewable energy sources considered in this study as well as the energy hubs and electric vehicle chargers.

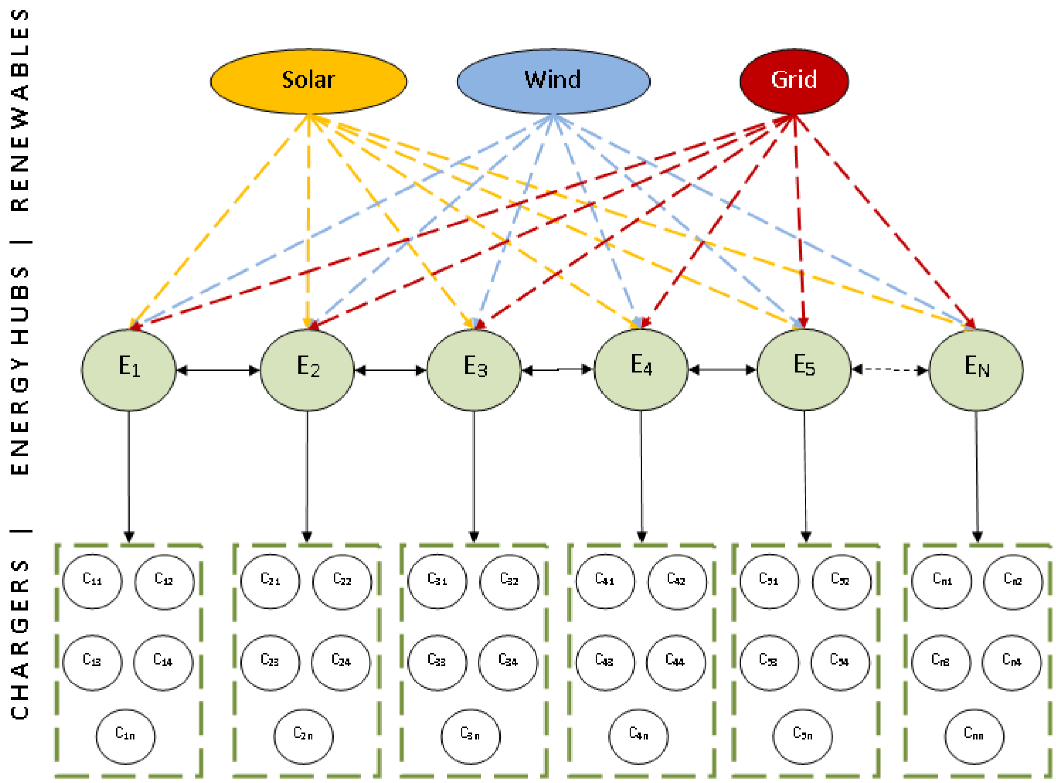

Figure 6.1 Superstructure of Electric Vehicle (EV) charging and energy infrastructure

Electric vehicle (EV) charging stations, powered by energy hubs, will be located in different areas in the city. These location may include residential sites, work locations, schools, hospitals and other notable places where vehicles may be parked for a significant amount of time. Even though superchargers exist for electric vehicles that could charge the battery for 30 minutes resulting in 270 kms of mileage, most vehicles get about an additional 18 km per hour charge with standard chargers[170]. Therefore, charging stations would be considered primarily for these locations.

The infrastructure would consist of several charging points across the city in areas where vehicles will be parked for a significant amount of time. These charging points would be powered by energy hubs that will facilitate the integration of renewables. In the superstructure, presented in Figure 6.1, E represents an energy hub at a particular site (i.e. rooftop) whilst C_{ij}, within the green rectangle, represents each charger, connected to this energy hub. In addition to charging electric vehicles, energy generated by these hubs may be used to partially meet the energy demand of Abu Dhabi city. For electricity generation from solar energy, both, solar PV and Micro-CSP technologies have been considered in this study. In addition, small wind turbines are used to generate electricity from wind energy.

6.3.2 Rooftop Area Estimation

MATLAB Image Segmenter and Image Region Analyzer tools were used to detect and analyze the rooftop area from map images. These satellite images of the studied area were captured using Google maps. In this section, the application of these tools is demonstrated.

Figure 6.2 Map image showing the aerial view of structures within the sample region considered in Abu Dhabi city

Abu Dhabi is the largest emirate that accounts for about 87% (67,640 km^2) of the United Arab Emirates, by land. However, Abu Dhabi city comprises of 972 km^2 with a population of about 1.5 million, as of 2013[171]. Moreover, the city is designed in blocks of localities. Satellite image of each block of structures is captured, as seen in Figure 6.2, as long as adequate details of each building can be observed. The image is then segmented where a threshold is applied to it. Based on the detail of the image, an appropriate level of threshold is applied, resulting in an image where the rooftop is made distinct from other noises (i.e. non-rooftop area), as evident from the last image in Figure 6.3.

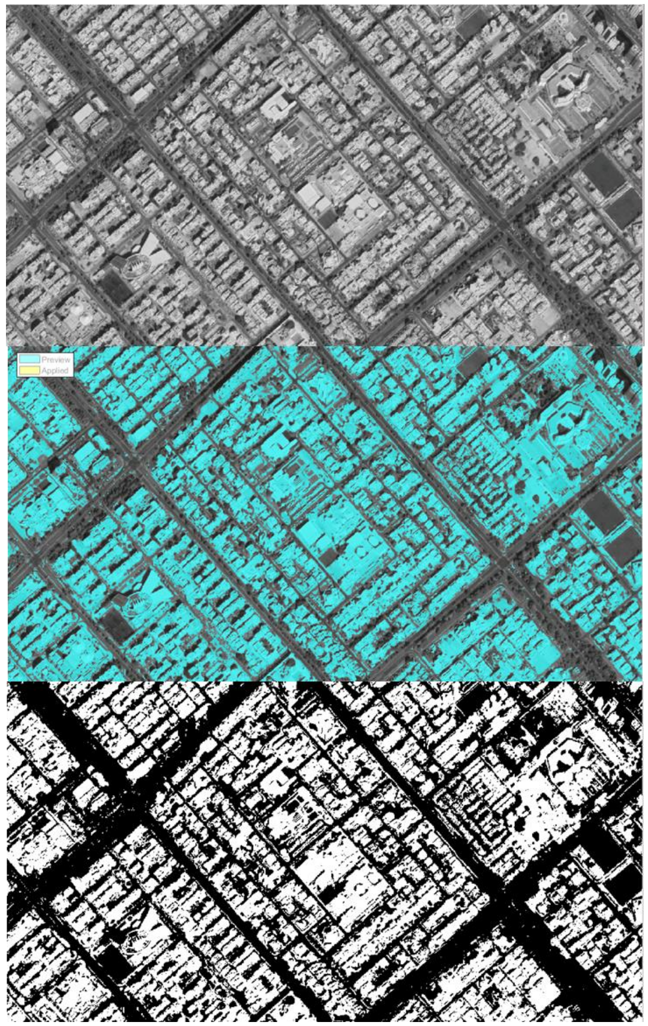

Figure 6.3 (a)Pre-processing, (b)threshold adaptation, and (c)post-processing images depicting the rooftop area of buildings in the sample region

Post-threshold adaptation, the image is transformed such that the identified areas within it can be analysed quantitatively. An area, based on the scale of the transformed image and its pixels, is calculated, as shown in Figure 6.4. The actual area of the rooftop is, then, obtained, using the scale at which the image was captured.

Figure 6.4 Rooftop area calculation for the sample region within Abu Dhabi city

<u>6.3.3 Model formulation</u>

6.3.3.1 Objective function

An objective function, *g*, is mainly developed based on the amount of CO_2 emissions produced from energy consumption (g^{Energy}) and utilization of electric/ICE vehicles (g^{Energy}), as seen from Equation 1. g^{Energy}, as seen in Eqn.2, is calculated by multiplying the amount of electricity production from each energy source with the associated CO_2 emissions per unit of electricity. g^{Veh}, expressed using Eqn. 3, considers the number of different types of vehicles, the emissions generated from them per km and the average mileage these vehicles have over the considered timeframe. For example, if the annual emissions reduction is studied, the average mileage over a year may be considered.

$$g^T = g^{Energy} + g^{Veh} \tag{1}$$

$$g^{Energy} = \sum_t \sum_s \sum_j P_{s,j,t} CO2_{s,j} \quad (2)$$

$$g^{Veh} = n^{ICE} g^{ICE} km^{ICE} + n^{EV} g^{EV} km^{EV} + n^{PHEV} g^{PHEV} km^{PHEV} \quad (3)$$

The total economic cost (z), of employing respective renewable energy and electric vehicle charging technologies, is evaluated using Eqn. 4. This cost comprises of energy generation cost (CE^T) as well as cost of electric vehicle charging infrastructure (CI^T).

$$z = CE^T + CI^T \quad (4)$$

The cost of energy includes the capital and operating cost as well as fuel costs if required by the energy generation plant. The cost of EV charging infrastructure comprises of capital costs and, operating and maintenance costs of charging infrastructure, as seen in Eqn. 5. The capital cost incurred at energy hub *s* at time *t* is represented using Eqn. 6. In this study, the total cost of chargers (CCH_s^T) installed at energy hub *s* is amortized considering a constant discount rate (D) and a similar lifetime for all chargers (N_{CH}). Moreover, CCH_s^T is equal to the total number of each type of charger (nCH_s) installed at energy hub *s* multiplied by the cost (CCH) of these chargers, respectively. The cost of each charger includes the cost of equipment, parts for installation and labor costs.

$$CI^T = \sum_s \sum_t \left(CCI_{s,t}^{cap} + CCI_{s,t}^{O\&M} \right) \quad (5)$$

$$CCI_{s,t}^{cap} = \frac{CCH_s^T}{\frac{(1+D)^{N_{CH}-1}}{D(1+D)^{N_{CH}}}} \quad (6)$$

$$CCH_s^T = \begin{pmatrix} nCH_s^{21} CCH^{21} + nCH_s^{22} CCH^{22} + nCH_s^{23} CCH^{23} \\ + nCH_s^{31} CCH^{31} + nCH_s^{32} CCH^{32} + nCH_s^{33} CCH^{33} \end{pmatrix} \quad (7)$$

6.3.3.2 Energy Hub

The energy hub, in this study, is modeled without a storage technology, using the following equation. Multiple input energy vectors and a single output energy vector (i.e. electricity) were considered.

$$L_{s,t} = \sum_j C_j P_{s,j,t} \tag{8}$$

The load ($L_{s,t}$) by each energy hub s at time t is met using electric power $P_{s,j,t}$, converted from energy vector j, and storage technology, q. In order to allow networking of energy hubs, this load is defined by the demand of the energy ($Dem_{s,t}$) and the energy transferred ($T_{s,b,t}$) from/to other energy hubs, provided a connection exists between them ($\alpha_{s,b}$). $Dem_{s,t}$ mainly constitutes of the electric chargers connected to this energy hub. Since this information is readily available, this demand can be simulated based on the number of electric vehicles that have penetrated the transport industry, as a percentage of total cars. In one the observed scenarios, this is extended to the region's electricity demand.

$$L_{s,i,t} = Dem_{s,t} + \sum_{b \in S-s} T_{s,b,t}\, \alpha_{s,b} \tag{9}$$

6.3.3.3 Renewable energy technology

Yield of electric power from each RET is subjected to technical limitations. Electricity generated from solar PV technology is defined by Equations 10 and 11 whereas electricity produced from solar CSP technologies is defined by Equations 12 and 13. Power derived from wind turbines are expressed using equations 14 and 15. Several other formulations exist in literature that consider additional parameters for added accuracy.

$$P_{s,PV,t} \leq \; Land_{s,PV} GHI_t PR_{PV} \tag{10}$$

$$\sum_t P_{s,PV,t} = \; N_{s,PV-module} CF_{PV} Power_{PV-module} PR_{PV} h_{PV} \tag{11}$$

$$P_{s,CSP,t} \leq \; Land_{s,CSP} DNI_t PR_{CSP} \tag{12}$$

$$\sum_t P_{s,CSP,t} = \; N_{s,CSP-SCA} CF_{CSP} Power_{CSP-SCA} PR_{CSP} h_{CSP} \tag{13}$$

$$P_{s,WT,t} \leq \; Land_{s,WT} 0.5 \rho_{air} A_{swept} ws_{s,t}^3 h \tag{14}$$

$$\sum_t P_{s,WT,t} = \; N_{s,WT} CF_{WT} Power_{WT} h_{WT} \tag{15}$$

The area needed for each type of RE technology is defined by Equations 16, 17 and 18.

$$Land_{s,PV} = 1.5 \times Area_{PV-module} N_{s,PV-module} \tag{16}$$

$$Land_{s,CSP} = 4 \times Aperture_{SCA} length_{SCA} N_{s,CSP-SCA} \tag{17}$$

$$Land_{s,WT} = 5 \times {rotor_{WT}}^2 \tag{18}$$

Moreover, the sum of these required spaces is constrained by the maximum roof area available at energy hub site, *s*.

$$\sum_s Land_{s,PV} + Land_{s,CSP} + Land_{s,WT} \leq Area_s^{max} \tag{19}$$

6.3.3.4 EV Charging

As part of the EV charging infrastructure, parking spaces need to be designated for electric vehicles where chargers are installed. Thus, each charger occupies a parking space. Parking ratio, ratio of parking spaces to building area, can be used to constraint the available EV parking spaces. Equations 20 and 21 can be used to define the minimum and maximum parking spaces available at each energy hub site. These conditions are necessary for the promotion of EVs whilst accommodating ICE vehicles in the transition period. Level 31 chargers ('Super-fast DC' public), in this study, are mainly perceived as chargers at dedicated EV charging stations. Therefore, the number of level 31 chargers at these stations are subjected to the constraint presented in Eqn. 22. At these stations, EVs would stopover and recharge in a similar manner as ICE vehicles would refuel at gas stations.

$$nch_s^{21} + nch_s^{22} + nch_s^{23} + nch_s^{32} + nch_s^{33} \ \geq Park^{min} \times Areamax(s) \quad (20)$$

$$nch_s^{21} + nch_s^{22} + nch_s^{23} + nch_s^{32} + nch_s^{33} \ \leq Park^{max} \times Areamax(s) \quad (21)$$

$$nch_{min}^{31} \ \leq \ nch_s^{31} \leq \ nch_{max}^{31} \quad (22)$$

In this study, rooftops of structures involving hospitals, high-rise buildings, schools and malls have been considered where vehicles are parked for a considerable amount of time. Not all chargers may be appropriate for each type of site. Thus, the types of chargers not suitable for a particular site need to be eliminated, as shown below.

$$nch_s^{23} + nch_s^{31} + nch_s^{32} + nch_s^{33} = 0 \qquad \forall s \in school \qquad (23)$$

$$nch_s^{23} + nch_s^{31} = 0 \qquad \forall s \in mall$$

$$nch_s^{23} + nch_s^{31} + nch_s^{32} = 0 \qquad \forall s \in hospital$$

$$nch_s^{31} + nch_s^{32} = 0 \qquad \forall s \in building$$

$$nch_s^{21} + nch_s^{22} + nch_s^{23} + nch_s^{32} + nch_s^{33} = 0 \quad \forall s \in station$$

The number of electric vehicles that can be charged by each type of charger needs to be constrained by values that are dictated by feasibility and technical limitations of the type of charger. For example, as seen from Table 6.2, the maximum number of 20kWh EVs that can be charged by level-21 charger (AC public 3ϕ) is 8 in 24 hours. They may not be feasible to use at sites where parking time is restricted to a couple of hours. On the other hand, if charging stations with level-31 chargers are studied, a minimum number of vehicles need to be considered that will be serviced by these stations. Thus, the following constraints are imposed.

$$Nev_{s,min}^{21} \leq Nev_{s,t}^{21} \leq Nev_{s,max}^{21} \tag{24}$$

$$Nev_{s,min}^{22} \leq Nev_{s,t}^{22} \leq Nev_{s,max}^{22}$$

$$Nev_{s,min}^{23} \leq Nev_{s,t}^{23} \leq Nev_{s,max}^{23}$$

$$Nev_{s,min}^{31} \leq Nev_{s,t}^{31} \leq Nev_{s,max}^{31}$$

$$Nev_{s,min}^{32} \leq Nev_{s,t}^{32} \leq Nev_{s,max}^{32}$$

$$Nev_{s,min}^{33} \leq Nev_{s,t}^{33} \leq Nev_{s,max}^{33}$$

6.4 Results and Discussion

In this section, the results from the rooftop area estimation analysis are presented. Additionally, various scenarios, involving EV demand, Abu Dhabi electricity demand and lifecycle emissions of RET and EVs, are studied. Impact of different

EV penetration within the transport sector on annual costs and carbon emissions is reported and discussed.

6.4.1 Rooftop Area

In this study, rooftop area of major structures within Abu Dhabi city was determined using the tools, discussed in the earlier sections. Area yielded from this method was compared to the actual rooftop area of the structures. Figure 6.5 shows the structures used with their respective unscaled areas, used for comparison.

After scaling the areas, the average percentage difference between the actual and calculated areas, based on MATLAB image segmentation and region analyzing tools, was found to be 18.55%. This area accounts for the entire rooftop, including rooftop area covered with installations such as HVAC equipment. In a study conducted by Koo et al.[172], the average rooftop area available for RET installation was found to be 61.2% of building area. Thus, this value is considered in this study, as well, when considering RET technologies.

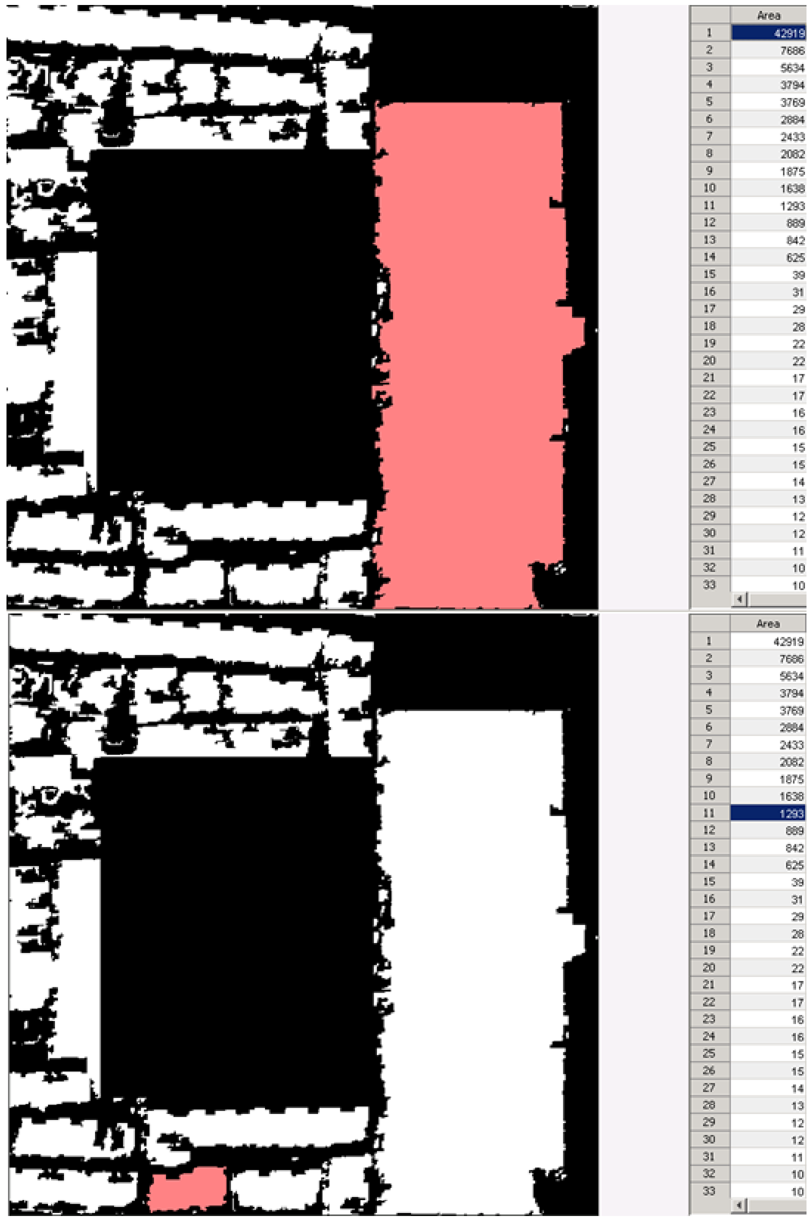

Figure 6.5 Example of unscaled areas of two structures used to calculate the percentage difference between the actual and detected rooftop area

6.4.2 EV Demand

In this scenario, rooftop renewable energy technologies are exclusively utilized to meet EV charging demand. The annual cost and CO_2 emissions realized for 10% EV penetration, for different energy generation configurations, have been recorded in Figure 6.6. The electricity produced by each of the technologies as well as the RET equipment installed is noted in Table 6.3.

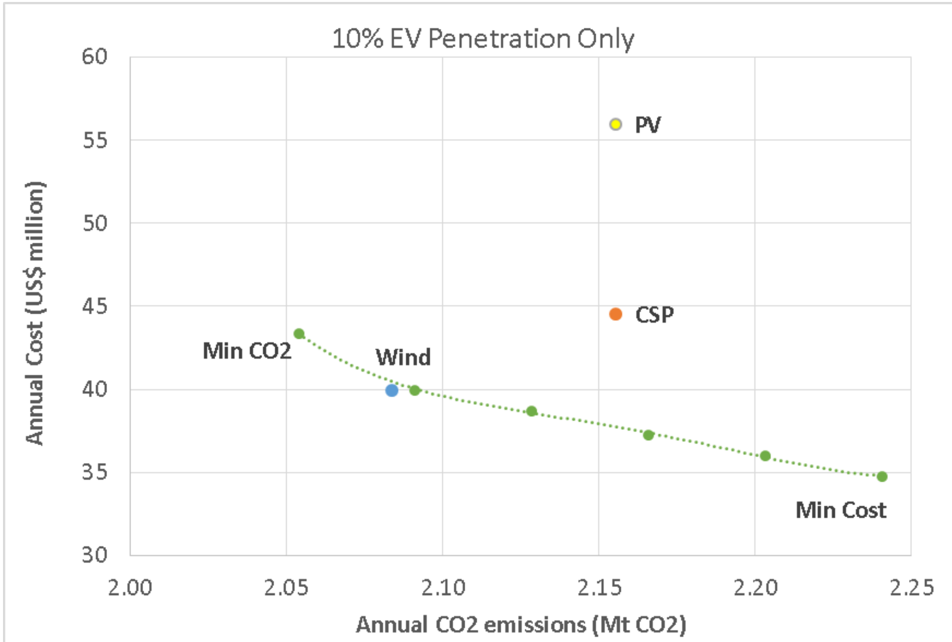

Figure 6.6 Annual cost and carbon emissions realized when utilizing different energy generation configurations for 10% EV charging demand

Table 6.3 Electricity produced by each energy generation technology and the number of RET equipment installed for results shown in Figure 6.6

Case	PV	CSP	Wind	Grid	PV Mod	SCA	WT
	GWh						
Min Cost	0.00	0.00	0.00	277.81	0	0	0
Min CO_2	0.00	44.31	233.41	0.09	0	79489	131578
PV only	126.88	0.00	0.00	150.93	2781672	0	0
CSP only	0.00	126.88	0.00	150.93	0	227607	0
Wind only	0.00	0.00	233.41	44.40	0	0	131578

As evident from Figure 6.6, the least amount of emissions annually are observed for the 'Min CO_2' case where almost all electricity demand is met via renewable energy technologies, mainly through wind energy (84%). In this case, 131,578 small wind turbines and 79,849 micro-CSP solar collector assemblies are installed. In contrast, the least annual cost for energy generation and EV charging infrastructure yields when all electricity is purchased from the local electrical grid. The difference in annual costs, as evident from Figure 6.6, for the two scenarios (i.e. min cost and min CO_2) is \$8.59 million. In addition, the reduction in emissions observed, by employing RET, is about 187 ktonnes CO_2, annually. This cost roughly translates to \$46 per ton of CO_2 mitigated. In comparison to the average carbon capture and storage (CCS) cost from point source, as reported by Rubin et al.[112], the cost appears to be \$8 cheaper per ton CO_2. The reported cost for utilizing RET also includes mitigating emissions that would, otherwise, be emitted to ambient air. Capturing these emissions, from ambient air, would be more difficult and result in higher costs.

If opting for a single RET, investing in wind energy would be more economically and environmentally beneficial, as indicated by the results in Figure 6.6. Generating electricity from wind is cheaper than generation through solar energy. Furthermore, solar PV and CSP, without energy storage systems, are only able to meet about 46% of given EV demand. Installation of storage system will allow these technologies to meet further demand; however, resulting in higher costs.

6.4.3 EV + Abu Dhabi city demand

In this scenario, rooftop RET installations were utilized in order to meet electric vehicle energy demand as well Abu Dhabi city electricity consumption. The hourly electricity demand for each month is shown in Figure 6.7. At least 80% of total energy demand of buildings is attributed towards cooling systems[173]. The average afternoon temperature in Abu Dhabi ranges from 24^{O}C to 42 ^{O}C, throughout the year. Thus, cooling systems are utilized all year around. As observed in Figure 6.7, the highest hourly electricity consumption in a day occurs at about 4 PM whereas the highest monthly electricity consumption takes place in July, reflecting increased usage of cooling systems in warm weather.

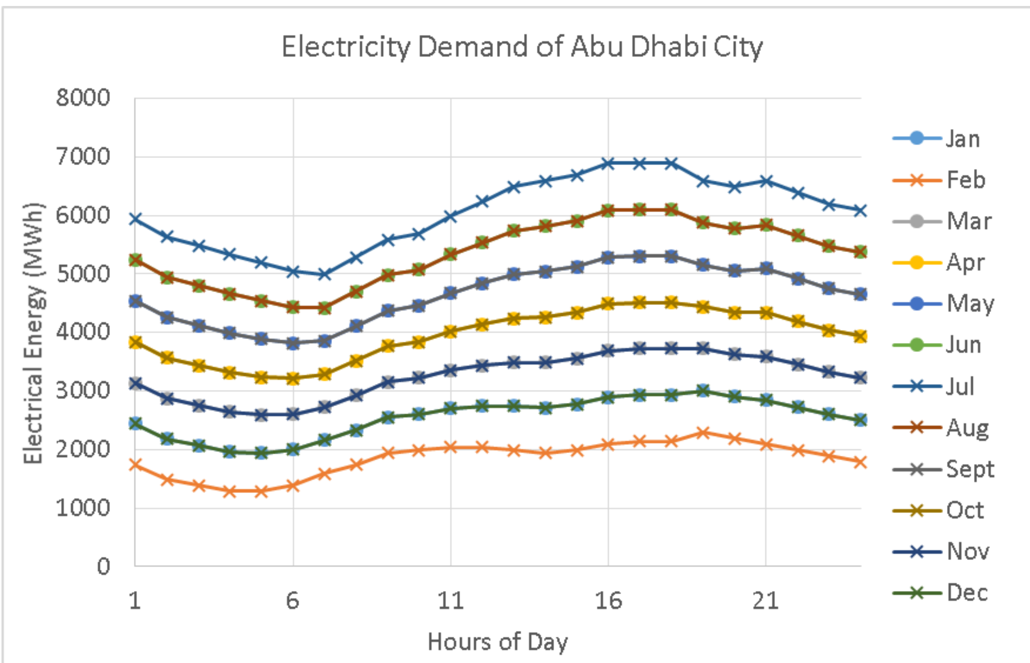

Figure 6.7 Hourly electricity demand of Abu Dhabi city for each month

[174]

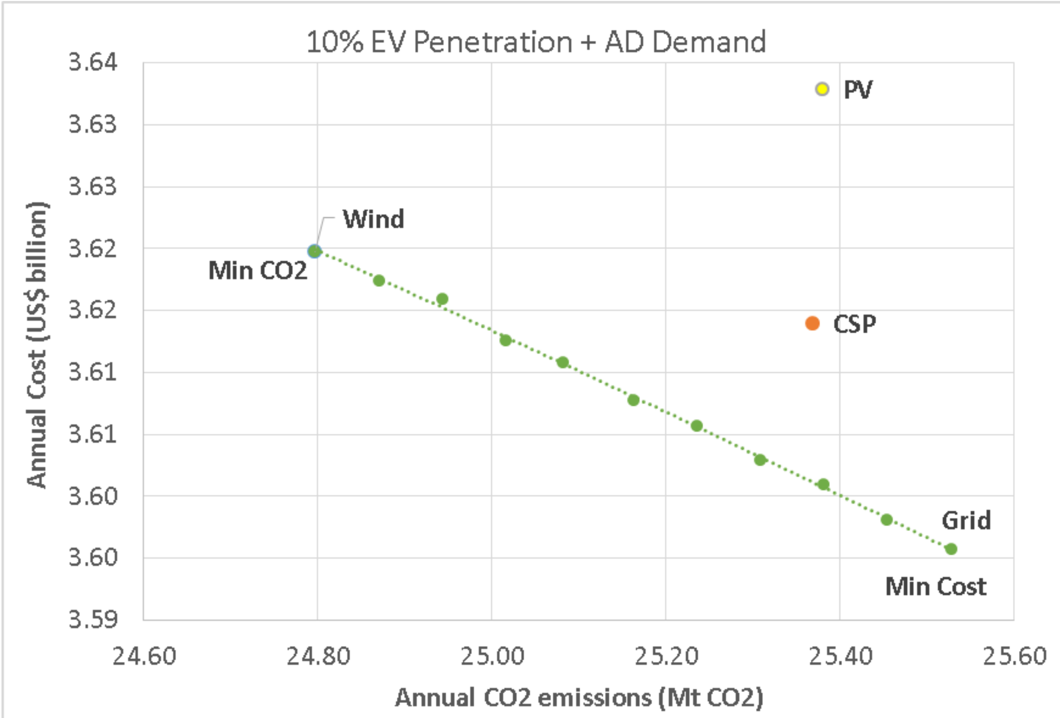

Figure 6.8 Annual cost and CO_2 emissions observed for meeting 10% EV and Abu Dhabi city electricity demand using different energy configurations

Figure 6.8 shows the cost incurred and the carbon emissions generated for the entire year when using different energy configuration. With the minimum carbon emissions scenario, about 730 ktonnes of CO_2 are mitigated, at an additional cost of $24 million, as compared to the minimum cost scenario where all electricity is purchased from the electrical grid, as evident from Table 6.4. Unlike the previous case (i.e. EV demand only), most of the electricity consumed is purchased from the electrical power grid. About 3.12% of electricity is generated via small wind turbines. A small contribution of about 23.3 MWh of electricity is made via 511 solar PV modules installed. In this study, the considered micro-CSP technology was found to be effective for sites with at least 2700 m^2 available area. Moreover, dedicated charging stations with level-31 chargers were only allowed solar PV technology. This restriction was placed as these stations are mainly surrounded with high-rise structures where small wind turbines may not prove to be efficient. Therefore, despite solar micro-CSP is a more economic option, the model suggests installation of PV modules. For the cases of PV only and CSP only, the latter was observed to produce 16 GWh more electricity than the former.

Another observation is made when comparing the two cases, meeting EV demand only and meeting EV + Abu Dhabi city demand. It is observed that in this case, more energy is generated via renewable energy technologies even though the same rooftop area is available. This is because excess energy is not allowed by the model since no energy storage systems are considered. Therefore, in the previous case, electricity generated via wind turbines is restricted by the demand of electric vehicles. Even if more wind speed was observed during a particular hour, an amount of electricity that suffices the hourly EV demand, is only generated. In this case, on the contrary, energy generated by wind turbines is used to meet Abu Dhabi (AD) demand as well. This demand is considerably much higher than the required EV demand. Consequently, the electricity generated is mainly dictated by the available wind speed rather the electricity demand. The same situation occurs for solar energy technologies. Electric power generated during sunlight hours is contributed towards meeting overall demand. Therefore, a much higher contribution of solar energy generated electricity is observed. Also, the optimality region, lying between min CO_2 and min cost, appears to be a straight line since the demand is very high as compared to RET produced electricity. Thus, it is highly dependent on grid connected electricity.

Table 6.4 Electricity produced by each energy generation technology and the number of RET equipment installed for results shown in Figure 6.8

Case	PV	CSP	Wind	Grid	PV Mod	SCA	WT
	TWh						
Min Cost	0.00	0.00	0.00	34.90	0	0	0
Min CO_2	~0	0.00	1.09	33.81	511	0	611984
PV	0.22	0.00	0.00	34.68	4824427	0	0
CSP	0.00	0.24	0.00	34.66	0	424890	0
Wind	0.00	0.00	1.09	33.81	0	0	611984

6.4.4 Lifecycle emissions

The United Arab Emirates takes pride in having the largest industrial battery plant in the Gulf. Moreover, it has already invested significantly in renewable energy and plans to increase the share of renewable energy. In addition, UAE plans to explore several manufacturing industries in the future[175]. It is possible that the UAE may consider manufacturing of RET equipment and electric vehicles parts, locally, as it currently does for some ICE vehicles. Hence, lifecycle emissions of RET and EVs are accounted for, in this scenario. The results obtained are depicted in Figure 6.9.

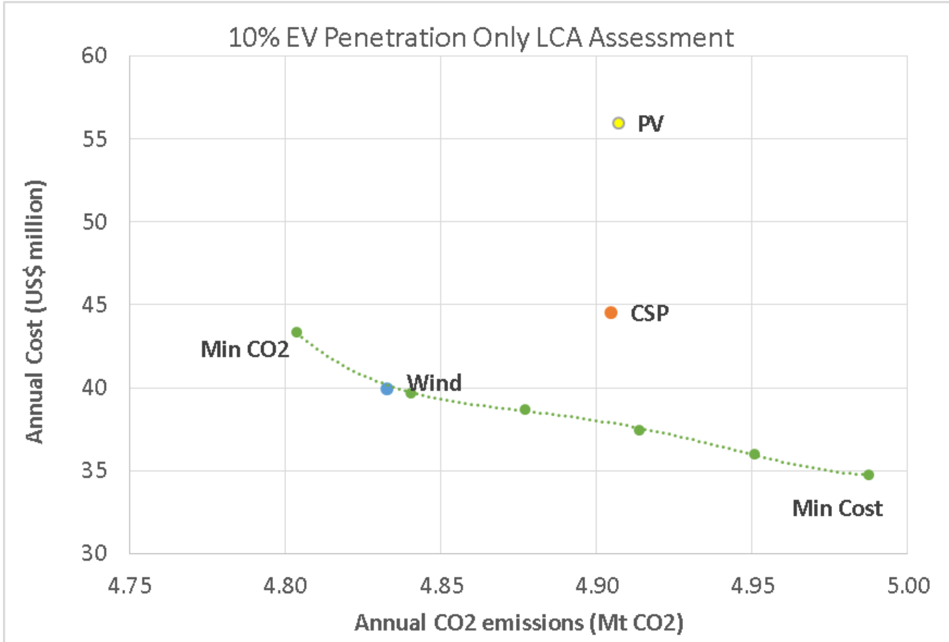

Figure 6.9 Annual cost and CO_2 emissions observed for meeting 10% EV demand whilst considering lifecycle emissions using different energy configurations

The general outlook appears to be very similar to the scenario where EV demand is only studied. However, comparing the minimum carbon emissions scenario with that of minimum cost, about 183 ktonnes of CO_2 is mitigated annually at a cost of $8.59 million. Implying, about 3 ktonnes less of CO_2 emissions will be reduced when considering lifecycle emissions. In this particular case study, lifecycle emissions of both, ICEs and EVs were considered. Since % EV penetration is considered, the resulting emissions will be offset. Nevertheless, to investigate the true impact, a detailed study on this aspect alone, needs to be conducted.

6.4.5 EV penetration

In the previous scenarios, the impact of 10% EV penetration on annual costs and emissions was studied. In this case, different share of EV penetration is studied when meeting EV demand only and coupled EV-AD demand. Figure 6.10 and Figure 6.11 show the results obtained for each of these cases, respectively.

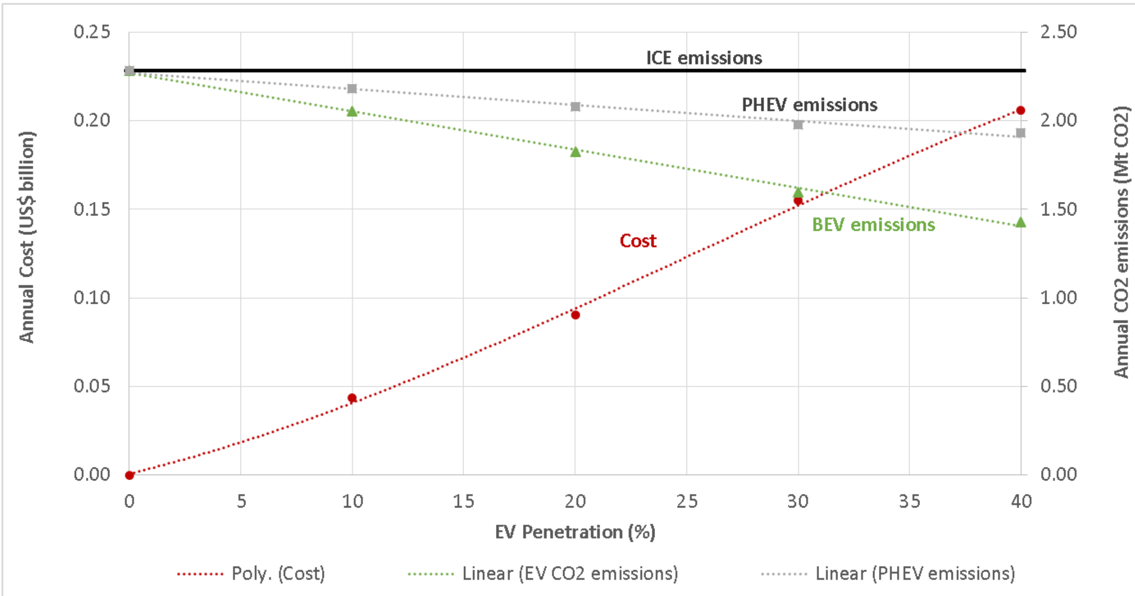

Figure 6.10 Annual cost and carbon emissions when considering different EV penetration ratios when meeting EV electricity demand only

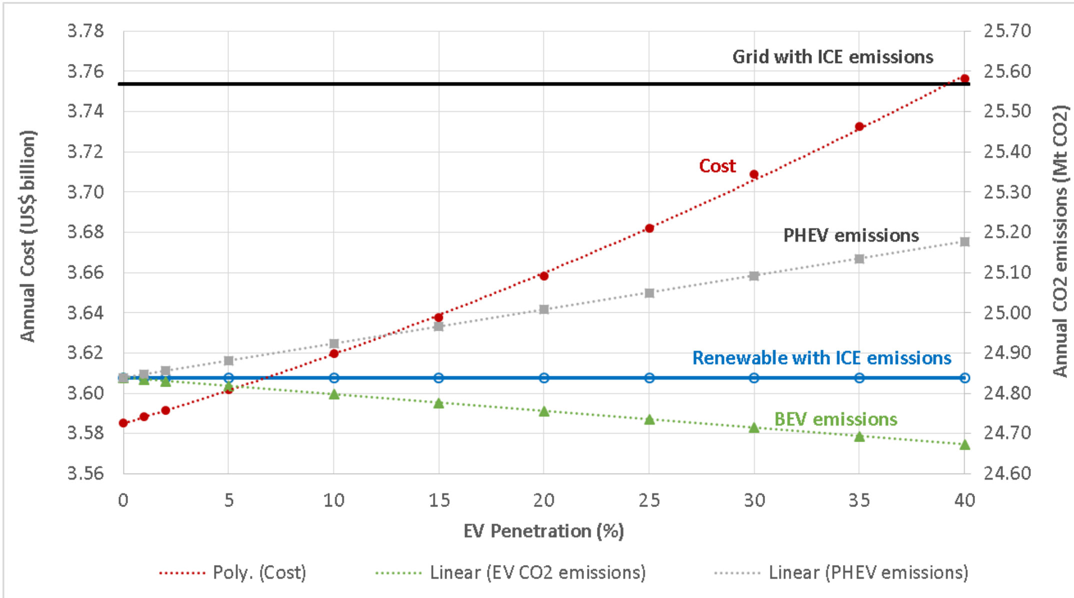

Figure 6.11 Annual cost and carbon emissions when considering different EV penetration ratios when meeting EV and AD electricity demand

As observed in Figure 6.10, as the EV penetration increases, the annual carbon emissions mitigated increases for both, BEVs and PHEVs. Moreover, the annual cost appears to increase as a result of more RET and EV charging infrastructure installed. On the other hand, in the case of EV+AD demand, the emissions generated by BEV decreases as more battery electric vehicles penetrate the transport sector. However, the annual emissions when considering PHEVs increases with increasing EV penetration. This is because, in the second case, EV charging demand is mainly met through electricity purchased from the grid. PHEVs do reduce ambient air emissions, but, conversely, increase the point sources emissions. However, due to increasing EV charging demand, amount of electricity consumed from the grid, eventually produced through fossil fuels, increases. This leads to an increase in point source emissions from power plants.

For PHEVs option, construction of further renewable energy projects may be planned to increase RE share to the grid or CCS technology may be utilized to mitigate these point source emissions.

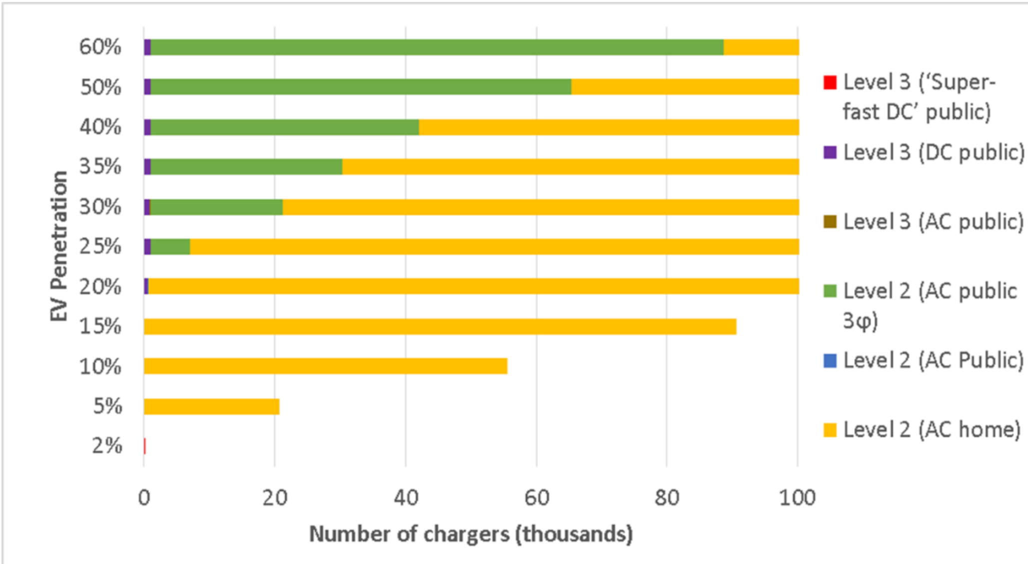

Figure 6.12 Number of each type of EV chargers installed for each ratio of EV penetration

As evident from Figure 6.12, as EV penetration ratio increases, the required number of chargers increase. However, the number of chargers does not exceed a maximum of 108,810, for this case study. Since all chargers occupy a parking space, each charger represents an available EV parking space. These parking spaces are restricted by a minimum and maximum, as indicated in Equations 20 and 21. Therefore, a different type of charger is selected rather than adding a parking space. Initially, at low EV penetration ratio, the results suggests operation of dedicated charging stations where level-31 chargers ('Super-fast DC' public) are installed, as evident from Table 6.5. Once the maximum is reached for these dedicated stations (i.e. 10 chargers per station), level-23 (AC home) chargers are installed. Once 20% of the transport sector comprises of EVs, level-32 (DC public) and level-22 (AC public) are utilized. However, at 25%, the maximum parking spaces allocated for EVs is reached. Thus, level-23 (AC home) chargers are compromised with level-21 (AC public 3ϕ) chargers. This trend continues until no more EV penetration can occur with the same designated parking ratio, stated in Equation 21. At that stage, since EVs would have penetrated most of the transport industry, the parking ratio can be increased in order to facilitate more chargers.

Table 6.5 Number of chargers shown in Figure 6.12

EV Penetration	Level 3			Level 2		
	'Super-fast DC' public	DC public	AC public	AC public 3ϕ	AC public	AC home
2%	49	0	0	0	0	0
5%	50	0	0	0	0	20600
10%	50	0	0	0	0	55600
15%	50	0	0	0		90600
20%	50	465	0	0	116	107725
25%	50	912	0	6032	0	101816
30%	50	715	184	20194	0	87654
35%	50	912	0	29365	3	78478
40%	50	912	0	41032	0	66816
50%	50	911	0	64378	0	43470
60%	50	912	0	87699	0	20149

6.5 Conclusion

In this study, optimal integration of renewable energy within the energy infrastructure was examined. Rooftop area of Abu Dhabi city was determined through the image segmentation technique. An electric vehicle charging infrastructure, based on these resources, was designed. Different scenarios were investigated where renewable energy, utilizing this rooftop area, was utilized to meet energy demand for the electric vehicle charging infrastructure as well the electricity demand of the city. Micro-CSP and small wind turbine technologies were found to be effective in attaining the greatest reduction in CO_2 emissions. However, the least cost was still observed when electricity demand was met completely by the grid. The study incorporated a scenario where life cycle emissions were also considered. A similar trend was observed; yet, signifying the magnitude of increase that may be increased when producing these technologies, domestically. In addition, the impact of varying EV penetration ratios on cost and emissions was also investigated. A decrease in carbon emissions as well as increase in cost was observed with increasing EV penetration.

Chapter 7 Conclusions & Future Work

All research objectives of the proposed work were successfully met. This dissertation presented the global problem of carbon emissions and the strong dependency of energy intensive industries and the existing energy infrastructure that heavily add to the problem. The area of renewable energies was explored along the path of integrating them to these carbon concentrated centers. A generic framework was developed based on superstructure optimization, outlining the various energy producers and consumers, along different echelons of the energy hub network, as discussed in Chapter 3. The constraints defining the technical limitations of various energy sources were shown. In addition, conditions pertaining to certain carbon mitigation measures were included in the framework modeling.

In the first study, a multi-period MILP model was successfully developed and a case study was conducted to investigate the applicability of the developed model. The results mainly showed the reduction of carbon emissions that may be obtained with the implementation of RET and the associated economic profit realized. Combined Heat and Power (CHP) systems were employed to realize the lowest economic costs. On the other hand, lowest carbon emissions were experienced when solar PV, CSP and wind technologies were utilized. Scenarios were considered through which the effect of EROI, crude oil flow, carbon pricing and CCS were studied. With decreasing EROI values, higher economic and environmental costs were observed. For varying crude oil flow, higher annual profit was realized alongside an increase annual carbon emissions. Under the

C&T program, a carbon credit value of \$87/tCO_2 (i.e. Switzerland) was found to be optimal as it resulted in the highest profit with least carbon dioxide emissions. Multi-objective optimization was carried out; resulting in a Pareto front that depicted the decrease in carbon emissions with decreasing profit.

In Chapter 5, the study of incorporating 'clean' energy within a refinery was presented. Different units and their significance that exist in a refinery were discussed, in detail. These units were successfully simulated using Aspen HYSYS V8.4 to determine the energy demand by each of these process units. Results showed that PV coupled with CSP(heat) as well as Wind coupled with CSP(heat) technologies resulted in lowest carbon dioxide emissions. On the contrary, CHP under excess conditions, resulted in the lowest economic-cost scenario. When storage technology was considered, Wind coupled with CSP(heat) resulted in further reduction of carbon emissions. Whilst studying the effect of carbon cap-and-trade program, three different carbon prices, which are already in effect in different economies, were investigated. In addition, the impact of different CCS costs on economic costs and CO_2 emissions was studied. When considering 70% CCS, as the cost of CCS increased, preference of using only CHP transitioned to CSP and later, coupled with wind technology.

Finally, research work on integrating renewable energy to existing energy infrastructure while utilizing rooftop area of structures within a region was successfully carried out. Using MATLAB segmentation and region analyzing tools, the average percentage difference between the actual and calculated areas was found to be 18.55%. An electric vehicle charging infrastructure was designed which is powered through rooftop RET systems. Cases were presented where produced energy was used to meet EV demand only, and EV and AD city demand, collectively. In the former case, deployment of wind turbines and CSP technology for electricity generation resulted in least emissions. Minimum economic cost was realized when electricity was purchased completely from grid. In the former scenario, due to the high demand of Abu Dhabi city, grid majorly contributed in meeting electricity demand whilst wind technology was considered to meet a part of this demand. The lifecycle emissions were also considered if the need arises for local production of technologies. Wind technology still resulted in least LCA carbon emissions. Further analysis was carried out that showed BEV reduced environmental impact with increased EV penetration. The number and type of chargers to be utilized under each scenario was also determined with increasing EV penetration.

There are other avenues that may be investigated when conducting further research in this area. Though a general framework was introduced in this work, specific studies may be carried out, incorporating stochasticity, such as varying demand, that would allow to observe the robustness of the proposed framework with respect to uncertainty. Complex situations may be analyzed, such as adding pool to pool flow in the pooling problem that would aid in the planning stages of the supply chain. Cases with MINLP formulations may be presented and different optimization techniques may be employed that would focus on finding the optimal solution in reduced computation time. Finally, studies can be carried out, incorporating the hydrogen vector as research interest is growing that focuses on constructing a hydrogen economy.

References

[1] U.S. Energy Information Administration, "Annual Energy Outlook 2015," *Off. Integr. Int. Energy Anal.*, vol. 1, pp. 1–244, 2015.

[2] A. K. Akella, R. P. Saini, and M. P. Sharma, "Social, economical and environmental impacts of renewable energy systems," *Renew. Energy*, vol. 34, no. 2, pp. 390–396, 2009.

[3] J. Adam, "Fact sheet: 6 things you should know about the value of renewable energy," 2012. [Online]. Available: https://thinkprogress.org/fact-sheet-6-things-you-should-know-about-the-value-of-renewable-energy-4f18647ed31e/. [Accessed: 12-Dec-2017].

[4] U.S. Energy Information Administration, "Renewable energy explained," 2017. [Online]. Available: https://www.eia.gov/energyexplained/?page=renewable_home. [Accessed: 03-Jan-2018].

[5] T. V. Ramachandra and B. V. Shruthi, "Spatial mapping of renewable energy potential," *Renewable and Sustainable Energy Reviews*, vol. 11, no. 7. pp. 1460–1480, 2007.

[6] Enerdata, "Global Energy Statistical Yearbook 2016," *Enerdata Intelligence + Consulting*. 2016.

[7] U.S. Energy Information Administration, "Total Electricity Generation," *International Energy Statistics*, 2015. [Online]. Available:

https://www.eia.gov/beta/international/data/browser/#/?pa=00000000000000000000000000000fvm&c=0g&ct=0&tl_id=2-A&vs=INTL.29-12-ARE-BKWH.A&ord=CR&vo=0&v=H&end=2015&showdm=y. [Accessed: 03-Jan-2018].

[8] T. Mezher, G. Dawelbait, and Z. Abbas, "Renewable energy policy options for Abu Dhabi: Drivers and barriers," *Energy Policy*, vol. 42, pp. 315–328, 2012.

[9] Open Energy Information, "Transparent Cost Database," *Annual Review of Resource Economics*, 2016. [Online]. Available: http://en.openei.org/apps/TCDB/.

[10] J. Logan, P. Sullivan, W. Short, L. Bird, T. L. James, and M. R. Shah, "Evaluating a Proposed 20% National Renewable Portfolio Standard," Golden, 2009.

[11] Lazard, "Lazard's Levelized Cost of Energy Analysis - Version 8.0," New York, 2014.

[12] H. M. Qiblawey and F. Banat, "Solar thermal desalination technologies," *Desalination*, vol. 220, no. 1–3, pp. 633–644, 2008.

[13] O. Younas, "Desalination of seawater/brackish by multi-effect solar still coupled with a point focus Fresnel lens," The Petroleum Institute, 2013.

[14] J. Nikoletatos and S. Tselepis, "Renewable Energy Integration in Power Grids," 2015.

[15] L. E. Jones and T. B. Tsuchida, *Renewable Energy Integration*. 2014.

[16] S. A. Abbasi and N. Abbasi, “The likely adverse environmental impacts of renewable energy sources,” in *Applied Energy*, 2000, vol. 65, no. 1–4, pp. 121–144.

[17] International Energy Agency, *Benign Energy?: The Environmental Implications of Renewables*. OECD, 1998.

[18] R. Pollin, J. Heintz, and H. Garrett-Peltier, “The economic benefits of investing in clean energy,” *Cent. Am. Prog. Polit. Econ. Res. Inst.*, p. 69, 2009.

[19] S. Abureden, S. Taqvi, I. H. Mustafa, I. H. Alhajri, A. Alsahli, and A. Elkamel, “Case study: Integrating Solar Energy in the Upstream Oil Supply Chain (USOSC) of Abu Dhabi, UAE,” in *International Conference on Science, Ecology and Technology I*, 2015, pp. 638–649.

[20] A. Abdullah, S. Sgouridis, S. Griffiths, D. Gielen, D. Saygin, and N. Wagner, “Renewable energy prospects: United Arab Emirates,” Abu Dhabi, 2015.

[21] N. Gagnon, C. A. S. Hall, and L. Brinker, “A preliminary investigation of energy return on energy investment for global oil and gas production,” *Energies*, vol. 2, no. 3, pp. 490–503, 2009.

[22] H. Lund, “Renewable energy strategies for sustainable development,” *Energy*, vol. 32, no. 6, pp. 912–919, 2007.

[23] J. Weiss and B. Tsuchida, “Integrating renewable energy into the electricity grid,” *The Brattle Group Report*, 2015. [Online]. Available: http://info.aee.net/hubfs/EPA/AEEI-Renewables-Grid-Integration-Case-Studies.pdf?t=1440089933677. [Accessed: 12-Dec-2017].

[24] O. Egbue and S. Long, “Barriers to widespread adoption of electric vehicles: An analysis of consumer attitudes and perceptions,” *Energy Policy*, vol. 48, pp. 717–729, 2012.

[25] M. Geidl, G. Koeppel, P. Favre-perrod, B. Klöckl, G. Andersson, and K. Fröhlich, “The Energy Hub – A Powerful Concept for Future Energy Systems,” in *Third Annual Carnegie Mellon Conference on the Electricity Industry*, 2007, pp. 1–10.

[26] M. Geidl, P. Favre-Perrod, B. Klöckl, and G. Koeppel, “A greenfield approach for future power systems,” in *41st CIGRE session 2006*, 2006, p. 10.

[27] P. Favre-Perrod, “A vision of future energy networks,” in *2005 IEEE Power Engineering Society Inaugural Conference and Exposition in Africa*, 2005.

[28] M. Geidl, G. Koeppel, P. Favre-Perrod, B. Klockl, G. Andersson, and K. Frohlich, “Energy hubs for the future,” *IEEE Power Energy Mag.*, vol. 5, no. 1, pp. 24–30, 2007.

[29] D. Grosspietsch, “Distributed multi-energy-hubs: a review and technoeconomic model to assess viability and potential pathways,” in

Energy Science Technology Conference 2015, 2015, p. 21.

[30] M. Geidl and G. Andersson, “A modeling and optimization approach for multiple energy carrier power flow,” in *2005 IEEE Russia PowerTech*, 2005, pp. 1–7.

[31] A. Walker, S. B., Mukherjee, U., Fowler, M., & Elkamel, “Benchmarking and selection of Power-to-Gas utilizing electrolytic hydrogen as an energy storage alternative,” *Int. J. Hydrogen Energy*, vol. 41, no. 19, pp. 7717–7731, May 2016.

[32] G. Koeppel and G. Andersson, “The Influence of Combined Power, Gas, and Thermal Networks on the Reliability of Supply,” in *The Sixth World Energy System Conference*, 2006, pp. 646–651.

[33] G. Koeppel and G. Andersson, “Reliability modeling of multi-carrier energy systems,” *Energy*, vol. 34, no. 3, pp. 235–244, 2009.

[34] M. D. Galus, R. La Fauci, and G. Andersson, “Investigating PHEV wind balancing capabilities using heuristics and model predictive control,” in *IEEE PES General Meeting, PES 2010*, 2010.

[35] A. Ulbig, M. D. Galus, and S. Chatzivasileiadis, “General Frequency Control with Aggregated Control Reserve Capacity from Time-Varying Sources : The Case of PHEVs,” in *2010 IREP Symposium – Bulk Power System Dynamics and Control – VIII (IREP)*, 2010, pp. 1–15.

[36] K. Hemmes, “Integration of fuel cells in multisource multiproduct energy

systems," *Proc. 4th Int. ASME Conf. Fuel Cell Sci. Eng. Technol. FUELCELL2006*, vol. 2006, no. D, pp. 4–8, 2006.

[37] H. Hajimiragha, C. Canizares, M. Fowler, M. Geidl, and G. Andersson, "Optimal Energy Flow of Integrated Energy Systems with Hydrogen Economy Considerations," in *Bulk Power System Dynamics and Control – VII*, 2007, pp. 1–11.

[38] V. Manusov, A. Kirgizov, and J. Ahyoev, "Construction and optimization of a power complex with a distributed generation on the basis of renewables and methods of artificial intelligence (on the example of the Republic of Tajikistan)," in *E3S Web of Conferences*, 2016, vol. 3006, pp. 1–8.

[39] R. Rubio-Barros, D. Ojeda-Esteybar, and A. Vargas, "Energy Carrier Networks: Interactions and Integrated Operational Planning BT," in *Handbook of Networks in Power Systems II*, A. Sorokin, S. Rebennack, P. M. Pardalos, N. A. Iliadis, and M. V. F. Pereira, Eds. Berlin, Heidelberg: Springer Berlin Heidelberg, 2012, pp. 117–167.

[40] M. D. Galus *et al.*, "Integrating power systems, transport systems and vehicle technology for electric mobility impact assessment and efficient control," *IEEE Trans. Smart Grid*, vol. 3, no. 2, pp. 934–949, 2012.

[41] S. Pazouki, M. R. Haghifam, and A. Moser, "Uncertainty modeling in optimal operation of energy hub in presence of wind, storage and demand response," *Electr. Power Energy Syst.*, vol. 61, pp. 335–345, 2016.

[42] S. Pazouki, M. R. Haghifam, and J. Olamaei, “Economical scheduling of multi carrier energy systems integrating Renewable, Energy Storage and Demand Response under Energy Hub approach,” in *Smart Grid Conference 2013, SGC 2013*, 2013, pp. 80–84.

[43] E. Fabrizio, M. Filippi, and J. Virgone, “Trade-off between environmental and economic objectives in the optimization of multi-energy systems,” *Build. Simul.*, vol. 2, no. 1, pp. 29–40, 2009.

[44] Y. Dai and J. Wang, “A modeling and optimization approach for multi-carrier energy system considering the interaction between energy, product and emission,” *Biotechnol. - An Indian J.*, vol. 8, no. 6, pp. 848–854, 2009.

[45] A. J. Del Real, A. Arce, and C. Bordons, “Combined environmental and economic dispatch of smart grids using distributed model predictive control,” *Int. J. Electr. Power Energy Syst.*, vol. 54, pp. 65–76, 2014.

[46] Y. Wang, P. Zeng, H. Zhang, Y. Liu, T. Wang, and F. Kuang, “Information-centric Industrial Internet of Things: Energy model,” in *Proceedings of IEEE CCIS2012*, 2012, pp. 1–6.

[47] A. R. Restrepo, D. F. Manotas, and C. A. Lozano, “Self-generation of Electricity, Assessment and Optimization under the New Support Schemes in Colombia,” *IEEE Lat. Am. Trans.*, vol. 14, no. 3, pp. 1308–1314, 2016.

[48] M. Rayati, A. Sheikhi, and A. M. Ranjbar, “Optimising operational cost of a smart energy hub, the reinforcement learning approach,” *Int. J. Parallel, Emergent Distrib. Syst.*, vol. 30, no. 4, pp. 325–341, 2015.

[49] S. Pazouki, M.-R. Haghifam, and S. Pazouki, “Transition from fossil fuels power plants toward Virtual Power Plants of distribution networks,” *Inst. Electr. Electron. Eng. Inc. Conf. Proceedings.*, pp. 82–86, 2016.

[50] R. Buehler, “Integration of Renewable Energy Sources Using Microgrids, Virtual Power Plants and the Energy Hub Approach,” ETH Zurich, 2010.

[51] M. C. Bozchalui, S. A. Hashmi, H. Hassen, C. A. Cañizares, and K. Bhattacharya, “Optimal operation of residential energy hubs in smart grids,” *IEEE Trans. Smart Grid*, vol. 3, no. 4, pp. 1755–1766, 2012.

[52] S. Paudyal, “Optimal Energy Management of Distribution Systems and Industrial Energy Hubs in Smart Grids,” University of Waterloo, 2012.

[53] C. Unsihuay, J. W. Marangon-Lima, and A. C. Zambroni De Souza, “Short-term operation planning of integrated hydrothermal and natural gas systems,” in *2007 IEEE Lausanne POWERTECH, Proceedings*, 2007, pp. 1410–1416.

[54] E. Robertson, A. Alarcon-Rodriguez, S. Galloway, and G. Ault, “Outline for an integrated multiple energy carrier model of the UK energy infrastructure,” in *2009 44TH INTERNATIONAL UNIVERSITIES POWER ENGINEERING CONFERENCE*, 2009, pp. 911–915.

[55] M. D. Galus and G. Andersson, “Integration of Plug-In Hybrid Electric Vehicles into energy networks,” in *2009 IEEE Bucharest PowerTech: Innovative Ideas Toward the Electrical Grid of the Future*, 2009.

[56] S. Pazouki and M. Haghifam, "Market based short term scheduling in energy hub in presence of responsive loads and renewable resources," in *22nd International Conference on Electricity Distribution*, 2013, pp. 1–4.

[57] S. Pazouki, M. R. Haghifam, and J. Olamaei, "Short term scheduling of multi carrier systems through interruptible load and Energy Storage toward future sustainable energy needs," *Electr. Electron. Eng. (ELECO), 2013 8th Int. Conf.*, no. 3, pp. 77–81, 2013.

[58] S. Pazouki, "Scheduling of Energy Hubs Including CCHP , Solar and Energy Storages in Different Climates," in *The 20th Iranian Electrical Power Distribution Conference*, 2015, no. April, pp. 28–29.

[59] A. Zidan and H. A. Gabbar, "Optimal scheduling of energy hubs in interconnected multi energy systems," in *2016 4th IEEE International Conference on Smart Energy Grid Engineering, SEGE 2016*, 2016, pp. 164–169.

[60] I. G. Moghaddam, M. Saniei, and E. Mashhour, "A comprehensive model for self-scheduling an energy hub to supply cooling, heating and electrical demands of a building," *Energy*, vol. 94, pp. 157–170, 2016.

[61] A. Vaccaro, C. Pisani, and A. F. Zobaa, "Affine arithmetic-based methodology for energy hub operation-scheduling in the presence of data uncertainty," *IET Gener. Transm. Distrib.*, vol. 9, no. 13, pp. 1544–1552, 2015.

[62] M. Arnold, R. R. Negenborn, G. Andersson, and B. De Schutter, "Model-

based predictive control applied to multi-carrier energy systems," *2009 IEEE Power {&} Energy Soc. Gen. Meet.*, vol. 19, 2009.

[63] M. Arnold and G. Andersson, "Model predictive control of energy storage including uncertain forecasts," *Power Syst. Comput. Conf. (PSCC), Stock. Sweden*, 2011.

[64] E. Fabrizio, "Feasibility of polygeneration in energy supply systems for health-care facilities under the Italian climate and boundary conditions," *Energy Sustain. Dev.*, vol. 15, no. 1, pp. 92–103, 2011.

[65] M. Schulze and P. C. Del Granado, "Implementation of Feed-in Tariffs into Multi-Energy Systems," *Int. J. Electr. Comput. Energ. Electron. Commun. Eng.*, vol. 3, no. May, pp. 1004–1010, 2009.

[66] S. Barsali, D. Poli, S. Scalari, L. Carradore, and R. Turri, "Integration of process-side energy storage and active distribution networks: Technical and economical optimisation," in *Electricity Distribution - Part 1, 2009. CIRED 2009. 20th International Conference and Exhibition on*, 2009, no. July, pp. 1–4.

[67] F. Kienzle, "Evaluation of Investments in Multi-Carrier Energy Systems under Uncertainty," ETH Zurich, 2010.

[68] F. Kienzle and G. Andersson, "Valuing Investments in Multi-Energy Generation Plants under Uncertainty : A Real Options Analysis by," in *IAEE European Conference*, 2009, no. September 2014, pp. 1–17.

[69] F. Kienzle, P. Ahcin, and G. Andersson, “Valuing investments in multi-energy conversion, storage, and demand-side management systems under uncertainty,” *IEEE Trans. Sustain. Energy*, vol. 2, no. 2, pp. 194–202, 2011.

[70] Y. Maniyali, A. Almansoori, M. Fowler, and A. Elkamel, “Energy hub based on nuclear energy and hydrogen energy storage,” *Ind. Eng. Chem. Res.*, vol. 52, no. 22, 2013.

[71] A. Sharif, A. Almansoori, M. Fowler, A. Elkamel, and K. Alrafea, “Design of an energy hub based on natural gas and renewable energy sources,” *Int. J. Energy Res.*, vol. 38, no. 3, pp. 363–373, 2014.

[72] K. Orehounig, G. Mavromatidis, R. Evins, V. Dorer, and J. Carmeliet, “Towards an energy sustainable community: An energy system analysis for a village in Switzerland,” *Energy Build.*, vol. 84, pp. 277–286, 2014.

[73] G. Chicco and P. Mancarella, “A unified model for energy and environmental performance assessment of natural gas-fueled poly-generation systems,” *Energy Convers. Manag.*, vol. 49, no. 8, pp. 2069–2077, 2008.

[74] M. D. Galus, R. A. Waraich, M. Balmer, G. Andersson, and K. W. Axhausen, “A framework for investigating the impact of PHEVS,” 2009, p. 9.

[75] B. Morvaj, R. Evins, and J. Carmeliet, “Decarbonizing the electricity grid: The impact on urban energy systems, distribution grids and district heating

potential," *Appl. Energy*, vol. 191, pp. 125–140, 2017.

[76] H. Jiayi, J. Chuanwen, and X. Rong, "A review on distributed energy resources and MicroGrid," *Renewable and Sustainable Energy Reviews*, vol. 12, no. 9. pp. 2465–2476, 2008.

[77] M. Schulze, L. Friedrich, and M. Gautschi, "Modeling and optimization of renewables: Applying the energy hub approach," in *2008 IEEE International Conference on Sustainable Energy Technologies, ICSET 2008*, 2008, pp. 83–88.

[78] K. Hemmes, J. L. Zachariah-wolff, M. Geidl, and G. Andersson, "Towards multi-source multi-product energy systems," *Int. J. Hydrogen Energy*, vol. 32, pp. 1332–1338, 2007.

[79] F. Adamek, "Optimal multi energy supply for regions with increasing use of renewable resources," in *2008 IEEE Energy 2030 Conference, ENERGY 2008*, 2008, no. November, pp. 1–6.

[80] A. Maroufmashat, A. Elkamel, S. S. Khavas, M. Fowler, R. Roshandel, and M. Elsholkami, "Development of the energy hub networks based on distributed energy technologies," in *Summer Computer Simulation Conference*, 2015, vol. 47, no. 10, pp. 216–223.

[81] A. J. Del Real, A. Arce, and C. Bordons, "Solar-hydrogen residential power system considering seasonal weather variations," in *IFAC Proceedings Volumes (IFAC-PapersOnline)*, 2010, vol. 1, no. PART 1, pp. 169–174.

[82] A. G. Anastasiadis, V. M. Argyropoulou, K. D. Pagonis, and N. D. Hatziargyriou, “Losses in a LV-Microgrid with the Presence of Reactive Power and CHP Units,” in *8th Mediterranean Conference on Power Generation, Transmission, Distribution and Energy Conversion (MEDPOWER 2012)*, 2013, p. 34.

[83] G. Chicco and P. Mancarella, “Distributed multi-generation: A comprehensive view,” *Renewable and Sustainable Energy Reviews*, vol. 13, no. 3. pp. 535–551, 2009.

[84] M. Schulze and P. Del Granado, “Optimization modeling in energy storage applied to a multi-carrier system,” *... Energy Soc. Gen. Meet. ...*, pp. 1–7, 2010.

[85] E. Robertson, S. Galloway, and G. Ault, “The impact of wide spread adoption of high levels of Distributed Generation in domestic properties,” in *IEEE Power and Energy Society General Meeting*, 2012, pp. 1–8.

[86] J. Divya, K. C., & Østergaard, “Battery energy storage technology for power systems—An overview,” *Electr. Power Syst. Res.*, vol. 79, no. 4, pp. 511–520, Apr. 2009.

[87] M. D. Galus and G. Andersson, “Power system considerations of plug-in hybrid electric vehicles based on a multi energy carrier model,” in *2009 IEEE Power and Energy Society General Meeting, PES ’09*, 2009.

[88] F. Andrade, J. J. Cardenas, L. Romeral, and J. Cusido, “Modeling and studying of power flow in a parking lot with plug-in vehicles and the

impact in the public utility," in *2012 IEEE PES Innovative Smart Grid Technologies, ISGT 2012*, 2012, pp. 1–7.

[89] M. Y. Damavandi, M. P. Moghaddam, M.-R. Haghifam, M. Shafie-khah, and J. P. S. Catalao, "Stochastic Modeling of Plug-In Electric Vehicles' Parking Lot in Smart Multi-Energy System," in *Technological Innovation for Collective Awareness Systems*, L. M. Camarinha-Matos, N. S. Barrento, and R. Medonca, Eds. Costa de Caparica: Springer, 2014, pp. 332–342.

[90] M. Rastegar and M. Fotuhi-Firuzabad, "Optimal charge scheduling of PHEV in a multi-carrier energy home," in *2014 14th International Conference on Environment and Electrical Engineering, EEEIC 2014 - Conference Proceedings*, 2014, pp. 199–203.

[91] B. Morvaj, K. Knezović, R. Evins, and M. Marinelli, "Integrating multi-domain distributed energy systems with electric vehicle PQ flexibility: Optimal design and operation scheduling for sustainable low-voltage distribution grids," *Sustain. Energy, Grids Networks*, vol. 8, pp. 51–61, 2016.

[92] M. R. Haghifam, S. Pazouki, and S. Pazouki, "Renewables and Plug in Electric Vehicles modeling on electricity and gas infrastructures scheduling in presence of responsive demand," in *2013 3rd International Conference on Electric Power and Energy Conversion Systems, EPECS 2013*, 2013, pp. 1–5.

[93] M. Geidl and G. Andersson, “Optimal power flow of multiple energy carriers,” *IEEE Trans. Power Syst.*, vol. 22, no. 1, pp. 145–155, 2007.

[94] A. Maroufmashat *et al.*, “Modeling and optimization of a network of energy hubs to improve economic and emission considerations,” *Energy*, vol. 93, pp. 2546–2558, 2015.

[95] Geidl and A. G. M., “Optimal Power Flow of Multiple Energy Carrier Systems.,” *IEEE Trans. power Syst.*, vol. 22, no. no.1, pp. 145–155, 2007.

[96] A. Sheikhi, M. S. Naderi, A. M. Ranjbar, G. B. Gharehpetian, and F. Safe, “CHP optimized selection methodology for a multi-carrier energy system,” *Int. Rev. Electr. Eng.*, vol. 6, no. 4, pp. 1839–1846, 2011.

[97] M. R. Haghifam and M. Manbachi, “Reliability and availability modelling of combined heat and power (CHP) systems,” *Int. J. Electr. Power Energy Syst.*, vol. 33, no. 3, pp. 385–393, 2011.

[98] P. Mitchell and S. Skarvelis-Kazakos, “Control of a biogas co-firing CHP as an Energy Hub,” in *Proceedings of the Universities Power Engineering Conference*, 2015, vol. 2015–Novem, pp. 1–6.

[99] Y. Mozafari, W. D. Rosehart, and H. Zareipour, “Integrated electricity generation, CHPs, and boilers expansion planning: Alberta case study,” in *IEEE Power and Energy Society General Meeting*, 2015, pp. 1–5.

[100] A. El-Zonkoly, “Optimal scheduling of observable controlled islands in presence of energy hubs,” *Electr. Power Syst. Res.*, vol. 142, pp. 141–152,

2017.

[101] S. Pazouki, A. Mohsenzadeh, M.-R. Haghifam, and M. E. Talebian, "Optimal allocation of wind turbine in multi carrier energy networks improving loss and voltage profile," in *ELECO 2013 - 8th International Conference on Electrical and Electronics Engineering*, 2013, pp. 67–71.

[102] M. A. Pellow, C. J. M. Emmott, C. J. Barnhart, and S. M. Benson, "Hydrogen or batteries for grid storage? A net energy analysis," *Energy Environ. Sci.*, vol. 8, no. 7, pp. 1938–1952, 2015.

[103] A. Maroufmashat, S. T. H. Taqvi, M. W. Fowler, and A. Elkamel, "A modeling and optimization approach for multiple energy carrier power flow," *Submitt. Publiaction*.

[104] M. Elsholkami and A. Elkamel, "General optimization model for the energy planning of industries including renewable energy: A case study on oil sands," *AIChE J.*, vol. 63, no. 2, pp. 610–638, 2017.

[105] International Energy Agency (IEA), "Technology roadmap-concentrating solar power," Paris, 2010.

[106] J. Hernández-Moro and J. M. Martínez-Duart, "Analytical model for solar PV and CSP electricity costs: Present LCOE values and their future evolution," *Renewable and Sustainable Energy Reviews*, vol. 20. pp. 119–132, 2013.

[107] J. Macknick, R. Newmark, G. Heath, and K. Hallett, "A Review of

Operational Water Consumption and Withdrawal Factors for Electricity Generating Technologies," Golden, Colarado, 2011.

[108] C. Parrado, A. Girard, F. Simon, and E. Fuentealba, "2050 LCOE (Levelized Cost of Energy) projection for a hybrid PV (photovoltaic)-CSP (concentrated solar power) plant in the Atacama Desert, Chile," *Energy*, vol. 94, pp. 422–430, 2016.

[109] X. Ouyang and B. Lin, "Levelized cost of electricity (LCOE) of renewable energies and required subsidies in China," *Energy Policy*, vol. 70, pp. 64–73, 2014.

[110] T. Ashuri, M. B. Zaaijer, J. R. R. A. Martins, G. J. W. van Bussel, and G. A. M. van Kuik, "Multidisciplinary Design Optimization of Offshore Wind Turbines for minimum Levelized Cost of Energy," *Renew. Energy*, vol. 68, pp. 893–905, 2014.

[111] B. Zakeri and S. Syri, "Electrical energy storage systems: A comparative life cycle cost analysis," *Renewable and Sustainable Energy Reviews*, vol. 42. pp. 569–596, 2015.

[112] E. S. Rubin, J. E. Davison, and H. J. Herzog, "The cost of CO2 capture and storage," *Int. J. Greenh. Gas Control*, vol. 40, pp. 378–400, 2015.

[113] S. A. Kalogirou and Y. Tripanagnostopoulos, "Hybrid PV/T solar systems for domestic hot water and electricity production," *Energy Convers. Manag.*, vol. 47, no. 18–19, pp. 3368–3382, 2006.

[114] R. Mahtta, P. K. Joshi, and A. K. Jindal, “Solar power potential mapping in India using remote sensing inputs and environmental parameters,” *Renew. Energy*, vol. 71, pp. 255–262, 2014.

[115] A. Swain, “Solar energy generation potential along national highways,” *Int. Res. J. Eng. Technol.*, vol. 4, no. 9, p. 16, 2017.

[116] M. M. Hoogwijk, “On the Global and Regional Potential of Renewable Energy Sources,” Utrecht University, 2004.

[117] F. Trieb, C. Schillings, M. O. ’ Sullivan, T. Pregger, and C. Hoyer-Klick, “Global Potential of Concentrating Solar Power,” *SolarPaces Conf. Berlin*, no. September, pp. 1–11, 2009.

[118] P. Heller, Ed., *The Performance of Concentrated Solar Power (CSP) Systems*, 1st ed. Sawston: Woodhead Publishing, 2017.

[119] T. Wizelius, *Developing wind power projects: Theory and practice*. London: Earthscan Publishers, 2006.

[120] T. B. M. J. Ouarda *et al.*, “Probability distributions of wind speed in the UAE,” *Energy Convers. Manag.*, vol. 93, pp. 414–434, 2015.

[121] M. Mohibullah, A. M. Radzi, and M. I. A. Hakim, “Basic design aspects of micro hydro power plant and its potential development in Malaysia,” in *National Power and Energy Conference (PECon) 2004 Proceedings*, 2004, pp. 220–223.

[122] S. J. Zarrouk and H. Moon, “Efficiency of geothermal power plants: A

worldwide review," *Geothermics*, vol. 51. pp. 142–153, 2014.

[123] C. Coskun, Z. Oktay, and I. Dincer, "Performance evaluations of a geothermal power plant," in *Applied Thermal Engineering*, 2011, vol. 31, no. 17–18, pp. 4074–4082.

[124] J. Phillips, "Evaluating the level and nature of sustainable development for a geothermal power plant," *Renew. Sustain. Energy Rev.*, vol. 14, no. 8, pp. 2414–2425, 2010.

[125] S. Jalilinasrabady, R. Itoi, P. Valdimarsson, G. Saevarsdottir, and H. Fujii, "Flash cycle optimization of Sabalan geothermal power plant employing exergy concept," *Geothermics*, vol. 43, pp. 75–82, 2012.

[126] F. H. Harlow and W. E. Pracht, "A theoretical study of geothermal energy extraction," *J. Geophys. Res.*, vol. 77, no. 35, pp. 7038–7048, 1972.

[127] IEA, "Key World Energy Statistics 2016," *Statistics (Ber).*, p. 80, 2016.

[128] A. Mokri, M. Aal Ali, and M. Emziane, "Solar energy in the United Arab Emirates: A review," *Renewable and Sustainable Energy Reviews*, vol. 28. pp. 340–375, 2013.

[129] A. Zahedi, "A review of drivers, benefits, and challenges in integrating renewable energy sources into electricity grid," *Renewable and Sustainable Energy Reviews*, vol. 15, no. 9. pp. 4775–4779, 2011.

[130] P. Mancarella, "MES (multi-energy systems): An overview of concepts and evaluation models," *Energy*, vol. 65. pp. 1–17, 2014.

[131] I. van Beuzekom, M. Gibescu, and J. G. Slootweg, “A review of multi-energy system planning and optimization tools for sustainable urban development,” in *2015 IEEE Eindhoven PowerTech*, 2015, pp. 1–7.

[132] M. Mohammadi, Y. Noorollahi, B. Mohammadi-ivatloo, and H. Yousefi, “Energy hub: From a model to a concept – A review,” *Renew. Sustain. Energy Rev.*, vol. 80, no. December 2016, pp. 1512–1527, 2017.

[133] Y. Choi, C. Lee, and J. Song, “Review of Renewable Energy Technologies Utilized in the Oil and Gas Industry,” *Int. J. Renew. Energy Res.*, vol. 7, no. 2, p. 7, 2017.

[134] IPIECA, “Saving energy in the oil and gas industry,” London, 2013.

[135] D. J. Murphy and C. A. S. Hall, “Adjusting the economy to the new energy realities of the second half of the age of oil,” *Ecol. Modell.*, vol. 223, no. 1, pp. 67–71, 2011.

[136] A. R. Brandt, Y. Sun, S. Bharadwaj, D. Livingston, E. Tan, and D. Gordon, “Energy return on investment (EROI) for forty global oilfields using a detailed engineering-based model of oil production,” *PLoS One*, vol. 10, no. 12, 2015.

[137] Energy Files, “Forecasting Oil and Gas Production, Consumption and Activity,” 2010. [Online]. Available: http://www.energyfiles.com/global/onshore.html. [Accessed: 12-Dec-2017].

[138] J. G. Speight, *Handbook of Offshore Oil and Gas Operations*. Amsterdam: Elsevier, 2014.

[139] F. S. Manning and R. E. Thompson, *Oilfield Processing Volume Two: Crude Oil*. Tulsa: PennWell Publishing Company, 1995.

[140] Keystone XL Project, "Appendix U: Lifecycle Greenhouse Gas Emissions of Petroleum Products from WCSB Oil Sands Crudes Compared with Reference Crudes," 2013.

[141] I. Moore, "Life Cycle Well to Wheels Assessment of GHG Emissions from North American and Imported Crude Oils," in *Workshop Comparing Approaches to Life Cycle Analysis of Crude Oil*, 2011, p. 34.

[142] Global CCS Institue, "Accelerating the Uptake of CCS: Industrial Use of Captured Carbon Dioxide," 2011.

[143] Scottish Centre for Carbon Storage, "Carbon Sequestration," *Science (80-.).*, vol. 325, no. 5948, p. 1644 LP-1645, Sep. 2009.

[144] IEA, "Storing CO2 through enhanced oil recovery," *Int. Energy Agency, Paris, Fr.*, 2015.

[145] Masdar, "Shams 1 Fact Sheet," 2017. [Online]. Available: http://www.masdar.ae/assets/downloads/content/230/shams_factsheet-final-jan_8,_2017.pdf. [Accessed: 12-Dec-2017].

[146] Masdar, "Masdar City Solar PV Plant." [Online]. Available: http://www.masdar.ae/en/energy/detail/masdar-city-solar-pv-plant.

[Accessed: 12-Dec-2017].

[147] L. H. Goulder and A. R. Schein, "Carbon Taxes versus Cap and Trade: A Critical Review," *Clim. Chang. Econ.*, vol. 4, no. 3, p. 1350010, 2013.

[148] C. A. S. Hall, J. G. Lambert, and S. B. Balogh, "EROI of different fuels and the implications for society," *Energy Policy*, vol. 64, pp. 141–152, 2014.

[149] A. Szklo and R. Schaeffer, "Fuel specification, energy consumption and CO2 emission in oil refineries," *Energy*, vol. 32, no. 7, pp. 1075–1092, 2007.

[150] J. H. Gary, G. E. Handwerk, and M. J. Kaiser, *Petroleum Refining Technology and Economics*, Fifth. Boca Raton: Taylor & Francis, 2007.

[151] U. R. Chaudhuri, *Fundamentals of Petroleum and Petrochemical Engineering*. Boca Raton: Taylor & Francis, 2011.

[152] B. Dunn, H. Kamath, and J. M. Tarascon, "Electrical energy storage for the grid: A battery of choices," *Science*, vol. 334, no. 6058. pp. 928–935, 2011.

[153] IEA-ETSAP and International Renewable Energy Agency (IRENA), "Thermal Energy Storage Technology Brief," 2013.

[154] K.-H. Dietsche and D. Kuhlgatz, "History of the automobile," in *Fundamentals of Automotive and Engine Technology*, 2014, pp. 1–7.

[155] J. Mills, "Test your knowledge: where and when was the world's first

petrol station established," *The Sunday Times*, 24-Jul-2015.

[156] J. Gerdes, "Estonia launches nationwide electric vehicle fast-charging network," *Forbes*, San Francisco, 26-Feb-2013.

[157] R. Matulka, "The History of the Electric Car," *Energy.gov*, pp. 1–11, 2014.

[158] L. Graves, "Dubai announces new electric vehicle incentives," *The National*, Dubai, 24-Sep-2017.

[159] D. Baldwin, "UAE paves way for zero-carbon electric cars," *Gulf News*, Dubai, 18-Dec-2017.

[160] S. Griffiths and R. Mills, "Potential of rooftop solar photovoltaics in the energy system evolution of the United Arab Emirates," *Energy Strateg. Rev.*, vol. 9, pp. 1–7, 2016.

[161] CAA, "Types of Electric Vehicles," *Canadian Automobile Association*, 2016. [Online]. Available: http://electricvehicles.caa.ca/types-of-electric-vehicles/. [Accessed: 01-Aug-2016].

[162] M. Granovskii, I. Dincer, and M. A. Rosen, "Economic and environmental comparison of conventional, hybrid, electric and hydrogen fuel cell vehicles," *J. Power Sources*, vol. 159, no. 2, pp. 1186–1193, 2006.

[163] J. Liu, "Electric vehicle charging infrastructure assignment and power grid impacts assessment in Beijing," *Energy Policy*, vol. 51, pp. 544–557, 2012.

[164] S. Edelstein, "Electric car price guide: every 2015-2016 plug-in car specs," *Green Car Reports*, 2016. [Online]. Available:

http://www.greencarreports.com/news/1080871_electric-car-price-guide-every-2015-2016-plug-in-car-with-specs-updated. [Accessed: 02-Aug-2016].

[165] fleetcarma, "A Lengthy List of Electric Vehicles Currently Available in the United States," 2017. [Online]. Available: https://www.fleetcarma.com/electric-vehicles-united-states/. [Accessed: 18-Oct-2018].

[166] K. Morrow, D. Karner, and J. Francfort, "U . S . Department of Energy Vehicle Technologies Program - Advanced Vehicle Testing Activity Plug-in Hybrid Electric Vehicle Charging Infrastructure Review Novem Charging Infrastructure Review," *Power*, no. 58517, p. 34, 2008.

[167] CAA, "Charging stations," *Canadian Automobile Association*, 2016. [Online]. Available: http://electricvehicles.caa.ca/types-of-electric-vehicles/charging-stations/. [Accessed: 02-Aug-2016].

[168] A. Schroeder and T. Traber, "The economics of fast charging infrastructure for electric vehicles," *Energy Policy*, vol. 43, pp. 136–144, 2012.

[169] O. van Vliet, A. S. Brouwer, T. Kuramochi, M. van den Broek, and A. Faaij, "Energy use, cost and CO2 emissions of electric cars," *J. Power Sources*, vol. 196, no. 4, pp. 2298–2310, 2011.

[170] Z. Shahan, "Electric Car Charging 101," *EV Obsession*, 2015. [Online]. Available: https://evobsession.com/electric-car-charging-101-types-of-charging-apps-more/. [Accessed: 02-Aug-2016].

[171] A. Ahmad, “Abu Dhabi population swells,” *The National,* Abu Dhabi, 04-Nov-2014.

[172] C. Koo, T. Hong, H. S. Park, and G. Yun, “Framework for the analysis of the potential of the rooftop photovoltaic system to achieve the net-zero energy solar buildings,” *Prog. Photovoltaics Res. Appl.*, vol. 22, no. 4, pp. 462–478, 2014.

[173] N. Kaul, “The bad boys of energy consumption,” *Gulf News,* Abu Dhabi, 08-Nov-2017.

[174] Abu Dhabi Water & Electricity Company (ADWEC), “Statistical Report 1999-2016,” Abu Dhabi, 2016.

[175] I. Wright, “UAE Aims to Become International Manufacturing Hub,” *Engineering.com,* 02-Jun-2016.